2011-05-02

Synthesis of Fluorescent Analogs of Neurotransmitters

Sharanappa Maduraya Bagale
University of Miami, sharanappabagale@yahoo.com

UNIVERSITY OF MIAMI

SYNTHESIS OF FLUORESCENT ANALOGS OF NEUROTRANSMITTERS

By

Sharanappa M. Bagale

A THESIS

Submitted to the Faculty

of the University of Miami

in partial fulfillment of the requirements for

the degree of Master of Science

Coral Gables, Florida

May 2011

UNIVERSITY OF MIAMI

A thesis submitted in partial fulfillment of
the requirements for the degree of
Master of Science

SYNTHESIS OF FLUORESCENT ANALOGS OF NEUROTRANSMITTERS

Sharanappa M. Bagale

Approved:

_____	_____
James N. Wilson, Ph.D.	Terri A. Scandura, Ph.D.
Assistant Professor of Chemistry	Dean of the Graduate School
_____	_____
Angel E. Kaifer, Ph.D.	Norito Takenaka, Ph.D.
Professor of Chemistry	Assistant Professor of Chemistry

SHARANAPPA M. BAGALE (M.S., Chemistry)

Synthesis of Fluorescent Analogs of Neurotransmitters (May 2011)

Abstract of a thesis at the University of Miami.

Dissertation supervised by Dr. James N. Wilson.

No. of pages in text. (77)

Fluorescent analogs of biomolecules have been known as useful probes to study the structure, conformations and dynamics of cellular processes. These probes are more ideal than fluorescent labeled probes, as fluorescent analog probes retain the shape, size, conformation, and recognition element of the natural substrate, while giving useful intracellular information about detection and dynamics of biomolecules. The monoamine neurotransmitters control the central and periphery nervous systems. Serotonin (5-HT), in particular, is a versatile chemical messenger responsible for a multitude of biological processes, such as regulation of emotion, vasoconstriction, and bone metabolism. The study of serotonergic complex pathways is vital and essential in drug discovery for the diseases that result from the depletion and deregulation of serotonin in synapse. The extracellular concentration of serotonin is controlled by several transporters, most preferably the serotonin transporter (SERT). Selective serotonin reuptake inhibitors (SSRIs), along with dual- and triple-acting inhibitors, affect SERT and hence 5-HT in depression and related diseases.

In this present investigation, firstly, a set of fluorescent analogs of neurotransmitter probes based on ethylamino-functionalized substrates were successfully designed and these fluorescent probes were synthesized by convenient synthetic methods. Secondly, optical properties of these fluorescent probes were investigated in organic medium, in order to test their suitability for screening and imaging the biological cells. Finally, their uptake was examined in the murine osteocytic cell line, MLO-Y4, platelets of blood sample and HEK-293 cells expressing the dopamine transporter (DAT), norepinephrine transporter (NET) or SERT. The fluorescent probes targeting bone-derived cell line expressing 5-HTT provide useful information in understanding the dynamics of 5-HT regulation with respect to SSRI treatment. A novel fluorescent analog of 5-HT probe was developed that may be utilized to study 5-HTT function in the context of 5-HT uptake or regulation in cell culture, tissue explants, or even in vivo.

Acknowledgements

I would like to express my deepest gratitude to my supervisor, Dr. James N. Wilson, who was abundantly helpful and offered invaluable assistance, support, and guidance. I would also like to express my deepest gratitude to the members of the supervisory committee, Professor Angel E. Kaifer and Dr. N. Takenaka, for their constant support and invaluable suggestions regarding my theory courses and research.

I am also thankful to all the faculty members of the Chemistry Department of the University of Miami who have helped me in gaining invaluable knowledge about Chemistry. I am also thankful to all the graduate students who helped me in my study process.

I acknowledge my gratitude to all my former professors for their fruitful guidance and invaluable suggestions concerning my research. I am also thankful to Professors K. Tosney, L. White, and A. Hayward for helping with cellular studies.

Finally, I take this opportunity to express my profound gratitude to my beloved parents for their moral support and patience during my studies.

TABLE OF CONTENTS

LIST OF FIGURES

LIST OF TABLES

Chapter IV

LIST OF SCHEMES

Chapter II

Chapter III

Chapter I

INTRODUCTION TO FLUORESCENT ANALOGS NEUROTRANSMITTER

1.1 Historical perspective of fluorescent probes

Fluorescent probes have been exsensively used for the detection and study of the dynamics of complex biomolecules such as protein, nucleic acids, and peptides and it is also known that these techniques enabled researchers to gain much information, which in turn was used to deal with problems associated with human health. Fluorescence was observed by several chemists such as August Koehler and Carl Reichert, but it was George G. Stokes who coined the term fluorescence in 1852 after his observations of blue luminescence in fluorite.[1] Since then, various fluorescence microscopes have been developed to observe fluorescence in living cells. In 1940, Albert Coon originated the new immunofluorescence field.[2] He used fluorescence labeling techniques to label antidotes with fluorescent dyes.[2] The development of fluorescence techniques carried out a revolution in the field of life science. Fluorescent probes have been used for the screening and imaging of live cells to get information about functions and the dynamics of complex biomolecules.

Electrochemical methods such as amperometry and voltametry can be used to study neurotransmitter release and related processes. But these methods don’t give actual spatial information from where neurotransmitters release. Fluorescent probes are the most efficient and most extensively used methods to address this problem. This method gives spatial information regarding neurotransmitter release at an individual synapse. This probe is mainly based on

fluorescent labeled techniques in which vesicle proteins are tagged with GFP or fluorescent dyes.[3] Fluorescent labeled probes are extensively used to study the uptake and release of neurotransmitters in brain neurons. Fluorescent technology is used routinely as a nondestructive method for detecting and assessing biomolecules in a myriad of basic and applied life science research. Fluorescent probes are the most widely used techniques to address the problems in biophotonic and biomedical fields.[4-7] It is also a powerful tool for in vivo imaging with minimum perturbation of cells under analysis.

The radioactive probes are also commonly used to detect and study the dynamics of biomolecules in intracellular processes. But the fluorescent probe gained a lot of popularity over the radioactive probe because of its low cost and environmental safety. There are two main types of fluorescent probes. One is based on fluorescent labeled biomolecules and the other is based on fluorescent analogs of biomolecules. In a fluorescent labeled probe, fluorophore, or the reactive derivative of fluorophore, is tagged covalently by chemical reactions to biomolecules such as antibody, protein, peptide, DNA, and RNA.[8-13] There are two types of fluorescent labeled probes based on the fluorescent staining technique and molecular tagging technique. In the fluorescent staining technique, chemical fluorophore is used for staining,[14,15] and in the molecular tagging technique, biomolecules are tagged with fluorescent protein such as GFP and YFP.[16] Fluorescence in situ hybridization (FISH) is one of the advanced fluorescent labeled probes based on molecular tagging technique used to study the DNA and RNA sequence on chromosomes in cells and tissues efficiently.[17-19]

FISH is a very specific, fast, and accurate technique if the gene under investigation is known. However, it is very expensive and doesn't work well with an unknown gene. Again, in the FISH probe, GFP which is used for tagging biomolecules, can cause steric and conformational problems in a target biomolecule. Hence, the bulkiness of GFP can alter or restrict the normal functions of biomolecules. These are the major problems of fluorescent labeled techniques.

In the fluorescent analogs probe, a fluorescent molecule analog to the biomolecule is used to study the functions and dynamics of cellular structures. The fluorescent probes based on fluorescent analogs of biomolecules are used to study the neurotransmission process.[20-22] Fluorescent analogs probes are widely used to study enzymatic binding abilities and enzymatic reaction dynamics. For example, the effect of change in the dimension of an enzyme cofactor on enzyme binding and activity was studied by the synthesis of lin-benzoadenosine 5'-triphosphate, 5'-diphosphate, and 3',5'-monophosphate fluorescent "stretched-out" analog of adenine nucleotides.[23] The fluorescent "stretched-out" analog of adenine nucleotide binds strongly and retards enzymatic activity. The fluorescent analogs probe can be used as a substitute for the coenzyme in various reactions. For example, nicotinamide 1, N (6) – etheno adenine dinucleotide was synthesized and used as the fluorescent analog of the coenzyme nicotinamide adenine dinucleotide for different dehydrogenase catalyzed reactions.[24]

Fluorescent analogs probes were also widely used for the study of protein synthesis and nucleic acids. Anthraniloyl-m^{7}GTP (Ant-m^{7}GTP), a fluorescent analog of 7-methylguanosine was designed and synthesized to study the cap binding reaction in protein synthesis.[25] The structure, interactions, and dynamics of nucleic acids have been studied by fluorescent probes which are based on intercalating agent,[26] linker group[27, 28] and fluorescent analog nucleoside.[29, 30] In some cases, intercalating agents have been found to cause severe problems such as unwinding of double strand and changing molecular elasticity. Fluorescent probes based on fluorescent linker groups have also been found to cause problems to the motion of nucleic acid, base sequences and native interactions.[31, 32] Fluorescent probes based on a fluorescent nucleoside analog have been used but they have not caused any problems in motion, winding, molecular elasticity, base sequence, or native interactions of nucleic acids.[33]

1.2 Neurotransmitters and monoamine transporter

Neurotransmitters are the biomolecules, which transmit signals from one neuron to another neuron through the synaptic cleft. Neurotransmitters are synthesized from amino acids in the body and released by the development of electrical potential at the synaptic cleft.[34] In 1921; Otto Loewi predicted that one neuron transmits chemical signals to another neuron through the synaptic cleft, which is about 20 nm to 40 nm, by releasing chemicals which are known as neurotransmitters. Furthermore, Otto Loewi discovered the first neurotransmitter **"**acetylcholine."[35] Neurotransmitters are mainly divided into three: amino acids, peptides, and monoamines. The most prevalent and abundant neurotransmitters

are mainly glutamate and γ-aminobutyric acid (GABA).[35] Neurotransmitters based on monoamines such as norepinephrine (NE), dopamine (DA), and serotonin (SER), are responsible for the major functions of brain nerves. These neurotransmitters are transferred into or out of the presynaptic cleft by transporters, which are known as monoamine transporters (MATs). Monoamine transporters (MATs) are protein structures responsible for the release and reuptake of monoamines in neurons. There are several monoamine transporters (MATs), including the dopamine transporter (DAT), the serotonin transporter (SERT), the norephinephrine transporter (NET). Neurotransmission involves the release of neurotransmitters from the vesicles present in the presynaptic neurons into the synaptic cleft and their subsequent binding to respective postsynaptic neurons. During their reuptake, a specific monoamine transporter transfers these monoamine neurotransmitters back into presynaptic neurons. Reuptake of the neurotransmitter depletes the level of neurotransmitters in the synaptic cleft. Thus, the reuptake depletes the process of neurotransmission. But the monoamine reuptake inhibiter blocks the transfer of the monoamine neurotransmitter into the presynaptic neuron. So in the presence of monoamine reuptake, the inhibiter level of monoamine neurotransmitter increases in the synaptic cleft and therefore enhances the process of neurotransmission. Monoamines and monoamine transporters are fruitful targets for drug discovery. A drug affects the levels of these monoamine neurotransmitters that are present in the synaptic cleft. For example, Prozac, a selective serotonin inhibitor (SSRI)

increases the level of serotonin in a synapse by blocking serotonin transporter (SERT) and therefore it has been used as a potential drug for depression.[36]

1.3 Fluorescent probes for neurotransmitters

Fluorescent analog probes were extensively used for the study of monoamine neurotransmitters. Monoamine neurotransmitters such as serotonin, dopamine, and noradrenalin play a vital role in the central and peripheral part of the human brain system. Monoamine reuptake inhibitors, such as NS2330, drastically affect these monoamine transporters and thus deplete the concentration levels of this monoamine neurotransmitter in various systems, which results in CNS diseases such as Parkinson's disease, Alzheimer disease, and depression. Monoamine transporter modulators have long been used as the first option in the treatment of depression and related diseases and these MATs have been treated as therapeutic targets for these diseases.[37] Although a verity of newly invented antidepressants, such as SSRIs, NARIs, and SNRIs, have fewer side effects than the former tricyclic antidepressant (TCAs), patients' response to medical treatment is low. There is a need to search for a new antidepressant. The mechanism of action of the first generation of tricyclic antidepressant (TCAs) was clear only in 1961 by the discovery of Alexrod.[38] All monoamine reuptake inhibiters have different selectivity but there is no difference in the mechanism of relieving depression. In fact, it has been shown that double and triple monoamine reuptake inhibitors are more powerful than single monoamine reuptake inhibitors with respect to therapeutic response and efficacy in treatment resistant

patients.[39, 40] Recently, nocaine/modafinil hybrid ligands have shown to be an efficient monoamine reuptake inhibiter for all SERT, DAT, and NET.[41]

Although MATs are the fruitful target since a long period in drug discovery process for the treatment of CNS disorder, the screening and imaging technique of neurotransmitters and inhibitors has progressed little because of a lack of high quality functional assays. To address this problem, fluorescent analogs of neurotransmitter probes have recently been developed. Recently, high quality fluorescent assay based on 4-(4-dimethylaminostyryl)-*N*-methyl pyridinium (ASP+) was used for screening and imaging NET inhibiter.[42, 43] Ranwagstaff, et al. have reported robust and throughput functional assay for NET inhibitor using high throughput cellular screening System, fluorometric imaging plate reader (FLIFER^{Tetra}) based on ASP^{+}.[44] Miacrodialysis and electrochemical methods have been used frequently to measure the release of monoamine. But cyclic voltammetry and amperometry have a limitation in measurements as these methods have poor spatial resolution in the brain.[45] To offer a solution to this problem, an optical tracer based on a “fluorescent false neurotransmitter (FFN)” has been recently designed to directly measure directly monoamine uptake, redistribution, and release.[46] P^{H} sensitive FFN probe, which act as a false neurotransmitter for VMAT was introduced by Dalibar Sames, et al.[47]

Fluorescent probes based on stilbazone dyes which are very specific for NET have also been reported recently.[48] The level of 5-HT is controlled by 5-HTT and SSRI affect this 5-HTT in depression and depression related diseases. The study of 5-HT uptake is mainly concerned with drug discovery for depression and

related diseases. The fluorescent probe analog of 5-HT has been reported to study 5-HT uptake process.[49] Fluorescent analog probes are potentially useful in understanding the molecular mechanism of neurotransmitters with less or no perturbation in the cellular process.

1.4 Approach to design fluorescent analogs neurotransmitters

Fluorescent substrates that closely mimic biogenic amino neurotransmitters with respect to structure and properties can act as fluorescent analogs neurotransmitters. Biogenic amino neurotransmitters, as shown in following **Figure 1.1,** have an aromatic core part and amino side chain.

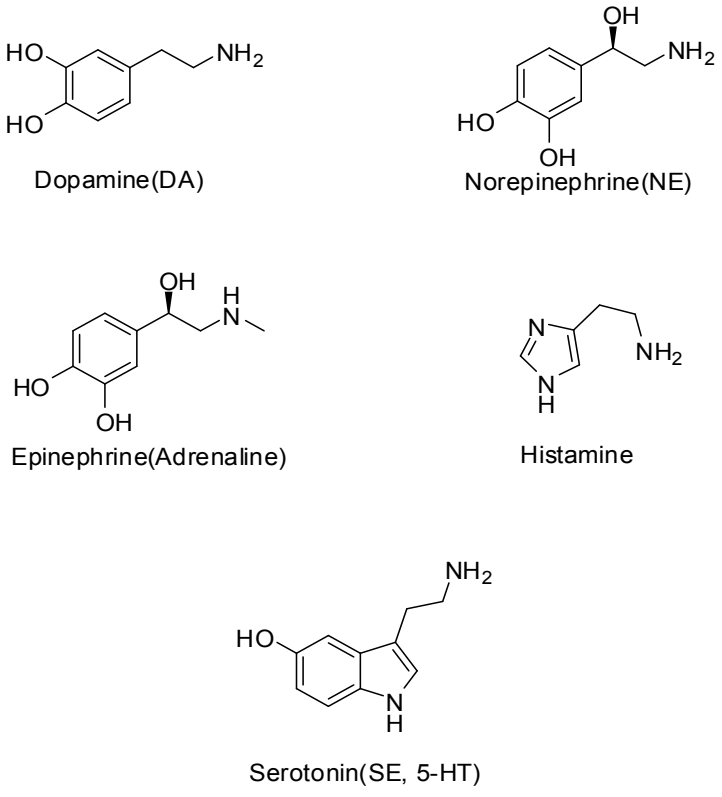

Figure 1.1: Structures of Monoamine Neurotransmitters

The natural monoamine neurotransmitter in protonated form consists of an aromatic core part and cationic part as shown in following **Figure 1.2**.

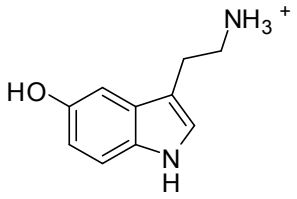

Serotonin (5-HTH$^+$)

Figure 1.2: Protonated 5-HT

Neurotransmitters bind to the transporter through their cationic portion. Success in designing a fluorescent analog neurotransmitter relies on the optical properties of the substrate and its ability to get into the cell. An ideal fluorescent analog neurotransmitter must have a high quantum yield, a higher absorption wavelength, and must be taken into the cell through a specific transporter easily.

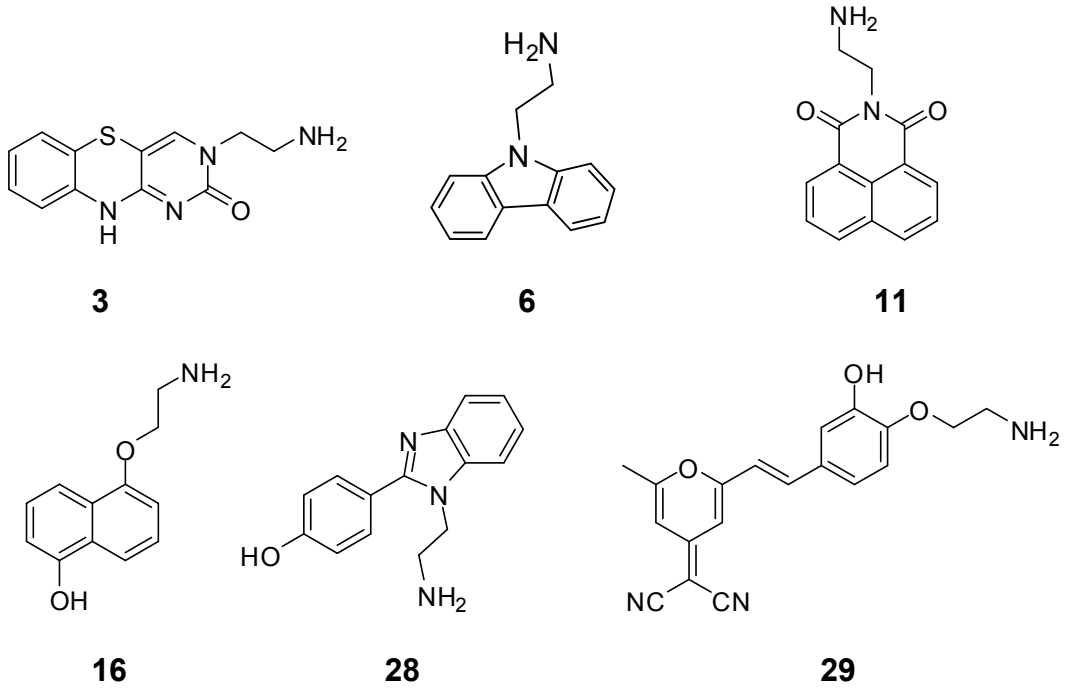

3 **6** **11**

16 **28** **29**

Figure 1.3: Structures of some possible probes

For imaging by confocal microscopy, fluorescent substrate should possess an absorption maximum above 405 nm and it should produce a bright image. The

following possible substrates **1** to **6** as shown in **Figure 1.3** could work as fluorescent analog neurotransmitters.

Based on the above possible substrates, a set of ethyl amine-functionalized fluorescent probes were synthesized and their optical properties were studied. Their uptake was examined in the murine osteocytic cell line, MLO-Y4 expressing SERT and HEK-293 cells expressing SERT, NET, and DAT. Their uptake was also examined in platelets expressing SERT in blood samples.

Chapter II

SYNTHESIS OF FLUORESCENT PROBES

The enormous interest in the development of chemical systems, such as fluorescent probes, in understanding the molecular mechanism of the neurotransmitter system and its significant importance in drug discovery has driven researchers to design and synthesis chemical substrates that have attractive optical properties. The detailed study of the serotonergic pathway is extremely important in investigating molecular mechanisms responsible for depression and related diseases.

2.1 Probe designing strategies

In our research, a series of ethylamine-functionalized fluorescent probes as shown in **Figure 2.1** were designed and synthesized to investigate the molecular mechanism of the serotonergic system. Probe **3** is based on the tricyclic cytosine core. The tricyclic cytosine is a fluorescent compound with attractive optical properties. Because of its unique fluorescent properties, its ethylamino functionalized fluorescent probe **3** was designed which mimics the fluorescent analog of 5-HT. Probes **6** and **9** are based on carbazole and the carbazole analog cores respectively. A large number of carbazole and carbazole derivatives have been designed and synthesized for the development of electro luminescent materials because of their excellent optical and electrical properties.

Carbazole and carbazole derivatives are known to emit blue, green and orange-red light. Because of their tunable optical properties with synthetic modifications, these compounds would be of great interest in screening and imaging techniques in cellular study.

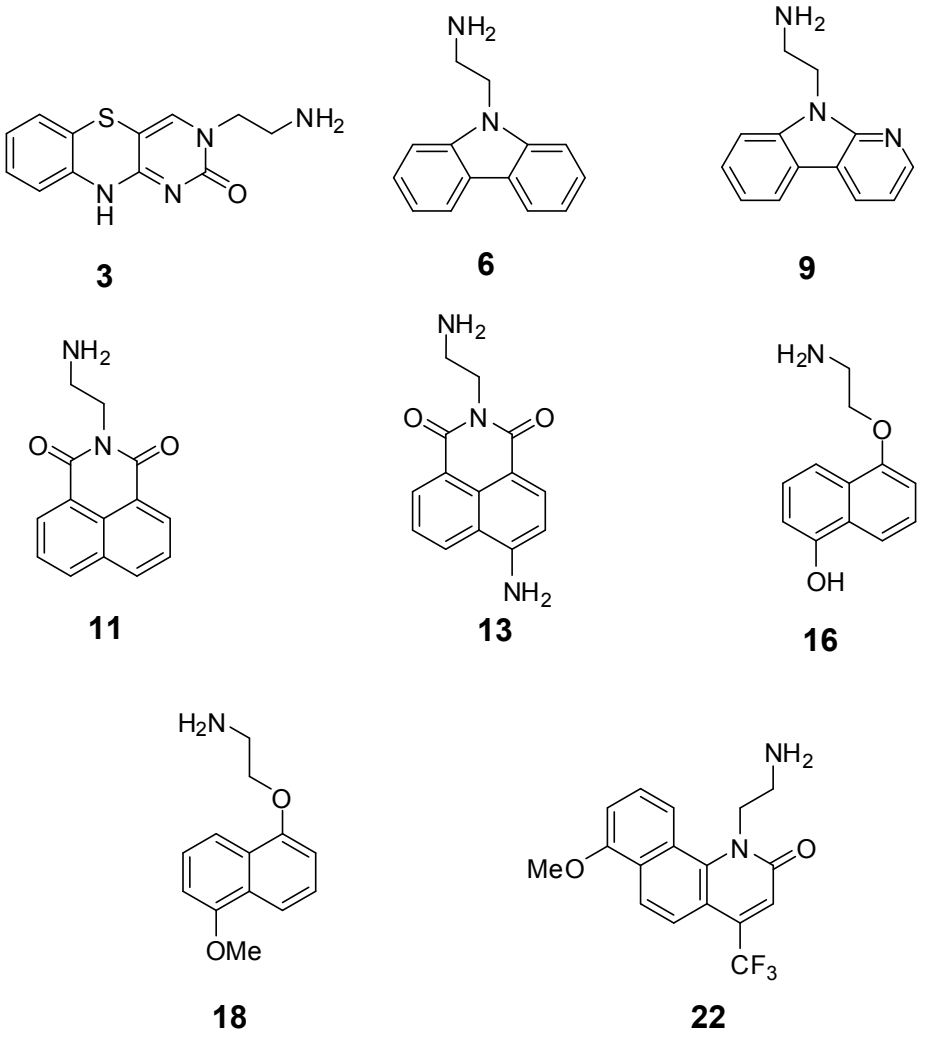

Figure 2.1: Structures of fluorescent probes

Probes **6** and **9** based on the carbazole core unit were designed and evaluated their optical properties for screening and imaging the cells to study the serotonergic system. The probes **11** and **13** are based on the naphthyl amide

(NI) core. Naphthyl imides have been used as fluorophore in the development of selective chemo sensors for biological and clinical applications because of their high sensitivity and selectivity.[50] Fluorescent Troger's bases, which were derived from 4-amino-1, 8-naphthyl imides, have been used to study bimolecular binding properties.[51] Again, their easy one-step synthesis and interesting optical properties have driven us to design ethylamino-functionalised naphthyl imide fluorescent probes **11** and **13**. Probes **16** and **18** are based on Naphthalene core. Naphthalene chromophore is of great value because of its interesting and potentially useful optical properties in the development of novel chemo sensors. For example, polyamidoamine (PAMAM) sensors have been developed recently which are based on the naphthalene chromophore core.[52] So probes **16** and **18** were designed to study neurotransmitter receptor and transporter systems. Probe **22** was designed around a carbostyril core. Carbostyril and its related compounds have been used for the investigation of the molecular mechanism of the neurotransmission process in the central nervous system. These compounds are interesting and potentially useful as novel antipsychotic agents for the excessive neurotransmission activity caused by a psychosis disease, such as Schizophrenia.[53]

2.2 Convenient synthetic routes

Tricyclic cytosine base **1** was synthesized according to the reported procedure.[54] Compound **1** was reacted with 1.2 equivalent of 2-azidoethyl tosylate in DMF with oven dry K_2CO_3 as base to obtain an intermediate **2**. This

intermediate **2** on reduction with PMe_3 in wet THF afforded aminoethyl functionalized tricyclic compound 3 as shown in the **Scheme 2.1**.

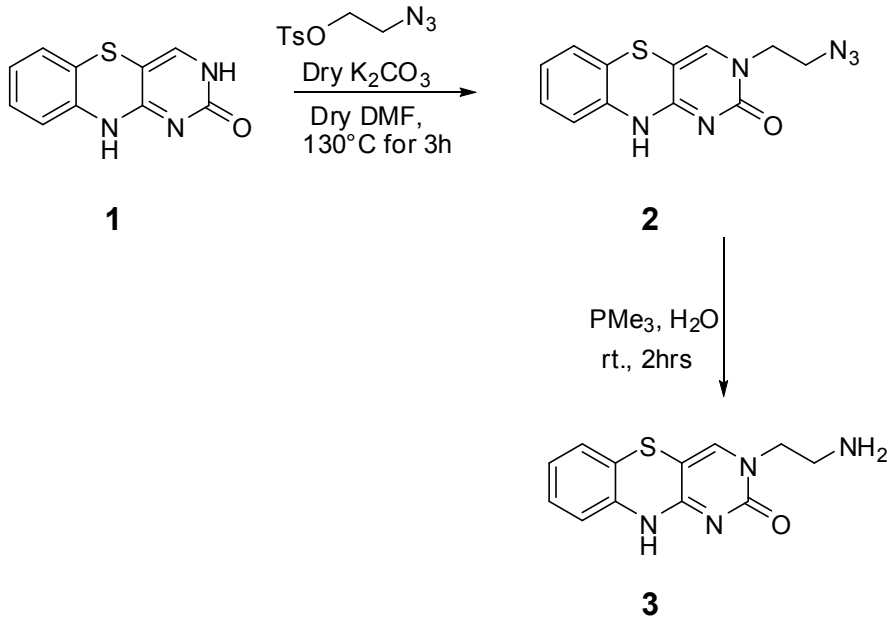

Scheme 2.1: Synthetic route for **3**

Probes **6**, **9**, **16**, and **18** were synthesized by following a similar route. Probes **6** and **9** were synthesized by similar alkylation with 1.2 equivalents of 2-azidoethyl tosylate followed by reduction with PMe_3 as described for 3. Compounds **11** and **13** were synthesized by a simple one-step condensation of ethylene diamine with Naphthyl anhydrides **10** and **12** respectively at 120^0C in 4 hours. Probe**16** was synthesized by similar alkylation of **14** with 1 equivalent of 2-azidoethyl tosylate followed by reduction with PMe_3 as described for **3** as shown in **Scheme 2.1.** Compound **14** on alkylation afforded both monoalkylated product as well as dialkylated product. Monoalkylated product **15** was separated by column chromatography from the dialkylated product and reduced to get **16**.

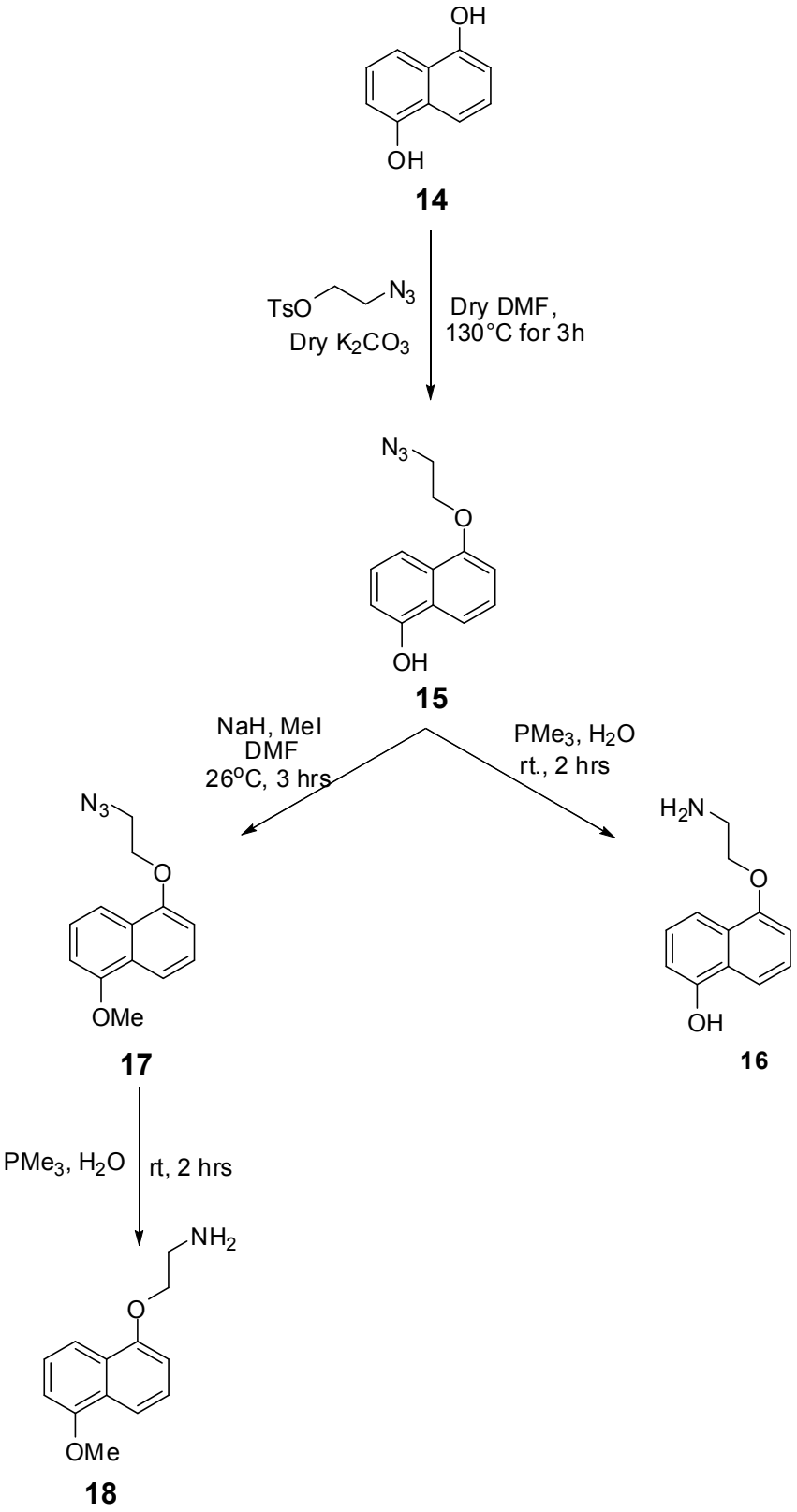

Scheme 2.2: Synthetic routes for **16** and **18**

Probe **18** was synthesized by methylation of **15** with MeI in DMF with NaH as base followed by reduction with PMe_3 as shown in the **Scheme 2**. Probe **22** was synthesized from carbostyril **20**. Compound **19** was reacted in an open flask with Ethyl - 3, 3, 3-trifluoro-2-oxopropanoate at 100^0C and the residual oil obtained was treated with 75% H_2SO_4 to get cyclic product **20**. The cyclic carbostyril **20** was reacted with 1.2 equivalent of 2-azido ethyl tosylate in DMF with dry K_2CO_3 as a base afforded azido intermediate **21**. The azide intermediate **20** on reduction with PMe_3 in wet THF afforded **22** as described in the **Scheme 2.3.**

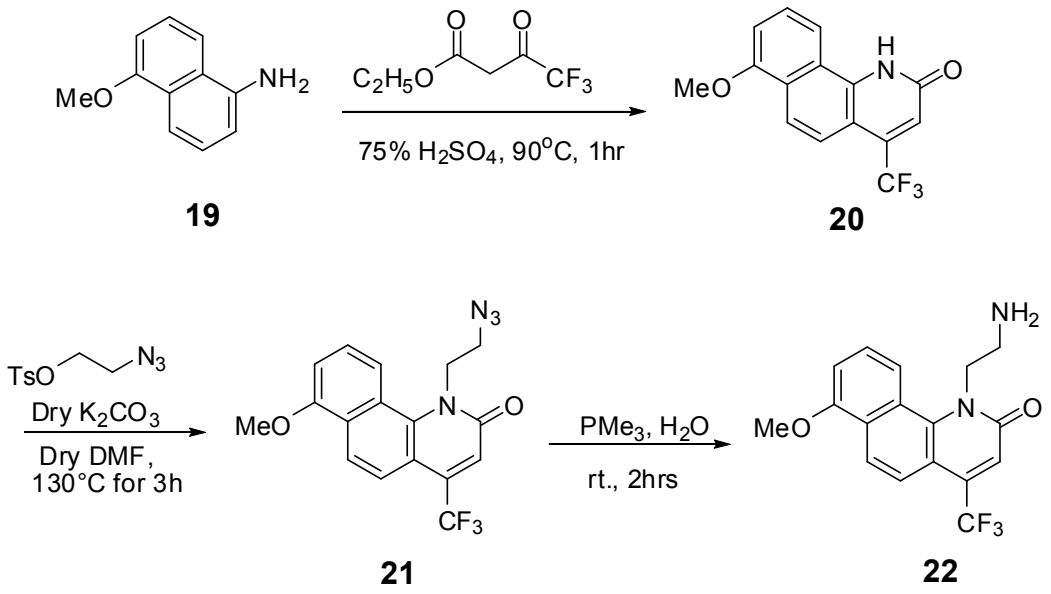

Scheme 2.3: Synthetic route for **22**

All compounds are freely soluble in the methanol solvent except **3**, **16,** and **18,** which are soluble at very low concentration (< 50μM) in methanol.

The synthesis of some of the exciting probes as shown in the following **Figure 2.2** was tried but later discontinued because of problems encountered in synthesis and optical properties.

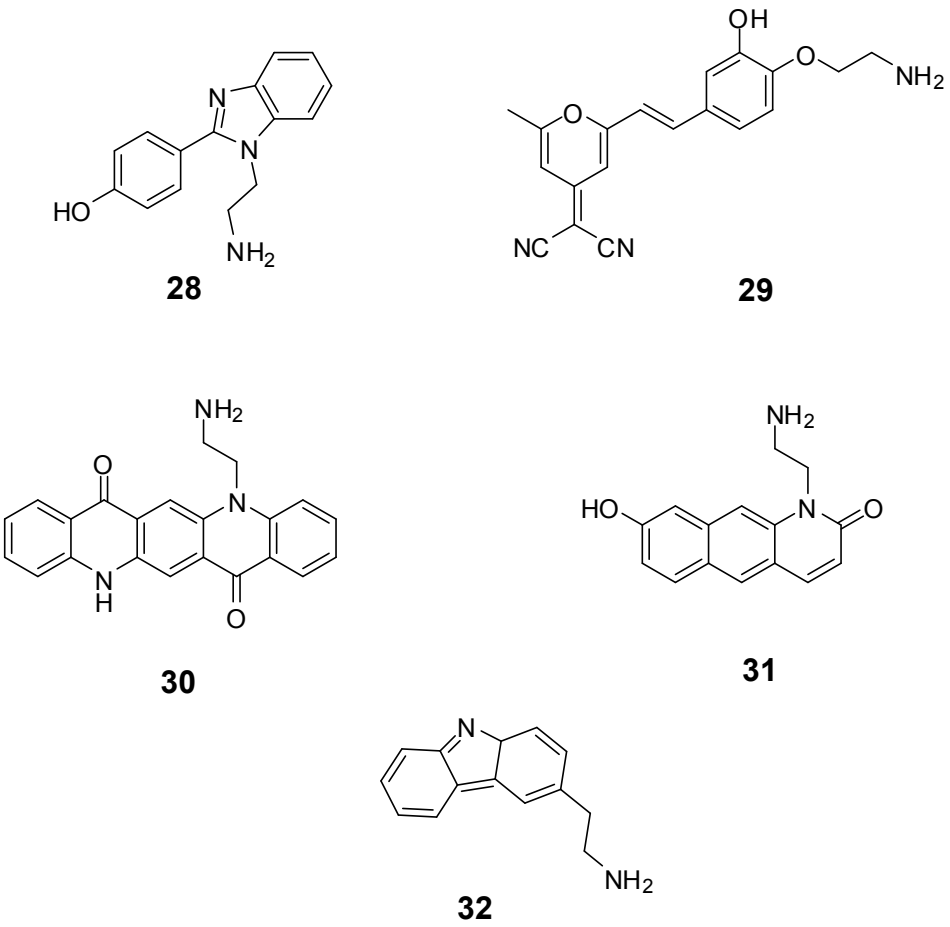

Figure 2.2: Some challenging fluorescent probes.

Chapter III

EXPERIMENTAL SYNTHESIS AND SPECTRAL CHARACTERIZATIONS

Materials and the methods: All chemicals including reactants, reagents, and solvents obtained from commercial suppliers such as Aldrich, sigma Aldrich, Fluka, and Alfa Asser were used as such without further purification. All reactions were carried out in dry conditions under an argon atmosphere with oven dry glass wares. NMR chemical shifts are given in ppm and coupling constants (J) are given in Hz. Column chromatography for purification was performed on a Biotag isolera machine with silica gel C-200.

3.1. 1, 3-diaza-2-oxophenothiazine (1)

Compound **1** was synthesised according to the reported procedure.[55]

3.2. 2-(2-azidoethyl)-2H-benzo[b]pyrido[4,3-e][1,4]thiazine-3(5H)-one(2)

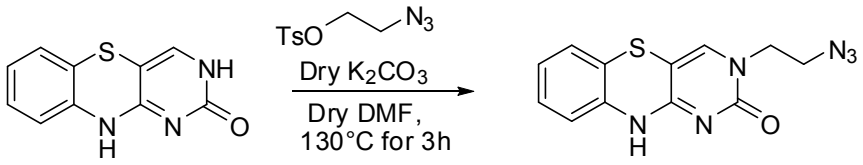

1 **2**

Scheme 3.1: Synthetic route for **2**

1,3-diaza-2-oxophenothiazine **1** (1 g, 4.6 mmol) was placed in a round bottom flask charged with a stir bar, 2-azidoethyl tosylate (1.3 g, 5.24 mmol) and oven dried K_2CO_3 (1.36 g, 10.0 mmol). DMF, as sufficient to allow the slurry to stir (~15 mL), was added and the reaction mixture was stirred at 130°C for 3 hours.

After cooling, the reaction was poured into water and extracted three times with ~50 mL of CH_2Cl_2. TLC indicated the presence of both major mono o-alkylated **2** and minor di o-alkylated intermediates in the organic layer. These were separated on a Biotage Isolera (25 g silica column with CH_2Cl_2 and MeOH). Yield (**2** only): 850 mg, 65%.

^{1}H NMR ($CDCl_3$, 400 MHz): δ_{ppm}: 3.55 (t, J = 5.6 Hz, 2H), 3.77 (t, J = 5.4 Hz, 2H), 6.80 (m, 1H), 6.84 (m, 2H), 6.93 (m, 1H), 7.11 (s, 1H).

^{13}C NMR ($CDCl_3$, 100.57 MHz): $\delta_{ppm:}$ 52.4, 52.7, 100.7, 119.2, 120.1, 127.6, 129.0, 130.5, 138.7, 142.1, 159.5, and 163.7.

MS (FAB+) Calculated 284, Found: 285 ($M + H^+$).

IR (cm^{-1}): 3266.7, 2966.8, 2409, 2139, 2098.3, 1625.9, 1464.7, 1445.4, 1333.1, 1291.6, 1231, 985.2, 773.9, 745.25, 727.2.

M.P. (1 atom.): 197^0C

3.3. 2-(2-aminoethyl)-2H-benzo [b] pyrido [4,3-e] [1,4] thiazine-3(5H)-one (3):

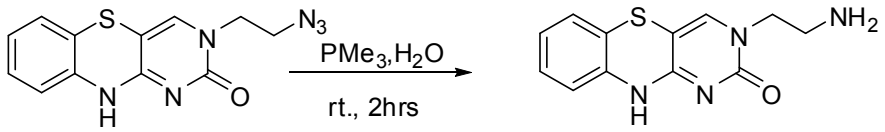

2 **3**

Scheme 3.2: Synthetic route for **3**

A round bottom flask was charged with **2** (500 mg, 1.75 mmol) and a stir bar. It was evacuated and filled with argon and then capped with a septum. Argon-purged THF (~ 5 mL) was added and the reactant was allowed to dissolve. A 1.0 M solution of PMe_3 (2.5 mL) was slowly added and vigorous bubbling was

observed. Argon-purged H_2O (1 mL) was then added and the reaction was allowed to proceed for 2 hours. Solvent, excess PMe_3, H_2O and $POMe_3$ were removed by vacuum distillation. The column purification was performed on a Biotage Isolera (10 g silica column with CH_2Cl_2 and MeOH). Yield: 299 mg, 66%.

^{1}H NMR ($CDCl_3$+MeOD, 400 MHz): δ_{ppm} 3.00 (t, J = 5.0 Hz, 2H), 3.38 (s, broad, 2H), 4.28 (t, J = 5.1 Hz, 2H), 6.72 (d, J = 8 Hz, 1H), 6.88 (m, 2H), 6.99(m, 1H), 7.58(s, 1H).

^{13}C NMR (DMSO, 100.57 MHz): δ_{ppm} 60.7, 69.9, 103.4, 116.8, 116.9, 124.7, 127.1, 128.5, 138.8, 152.5, 160.5, 164.6.

MS (FAB+) Calculated: 260, Found: 261 (M + H^+).

HRMS (ESI+) Calculated: 261.0805 (M + H^+), Found: 261.0814 (M + H^+).

IR (cm^{-1}): 3413.7, 3335.7, 3191.7, 2873.8, 1598.58, 1578.22, 1557.55, 1528.75, 1484.28, 1467.54, 1418.80, 1375.09, 1294.66, 1258.72, 1132.3, 774.6, 736.2.

M.P. (1 atom.): 173^0C

3.4 9-(2-azidoethyl)-9H-carbazole(5)

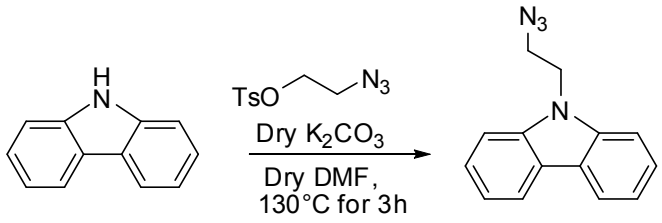

4 **5**

Scheme 3.3: Synthetic route for **5**

Product **5** was obtained from the reaction of **4** (500 mg, 2.97 mmol) and 2-azidoethyl tosylate (0.86 g, 3.5 mmol) according to the method described for the preparation of **2**. Yield: 585 mg, 82.9%.

^{1}H NMR ($CDCl_3$, 400 MHz): δ_{ppm} 3.62 (t, J = 6.0 Hz, 2H), 4.34 (t, J = 5.9 Hz, 2H), 7.60 (m, 4H), 7.74 (m, 2H), 8.37 (d, J = 7.0 Hz, 2H).

^{13}C NMR ($CDCl_3$, 100.57 MHz): δ_{ppm} 42.6, 50.3, 111.37(2C), 121.18(2C), 121.6(2C), 123.8 (2C), 126.6(2C), 140.8(2C).

MS (ESI+) Calculated: 237.1135 ($M + H^+$), Found: 237.1135 ($M + H^+$).

IR (cm^{-1}): 2929, 2108.7, 2081.6, 1592, 1507.8, 1453.7, 1408.6, 1336.5, 1267.4, 1237.4, 1084.1, 1066.1, 997.2, 939.9, 774.6, 747.6, 726.6.

M.P. (1 atom.): 66^0C

3.5 9-(2-aminoethyl)-9H-carbazole(6)

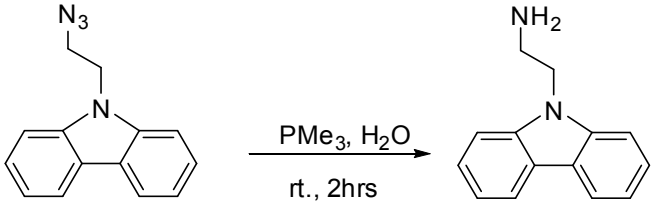

5 **6**

Scheme 3.4: Synthetic route for **6**

Product **6** was obtained from the reaction of **5** (200 mg, 0.84 mmol) and 1.0 M solution of PMe_3 according to the method described for the preparation of **3**. Yield: 134mg, 75.3%.

^{1}H NMR ($CDCl_3$, 400 MHz): δ_{ppm} 8.17 (d, J = 7.8 Hz, 2H), 7.51 (t, J = 8.2 Hz, 2H), 7.42 (d, J = 8.2 Hz, 2H), 7.32 (t, J = 8.4 Hz, 2H), 4.22 (t, J = 6.1 Hz, 2H), 3.05 (t, J = 6.1 Hz, 2H), 1.27 (s, broad, 2H).

^{13}C NMR ($CDCl_3$, 100.57 MHz): δ_{ppm} 42.0, 46.1, 109.4, 119.9, 120.5, 123.4, 126.0, 141.1.

MS (ESI+) Calculated: 210.1157(M + H^+), Found: 251.1562 (M+ acetone adduct).

IR (cm^{-1}): 3349.5, 3160.2, 3049, 2929, 1595, 1483.7, 1450.7, 1342.5, 1324.5, 1303.5, 1240.4, 1174.3, 1150.2, 1126.2, 1036, 900.87, 750.6, 720.6.

M.P. (1 atom.): 98-107^{0}C

3.6. 9-(2-azidoethyl)-9*H*-pyrido [2, 3-*b*] indole (8)

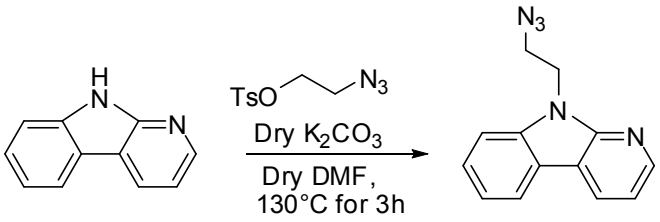

7 **8**

Scheme 3.5: Synthetic route for **8**

Product **8** was obtained from the reaction of **7** (500 mg, 2.98 mmol) and 2-azidoethyl tosylate (0.86 g, 3.5 mmol) according to the method described for the preparation of **2**. Yield: 549 mg, 79%.

^{1}H NMR ($CDCl_3$, 300 MHz): δ_{ppm} 2.81 (m, 2H), 3.61 (m, 2H), 6.21 (dd, J = 4.8 Hz, 2.2 Hz, 1H), 6.35 (t, 7.4 Hz, 1H), 6.54 (m, 2H), 7.09 (d, J = 7.5 Hz, 1H), 7.30 (d, J = 7.5Hz, 1H), 7.57 (d, J = 12.6 Hz, 1H).

^{13}C NMR ($CDCl_3$, 100.57 MHz): δ_{ppm} 41.90, 50.37, 109.52, 115.92, 118.46, 120.54, 120.59, 121.55, 127.32, 128.61, 139.89, 146.26, 151.72.

MS (ESI+) Calculated: 238.1087 ($M + H^+$), Found: 238.1087 ($M + H^+$).

IR (cm^{-1}): 3061, 2941, 2096.7, 1625, 1589, 1573.9, 1486.7, 1465.7, 1417.6, 1348.5, 1291.5, 1207.3, 1123.2, 997.02, 774.6, 735.6.

3.7. 2-(9*H*-pyrido [2, 3-*b*] indol-9-yl) ethanamine (9)

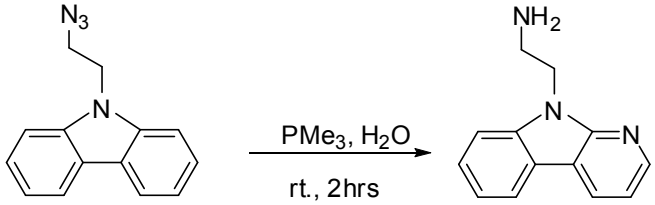

8 **9**

Scheme 3.6: Synthetic route for **9**

Product **9** was obtained from the reaction of **8** (200 mg, 0.85 mmol) and 1.0 M solution of PMe_3 according to the method described for the preparation of **3**. Yield: 138 mg, 78%

^{1}H NMR($CDCl_3$,300 MHz): δ_{ppm} 1.42 (s, broad, 2H), 3.14 (t, J = 6.2Hz, 2H), 4.44 (t, J = 6.3 Hz, 2H), 7.08 (d, J = 4.9 Hz, 1H), 7.22 (t, J = 4.8 Hz, 1H), 7.43 (m, 2H), 7.96 (d, J = 7.1 Hz, 1H), 8.20 (d, J = 6.0 Hz, 1H), 8.44 (d, J = 4.9Hz, 1H).

^{13}C NMR ($CDCl_3$, 100 MHz): δ_{ppm} 42.07, 45.15, 109.66, 115.21, 116.14, 120.39, 120.77, 121.42, 127.09, 128.44, 140.05, 146.34, 152.13.

HRMS (ESI+) Calculated: 212.1182 ($M + H^+$), Found: 212.1196 ($M + H^+$).

IR (cm^{-1}): 3367.6, 3283.4, 3052, 2919.9, 1592, 1573.9, 1483.7, 1417.6, 1333.5, 1297.5, 1228.4, 1120.2, 1000, 921, 840.7, 771.6, 741.6.

3.8. 2-(2-aminoethyl)-1H-benzo [de]isoquinoline-1, 3(2H)-dione (11)

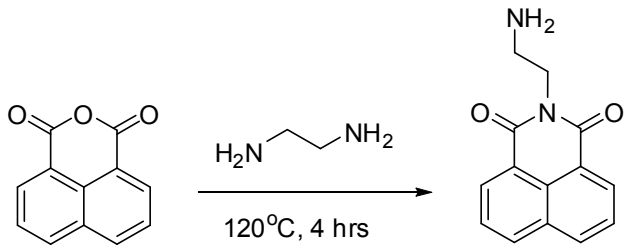

10 **11**

Scheme 3.7: Synthetic route for **11**

A pressure tube was charged with **10** (100 mg, 0.50 mmol), Ethyldiamine (3ml), and a stir bar. The reaction mixture was heated to 120°Cfor 4 hours. After cooling, the excess ethyldiamine was removed by vacuum distillation. The resultant mixture was purified to get **11**, on a Biotage Isolera (25 g silica column with CH_2Cl_2 and MeOH). Yield: 90 mg, 78%.

^{1}H NMR (MeOH, 400 MHz): δ_{ppm} 2.73 (t, J = 6.6 Hz, 2H), 4.10 (t, J = 6.6 Hz, 2H), 7.58 (t, J = 7.6 Hz, 2H), 8.07 (d, J = 8.0 Hz, 2H), 8.24 (d, J = 7.1Hz, 2H).

^{13}C NMR (MeOH, 100.57 MHz): δ_{ppm} 39.88, 42.43, 122.29 (2C), 126.87, 126.97, 127.86, 130.82, 130.87, 131.75, 134.21(2C), 164.56(2C).

MS (FAB+) Calculated: 240, Found: 241 ($M + H^+$).

IR (cm^{-1}): 3343.5, 3325.5, 2956, 2922.9, 2862.8, 2496.3, 1700, 1661, 1589, 1435.7, 1237.4, 1054.1, 846.8, 777.7.

M.P. (1 atom.): 138°C

3.9.6-amino-2-(2-aminoethyl)-1H-benzo[de]isoquinoline-1,3(2H)-dione (13)

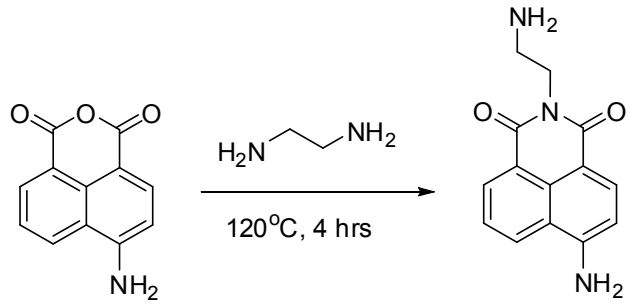

12 **13**

Scheme 3.8: Synthetic route for **13**

A pressure tube was charged with **12** (100 mg, 0.47 mmol), Ethyldiamine (3ml), and a stir bar. The reaction mixture was heated to 120°Cfor 4 hours. After cooling, the excess ethyldiamine was removed by vacuum distillation. The resultant mixture was purified to get **13**, on a Biotage Isolera (25 g silica column with CH_2Cl_2 and MeOH) Yield: 83 mg, 69%.

^{1}H NMR (DMSO, 400 MHz) δ_{ppm} 2.73 (t, J = 7.0 Hz, 2H), 4.00 (t, J = 6.1 Hz, 2H), 6.82 (dd, J = 8.4 Hz, 5.6 Hz, 2H), 7.41 (s, 2H), 7.63 (dd, J = 8.3 Hz, 7.3 Hz, 2H), 8.17 (dd, J = 8.3 Hz, 5.5 Hz, 2H), 8.41 (m, 2H), 8.59 (dd, J = 7.4Hz, 4.6Hz, 2H).

^{13}C NMR (DMSO, 100.57 MHz): δ_{ppm} 39.69, 43.05, 108.48, 108.95, 120.16, 122.68, 124.70, 130.02, 130.53, 131.72, 134.68, 153.47, 163.95, 164.82.

HRMS (ESI+) Calculated: 256.1081 ($M + H^+$), Found: 256.1093 ($M + H^+$).

M.P. (1 atom.): 171^{0}C

3.10. 5-(2-azidoethoxy) naphthalene-1-ol (15)

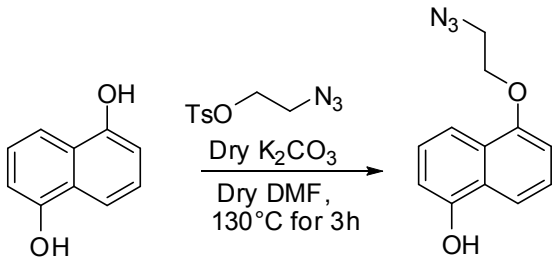

14 **15**

Scheme 3.9: Synthetic route for **15**

Product **15** was obtained along with a minor dialkylated compound from the reaction of **14** (1 g, 6.25 mmol) and 2-azidoethyl tosylate (1.6 g, 6.45 mmol) according to the method of the preparation of **2**. Yield: 800 mg, 57%.

^{1}H NMR ($CDCl_3$, 400 MHz): δ_{ppm} 3.72 (t, J = 4.6 Hz, 2H), 4.28 (t, J = 4.6 Hz, 2H), 5.23 (s, broad, 1H), 6.83 (dd, J = 12.5 Hz, 7.6 Hz, 2H), 7.39 (m, 2H), 7.79 (dd, J = 8.48 Hz, 0.56 Hz, 1H), 7.88 (d, J = 8.52 Hz, 0.68 Hz, 1H).

^{13}C NMR ($CDCl_3$, 100.57 MHz): δ_{ppm} 50.9, 67.6, 105.7, 109.9, 114.9, 115.1, 125.4, 125.8, 127.2, 151.5, 154.4(2C).

MS (FAB+) Calculated: 229, Found: 229(M +), 230(M + H^+).

IR (cm^{-1}): 3280.4, 2938, 2102.7, 2087.6, 2063.6, 1598, 1525.8, 1417.6, 1372.6, 1267.4, 1246.4, 1210.3, 1162.3, 1060.1, 954.6, 882.85, 852.8, 831.7, 774.6, 699.5.

M.P. (1 atom.): 145^0C

3.11. 5-(2-aminoethoxy) naphthalene-1-ol (16)

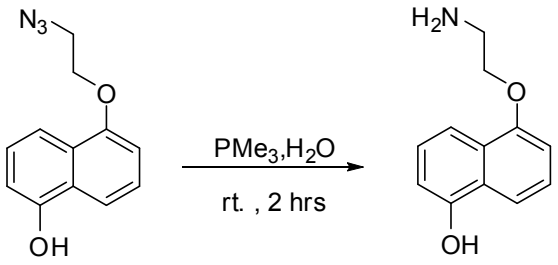

15 **16**

Scheme 3.10: Synthetic route for **16**

Product **16** was obtained from the reaction of **15** (500 mg, 2.84 mmol) and 1.0 M solution of PMe_3 according to the method described for the preparation of **3**.

Yield: 354 mg, 80%.

^{1}H NMR (DMSO, 400 MHz): δ_{ppm} 3.02 (t, J = 5.4 Hz, 2H), 4.07 (t, J = 5.3 Hz, 2H), 4.74 (s, broad, 2H), 6.89 (t, J = 7.1Hz, 2H), 7.29 (m, 2H), 7.69 (m, 2H).

^{13}C NMR (DMSO, 100.57 MHz): δ_{ppm} 41.84, 71.3, 106.14, 109.58, 112.96, 115.02, 125.36, 126.37, 126.54, 127.32.

HRMS (ESI+) Calculated: 204.1019 ($M + H^+$), Found: 204.1031($M + H^+$).

IR (cm^{-1}): 3346.5, 3289.4, 2956, 2916.9, 2865.8, 1592, 1519.8, 1465.7, 1408.6, 1366.6, 1276.4, 1255.4, 1015, 777.7.

M.P. (1 atom.): 181^{0}C

3.12. 1-(2-azidoethoxy)-5-methoxynaphthalene (17)

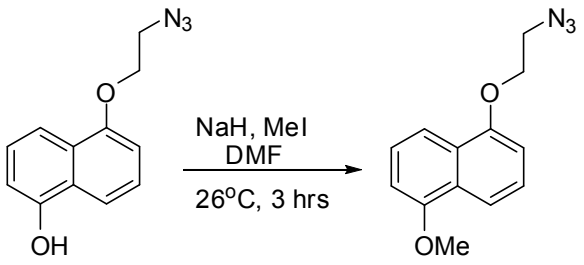

16 **17**

Scheme 3.11: Synthetic route for **17**

Compound **16** (285 mg, 1.24 mmol) was placed in a round bottom flask charged with a stir bar and dry NaH (60 mg, 2.5 mmol). DMF, as sufficient to allow the slurry to stir (~20 mol), was added. Then MI (0.4 ml, 6.42 mmol) solution in DMF was added slowly maintaining the temperature below 25^{O}C. The reaction mixture was stirred at room temperature for 5 hours. Product **17** was precipitated out from water and was recrystalized with DCM and methanol. Yield: 239 mg, 79%.

^{1}H NMR ($CDCl_3$, 400 MHz): δ_{ppm} 3.02 (t, J = 4.6 Hz, 2H), 4.02 (s, 3H), 4.31 (t, J = 4.6 Hz, 2H), 6.84 (dd, J = 17.6 Hz, 7.5Hz, 2H), 7.38 (m, 2H), 7.90 (t, J = 8.3 Hz, 2H).

^{13}C NMR ($CDCl_3$, 100.57 MHz) δ_{ppm} 50.93, 55.96, 67.62, 105.09, 105.86, 114.64, 115.43, 25.35, 125.93, 126.90, 127.11, 154.28, 155.61.

MS (FAB+) Calculated: 243, Found: 243(M +).

IR (cm^{-1}): 2944, 2108.7, 2081.6, 2066.6, 1592, 1507.8, 1408.6, 1375.6, 1264.4, 1237.4, 1213.3, 1084.1, 1069.1, 1030, 942.9, 861.8, 834.7, 774.6.

M.P. (1 atm.): 107^{0}C

3.13. 2-(5-methoxynaphthalen-1-yloxy) ethanamine (18)

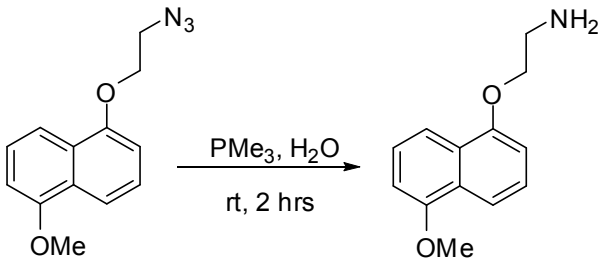

17 **18**

Scheme 3.12: Synthetic route for **18**

Product **18** was obtained from the reaction of **17** (200 mg, 0.84 mmol) and 1.0 M solution of PMe_3 according to the method described for the preparation of **3**.

Yield: 147 mg, 81%.

^{1}H NMR (MeOH, 300 MHz): δ_{ppm} 3.33 (t, J = 4.8 Hz, 2H), 3.97 (s, 3H), 4.28 (t, J = 7.5 Hz, 2H), 6.93 (t, J = 7.3 Hz, 2H), 7.38 (m, 2H), 7.83 (d, J = 8.5 Hz, 1H), 7.90 (d, J = 9.1 Hz, 1H).

^{13}C NMR (MeOH, 100.57 MHz): δ_{ppm} 40.04, 55.03, 66.87, 104.67, 105.81, 114.09, 114.90, 125.05, 125.39, 126.80, 126.96, 154.227, 155.58.

MS (ESI+) Calculated: 218.1176 ($M + H^+$), Found: 218.1176 ($M + H^+$).

IR (cm^{-1}): 3370.6, 2941, 1595, 1510.8, 1408.6, 1267.4, 1213.3, 1042, 783.7.

M.P. (1 atom.): 152^{0}C

3.14.7-methoxy-4-(trifluoromethyl)-6,10b-dihydrobenzo[*h*]quinolin-2(1*H*)-one(20)

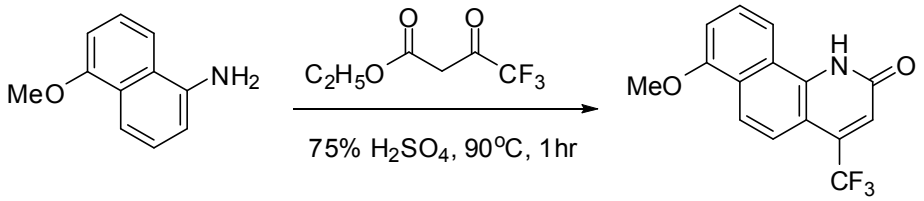

19 **20**

Scheme 3.13: Synthetic route for **20**

Ethyl 3, 3, 3-trifluoro-2-oxopropanoate (8 g, 43.4mmol) was heated in an open flask with the the primary 5-methoxy-1, 4-dihydronaphthalen-1-amine **19** (3.5 g, 20.3mmol.) for 30 minutes. The contents of the flask were stirred occasionally to facilitate the removal of alcohol formed, and heating was continued under argon flow for another 30 minutes at a temperature of 100^{O}C to remove the excess ester. On cooling the mixture, a dark liquid formed. The residual oil, representing the corresponding 3-oxonaphthalene carboxamide, was not crystallized, but used directly for the ring closure. To this oil, 75% H_2SO_4 was added, and the mixture was heated carefully to 90 ^{O}C for 40 minutes and was cooled to room temperature and poured into ice H_2O. The precipitate of **20** formed was isolated and finally recrystallized from methanol. Yield: 3.32 g, 56%.

^{1}H NMR (DMSO, 400 MHz): δ_{ppm} 0.91 (s, broad, 1H), 4.00 (s, 3H), 7.24 (s, 1H), 7.22 (d, J = 7.7 Hz, 1H), 7.64 (t, J = 8.0Hz, 1H), 8.01 (d, J = 8.8 Hz, 1H), 7.58 (d, J = 8.5 Hz, 1H).

^{13}C NMR: Not obtained.

HRMS (ESI+): Not Obtained.

IR (cm^{-1}): 3027.8, 1664.6, 1628.9, 1588.8, 1516.5, 1426.02, 1397.3, 1373.9, 1135.2, 1071.7, 1026.5, 882.7, 700.47, 683.6.

3.15.1-(2-azidoethyl)–7–methoxy–4-(trifluoromethyl)-6,10b–dihydrobenzo [*h*] quinolin-2(1*H*)-one (21)

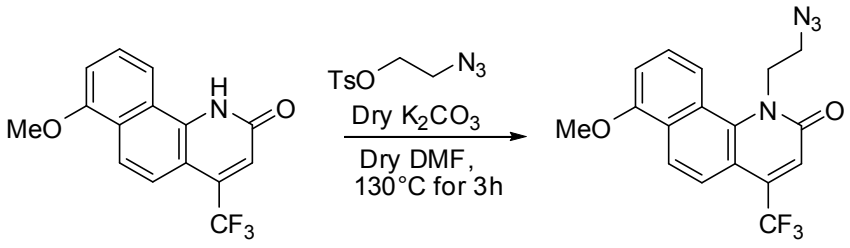

20 **21**

Scheme 3.14: Synthetic route for **21**

Product **21** was obtained from the reaction of **20** (1.32 g, 5.88 mmol) and 2-azidoethyl tosylate (1.5 g, 6.23 mmol) according to the method described for the preparation of **2**. Yield: 896 mg, 55%.

^{1}H NMR(DMSO,400 MHz): δ_{ppm} 3.84 (t, J = 4.4 Hz, 2H), 4.07 (s, 3H), 4.81(t, J = 4.2 Hz, 2H), 7.29 (d, J = 7.7 Hz, 1H), 7.59 (s,1H), 7.68 (t, J = 3.5 Hz, 1H), 7.85 (d, J = 9 Hz, 1H), 8.21 (d, J = 8.9 Hz, 1H), 8.64 (d, J = 8.3 Hz, 1H).

^{13}C NMR (DMSO, 100 MHz): δ_{ppm} 44.8, 56.2, 65.6, 108.8, 110.5, 116.6, 117.0, 119.5, 120.6, 124.6, 128.1, 131.0, 136.4, 136.7, 145.0, 155.2, 160.3.

MS (FAB+): Calculated 362, Found: 363 ($M + H^{+}$).

IR (cm^{-1}): 2929, 2105.7, 1573.9, 1507.8, 1438.7, 1402.6, 1375.6, 1264.4, 1237.4, 1084.1, 1048, 774.69.

3.16.1-(2-aminoethyl)-7-methoxy-4-(trifluoromethyl)-6,10b-dihydrobenzo[*h*] quinolin-2(1*H*)-one(22)

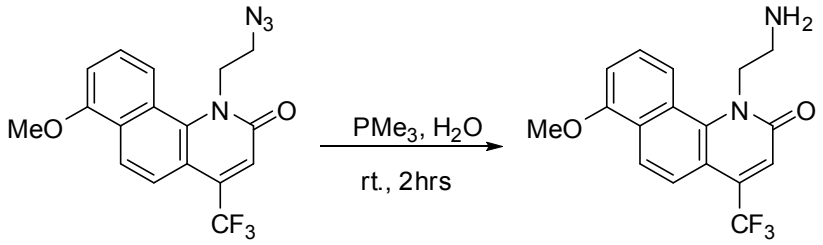

21 **22**

Scheme 3.15: Synthetic route for **22**

Product **22** was obtained from the reaction of **21** (150 mg, 0.84 mmol) and 1.0 M solution of PMe_3 according to the method described for the preparation of **3**. Yield: 85 mg, 62%.

^{1}H NMR(DMSO,400 MHz): δ_{ppm} 3.20 (s, 2H), 4.02 (s, 3H), 4.07 (t, J = 5.5Hz, 2H), 7.29 (d, J = 7.8Hz, 1H), 7.52 (s, 1H), 7.71 (t, J = 7.7 Hz, 1H), 7.86 (d, J = 9.0 Hz, 1H), 8.22 (d, J = 9.3 Hz, 1H), 8.66 (d, J = 8.2Hz,1H).

^{13}C NMR (DMSO, 400 MHz): δ_{ppm} 55.8, 64.1, 68.1, 108.3, 110.7, 116.2 116.5, 119.1, 120.2, 124.2, 127.8, 130.5, 135.5, 136.4, 144.5, 154.8, 159.9.

MS (FAB+): Calculated 336, Found: 337 ($M + H^+$).

IR (cm^{-1}):3346.5, 2910.9, 1670, 1634, 1613, 1573.9, 1459.7, 1438.7, 1396, 1339.5, 1120, 1027, 771.6.

3.17. Measurement of absorption, emission, and quantum yield

Solution of each probe with known concentration (≈100 μM) in methanol was prepared and then the absorbance of each probe was obtained from an *UV*-Visible absorption spectrophotometer. Absorption intensity for each probe is about 0.5. Then molar absorbance was calculated for each probe using formula A=εlC, where A is actual absorbance, ε is molar absorbance, l is path length and C is concentration of probe. The absorbance of standard perylene was obtained by using a similar procedure. Then the solution of each probe was further diluted 10 times to get ≈ 0.05 absorbance for the measurement excitation and emission wavelength range on fluorimeter instrument. The measurement of excitation and emission for standard was done with a similar procedure. The quantum yield was calculated for each probe according to the following equation:

$$\frac{\Phi_f^u}{\Phi_f^s} = \frac{I_f^u}{I_f^s} \times \frac{n^2(u)}{n^2(s)}$$

Where the s and u denote standard and unknown respectively, Φ is the fluorescence quantum yield, I is the gradient from the plot of integrated fluorescence intensity *vs.* absorbance and n the refractive index of the solvent.

3.18. Microwell plate preparation and microwell plate assays

Isolation of mid brain, hind brain and their plating on a 96-wellplate was done according to the reported procedure given below.[48] Then the microwell plate was incubated for 72 hours. Two rounds of screening fluorescent probes with neuronal cells were done in neuronal media (NM, Sciencell 1521containing basal medium, neuronal growth supplement and streptomycin supplement). For the

first round of screening, fluorescent probes were added to 200 µL neuronal media to adjust 100 µM net concentrations. Neuronal cells were incubated with this concentration for 10 minutes. After 10 minutes plates were rinsed to get rid of the remaining unacumulated probe solution from cells. A 200µM solution of Neuronal Media was then added in each plate well. A Perkin – Elmer LS55 equipped with plate reader attachement was used to read microwell plates. Excitation and emission wavelengths were adjusted depending on the initially observed optical properties of each fluorescent probe. In the second round of screening, neuronal cells were first pretreated with the desired inhibitor for 10 minutes and then exposed to the solution of fluorescent probe. The remaining steps which were used for the first round of screening, were carried out in exactly the same way. At the end, the microwell plates were read with a Perkin-Elmer LS55.

3.19. Midbrain and hind brain isolation

Isolation of the midbrain and hind brain was done according to the procedure given below.[48] The metencephelon, myelencephelon, and myelincephelon from e19 chick were isolated. These were placed in an aluminum foil mold. The tissue was submerged in 2.5% low melting agarose gel and kept on ice for few minutes to solidify. Then the solidified block was removed from the gel with a razor blade. The block was positioned on the stage of microtome with instant dry glue and allowed some time to dry. Then it was submerged in Dulbecco's phosphate buffered saline solution (DPBS, Mediatech #21-031-CV) at 0^0C. To obtain the sagittal section, the anterior side of the cube is positioned facing up. Transverse

slices were taken with 100μm increments, starting at the anterior edge of the mecencephelon and continuing posterioly to the hinder brain. A stereotaxic atlas of a chick brain was used to locate brain region. Slices from mesencephelon and metencephelon were retrieved using an inoculated loop and placed onto an 8-chambered glass vessel treated with 100 μL NM. Sagittal slices were obtained in a similar manner and slices from the sagittal midline were retrieved and placed onto the cover slip slides. The fluorescent probes were added to the NM to reach final 100 μM concentration. Then the brain section incubated with fluorescent probe solution for 10 minutes. The slices were rinsed with 80 gauge aspirating needle to remove the NM and then a fresh 50 μL of NM solution was added to the tissue. The chamber compartments were removed and the tissue was covered with 24X60 mm micro cover glass and sealed with clear nail polish.

3.20. Confocal imaging

Confocal imaging of tissue samples treated with fluorescent probes was done on a Leica SP5 confocal microscope with a standard 405 nm diode laser as an excitation source. XYZ – scans were taken within 2 μm sections and images were analyzed with J-1.41 software.

Chapter IV

PHOTOPHYSICAL PROPERTIES

4.1. 2-(2-aminoethyl)-2H-benzo[b]pyrido[4,3-e][1,4]thiazine-3(5H)-one (3)

The ethylamino-functionalized compound **3** has shown excellent optical properties. It absorbed at wavelength 300 nm - 435 nm with absorption maximum at 319 nm and emitted in the range 400 nm – 650 nm with emission maximum at 465 nm as shown in the **Figure 4.1**. Its absorption at longer wavelengths, as compared to probes **7** and **9**, may be because of the extended resonance effect of phenothiazine group in tricyclic compound **3**.

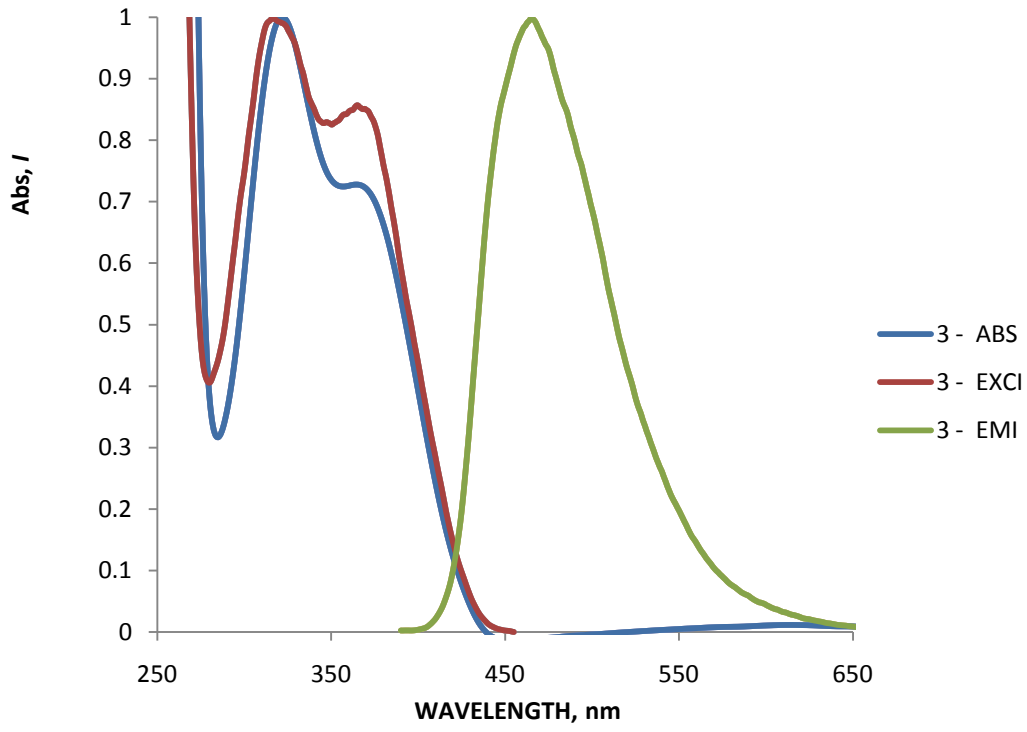

Figure 4.1: Absorption, Excitation, and Emission spectra of **3**

This red shift attributed to the large delocalization of the electron system over all three fused six member rings of tricyclic compound. The absorption range from 400 nm – 435 nm of this compound enabled us to use a confocal microscope with 405 diode laser as an excitation source for imaging. Its molar absorptivities was 6.8 X 10^3 L mol^{-1} cm^{-1} and its quantum yield was Φ = 4.7 X 10^{-1}, as shown in **Table 4.1**. Its high quantum yield, extended absorption range over 400 nm – 435 nm, and good molar absorption are vital for screening and imaging of the biological cells.

4.2. 9-(2-aminoethyl)-9H-carbazole(6)

The ethyl amino functionalized compound **6** absorbed at wavelength 305 nm - 375 nm with absorption maximum at 332 nm and emitted in the range 315 nm – 425 nm with emission maximum at 359 nm as shown in the **Figure 4.2**.

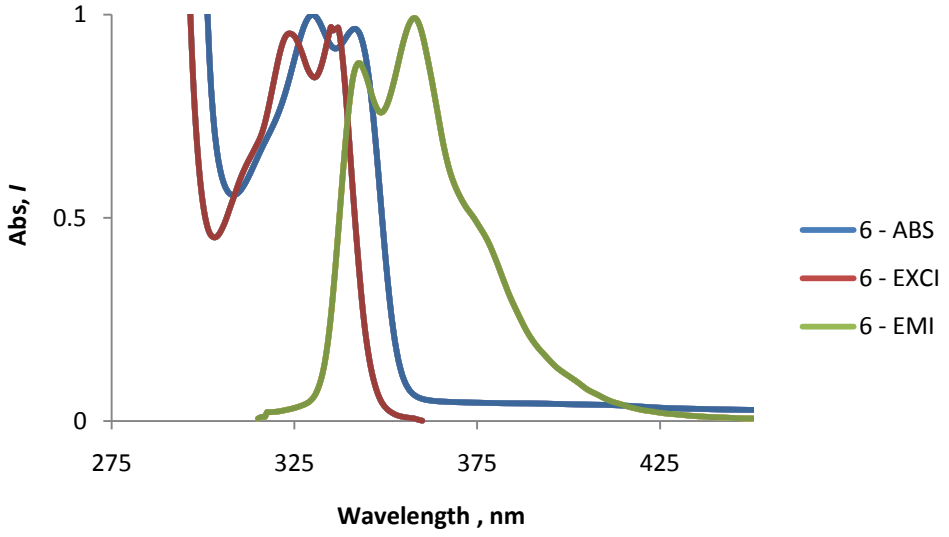

Figure 4.2: Absorption, Excitation, and Emission spectra of **6**

Molar absorptivities of compound **6** was 5.1 X 10^3 L mol^{-1} cm^{-1} and its quantum yield was 1.3 X 10^{-1} as shown in **Table 4.1**.

4.3. 2-(9*H*-pyrido [2, 3-*b*] indol-9-yl) ethanamine (9)

Compound **9** absorbed in the range wavelength 310 nm - 425 nm with an absorption maximum at 338 nm and emitted in the range 330 nm – 555 nm with an emission maximum at 390 nm as shown in the **Figure 4.3**. Compound **9**, which bears an electronegative nitrogen heteroatom atom in the phenyl ring, absorbs at a longer wavelength than compound **6,** which has no nitrogen in the phenyl ring. This red shift in absorption was attributed to the electron withdrawing effect of the nitrogen atom present in the phenyl ring. Compound **9** emitted at a higher wavelength than compound **6**. The excitation spectrum of compound **9** was almost similar to its absorption spectrum. It indicates that the same species was responsible for an emission which was visible on the absorption spectrum.

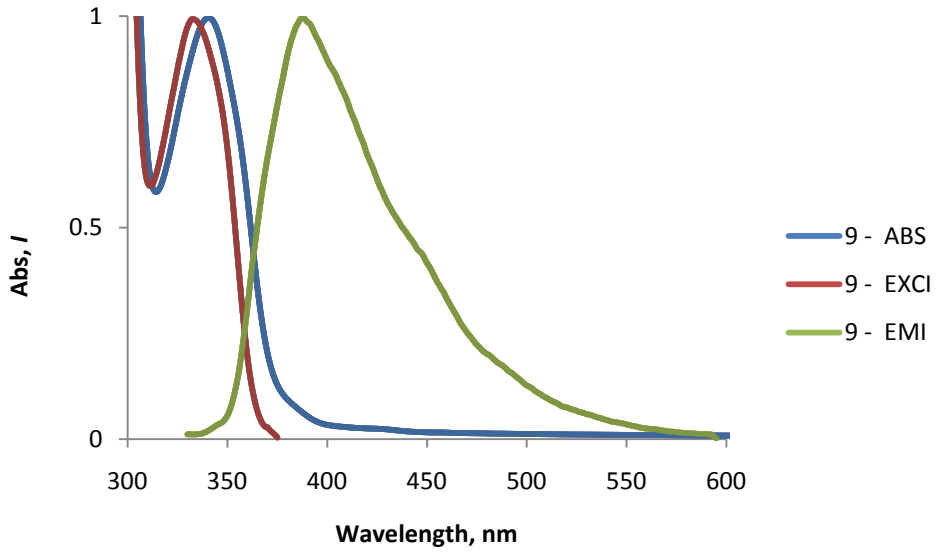

Figure 4.3: Absorption, Excitation, and Emission spectra **of 9**

Molar absorptivity of **9** was 4.5 X 10^3 L mol^{-1} cm^{-1} and its quantum yield was Φ = 6.0 X 10^{-2} as shown in **table 4.1**.

4.4. 2-(2-aminoethyl)-1H-benzo [de]isoquinoline-1, 3(2H)-dione (11)

Compound **11** absorbed in the range of 310 nm – 395 nm with an absorption maximum at 333 nm and emitted in the range 320 nm – 550 nm with an emission maximum at 386 nm as shown in **Figure 4.4**.

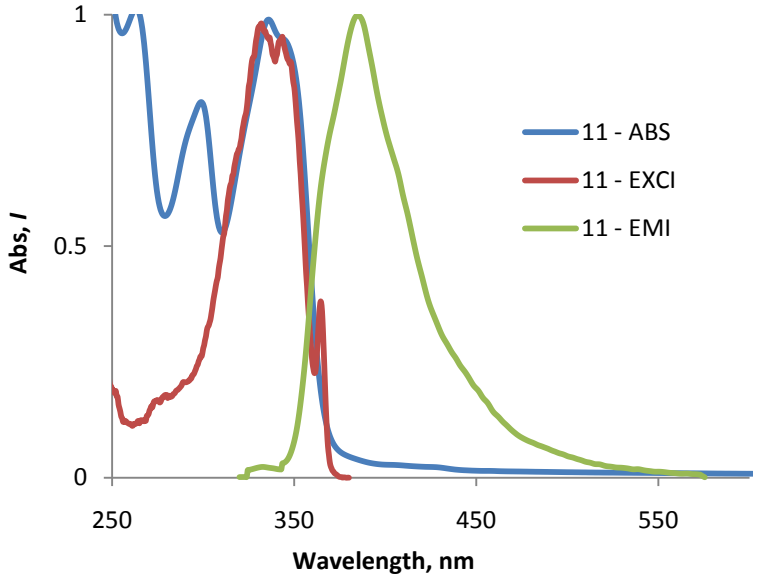

Figure 4.4: Absorption, Excitation, and Emission spectra of **11**

Molar absorptivity of **11** was very good i. e. 1.3 X 10^4 L mol^{-1} cm^{-1} and its quantum yield was Φ = 8.8 X 10^{-2} as shown in **table 4.1**.

4.5. 6-amino-2-(2-aminoethyl)-1H-benzo [de]isoquinoline-1, 3(2H)-dione (13)

The fluorescent probe **13** absorbed in the range of 350 nm - 500 nm with an absorption maximum at 432 nm and emitted in the range 450 nm - 680 nm with an emission maximum at 534 nm as shown in the **Figure 4.5**.

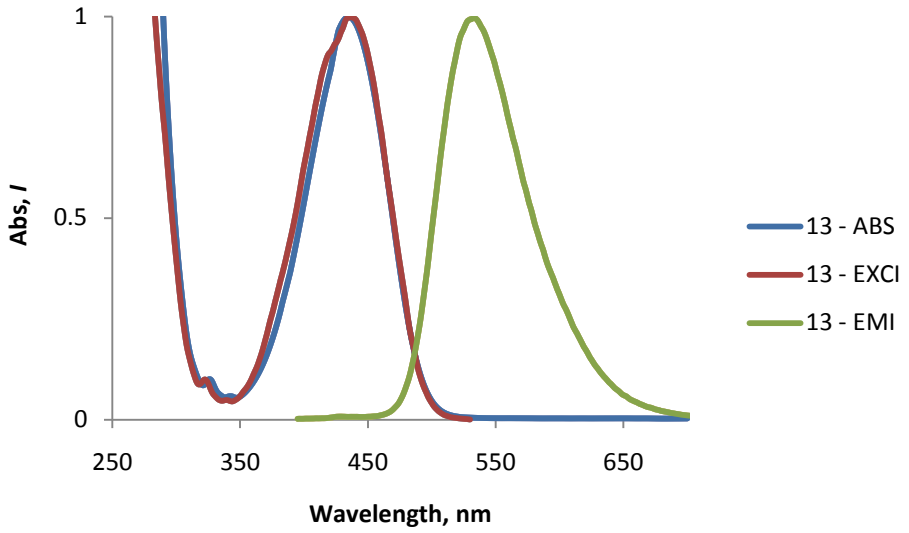

Figure 4.5: Absorption, Excitation, and Emission spectra of **13**

The absorption maximum was 432 nm, which was higher than 405 nm enabled to use confocal microscopy for imaging. It also emited in the range 400 nm – 650 nm which was also important for screening and imaging. This compound absorbed at a longer wavelength than compound **11**. This red shift in absorption was mainly attributed the presence of an amino group at the 4th position on the phenyl ring which increases the conjugated electron system via electron releasing mesomeric effect. There was also a red shift in the emission spectrum as compared to the emission spectrum of compound **11** because of the presence of amino group in compound **13** at the 4 th carbon on the ring. Molar

absorptivity of this compound was very high i.e. 3.9 X 10^4 L mol^{-1} cm^{-1} and its quantum yield was i.e. Φ = 6.2 X 10^{-2} as shown in **Table 4.1**. Because of its very good photophysical properties this compound was selected for screening and imaging the cells.

4.6. 5-(2-aminoethoxy) naphthalene-1-ol (16)

Compound **16** absorbed in the range 250 nm - 340 nm with an absorption maximum at 299 nm and emitted in the range 280 nm – 425 nm with an emission maximum at 347 nm as shown in the **Figure 4.6.**

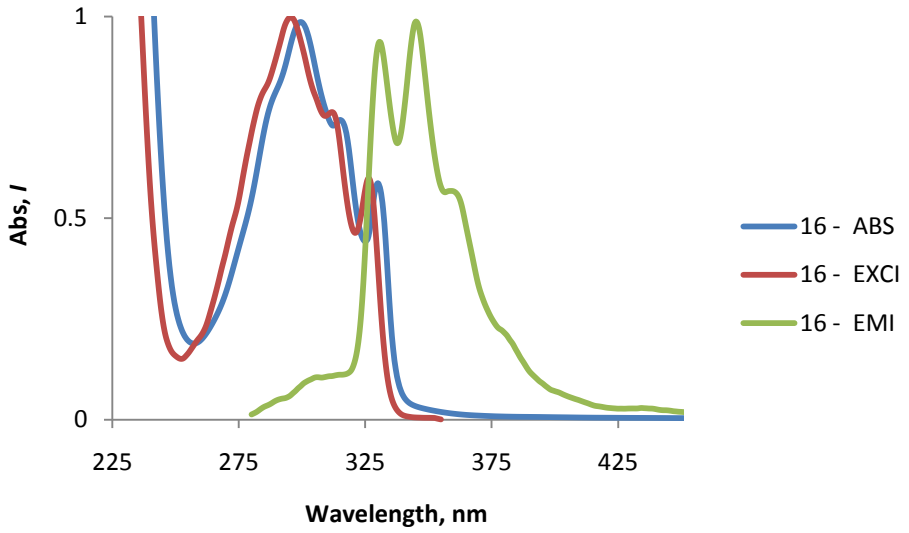

Figure 4.6: Absorption, Excitation, and Emission spectra of **16**

Molar absorptivity of compound **16** was relatively good i.e. 9.4 X 10^3 L mol^{-1} cm^{-1} and its quantum yield was Φ = 2.4 X10^{-2} as shown in **Table 4.1**.

4.7. 2-(5-methoxynaphthalen-1-yloxy) ethanamine (18)

Compound **18** absorbed in the range 250 nm - 330 nm with an absorption maximum at 261 nm and emitted in the range 280 nm – 400 nm with an emission maximum at 342 nm as shown in **Figure 4.7**. The absorption maximum of compound **18** shifted to a shorter wavelength as compared to the absorption maximum of compound **16**. The hydroxyl group present in compound **16** enabled a proton transfer excited state but 18 lacks a proton transfer in excited state. Thus, the blue shift was mainly attributed to the methoxy group present in compound **18** instead of the hydroxyl group present in compound **16**.

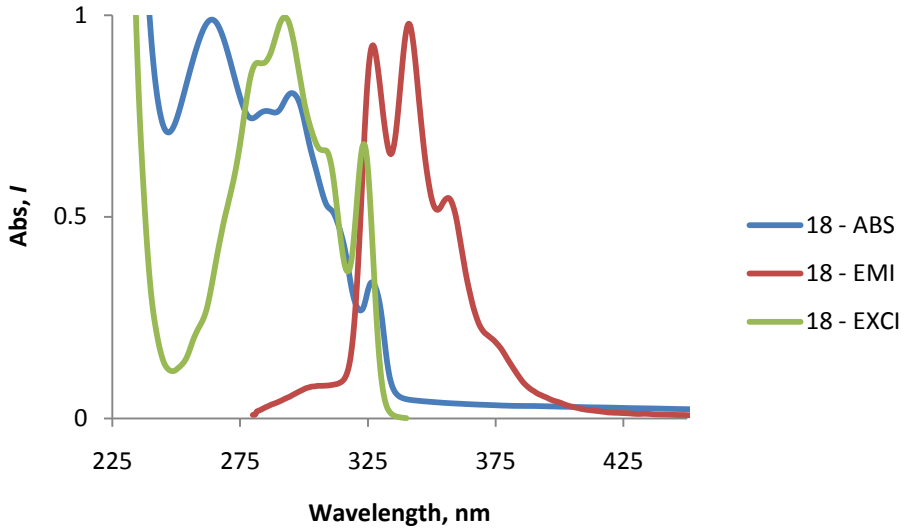

Figure 4.7: Absorption, Excitation, and Emission spectra of **18**

Molar absorptivity of compound **18** was 8.5 X 10^3 L mol^{-1} cm^{-1} and its quantum yield was Φ = 1.1 X 10^{-1} as shown in **Table 4.1**.

4.8.1-(2-aminoethyl)-7-methoxy-4-(trifluoromethyl)-6,10b-dihydrobenzo[*h*] quinolin-2(1*H*)-one(22)

Compound **22** absorbed in the range 325 nm - 400 nm with an absorption maximum at 377 nm and emitted in the range 350 nm – 550 nm with an emission maximum at 428 nm as shown in the **Figure 4.8**.

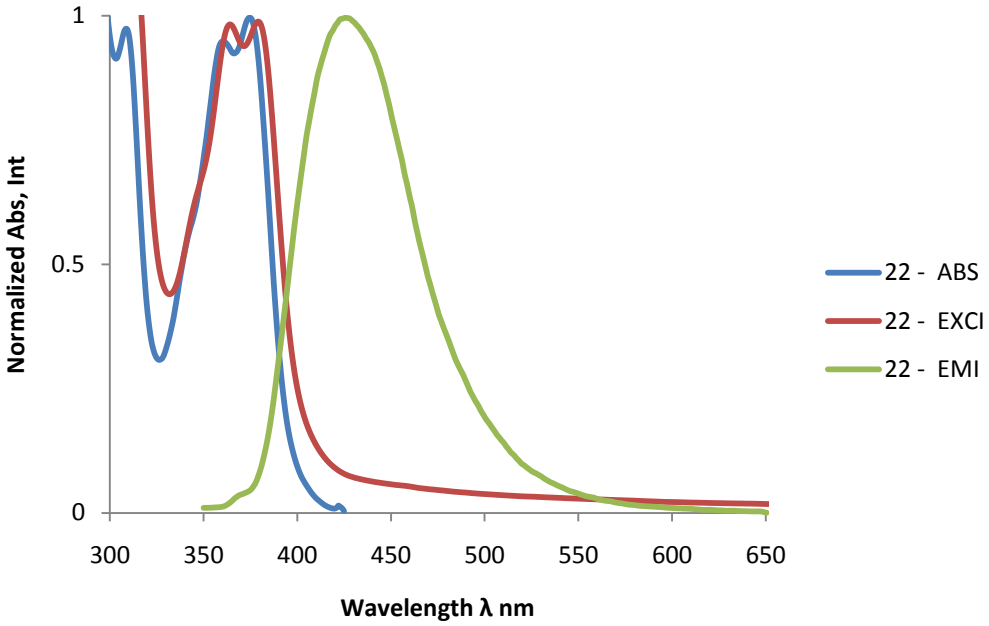

Figure 4.8: Absorption, Excitation, and Emission spectra of **22**

The absorption at a longer wavelength was mainly because of large delocalisation of π electrons over tricycalic compound. The quantum yield of **22** was $\Phi = 5.7 \times 10^{-2}$ and its molar absorptivity was very good i. e. 1.6×10^{4} L mol^{-1} cm^{-1} as shown in **table 4.1**.

Table 4.1: Optical properties of fluorescent probes

Compounds	Quantum Yield	Molar Abs. $L\ mol^{-1}cm^{-1}$	Absorption Max. nm	Emission Max. nm
3	4.7×10^{-1}	6.8×10^{3}	319	465
6	1.3×10^{-1}	5.0×10^{3}	237	359
9	6.0×10^{-2}	4.5×10^{3}	338	390
11	$8.8. \times 10^{-2}$	1.3×10^{4}	333	386
13	6.2×10^{-2}	3.9×10^{4}	432	534
16	2.4×10^{-2}	9.4×10^{3}	299	347
18	1.1×10^{-1}	8.5×10^{3}	261	342
22	5.7×10^{-2}	1.6×10^{4}	377	428

Chapter V

CELLULAR UPTAKE AND INHIBITION STUDIES

Prior to cellular uptake and inhibition studies, the various possible fluorescent probes **3**, **6**, **9**, **11**, **13**, **16**, **18**, and **22** were synthesized by using convenient synthetic routes. Then, optical properties of these fluorescent probes were investigated in detail and these optical properties were used for the screening and imaging of the cells. 20 uM solutions of these probes were used for cellular study.

5.1. Fluorescent probes for HEK-293 cells

Live cell and tissue imaging:

HEK-293 cells expressing DAT, NET, or SERT isolated from brain stem of E-14 chick embryos were exposed to the solutions of these compounds. The images of these exposed cells were taken with confocal microscopy. Some of the compounds, namely **3** and **13**, have shown affinity to the HEK-293 cells, indicating that these compounds can act as neurotransmitter analogs. The high emission responses were observed from the images obtained from compounds **3** and **13**. This emission response was either because of active transport of these compounds via DAT, NET, or SERT or because of just binding of these compounds to the surface of the transporters or receptors. To ensure that the interaction between cells and compounds was an active transport and compounds were accumulated into the cells via transporters, HEK-293 cells expressing DAT, NET or SERT were pretreated with 10 uM solutions of GBR-

12909, desipramine and clomipramine, respectively for 1 minute before introducing the probes. Pretreatment of cells with a reuptake inhibitor was done with the same concentration for the same duration.

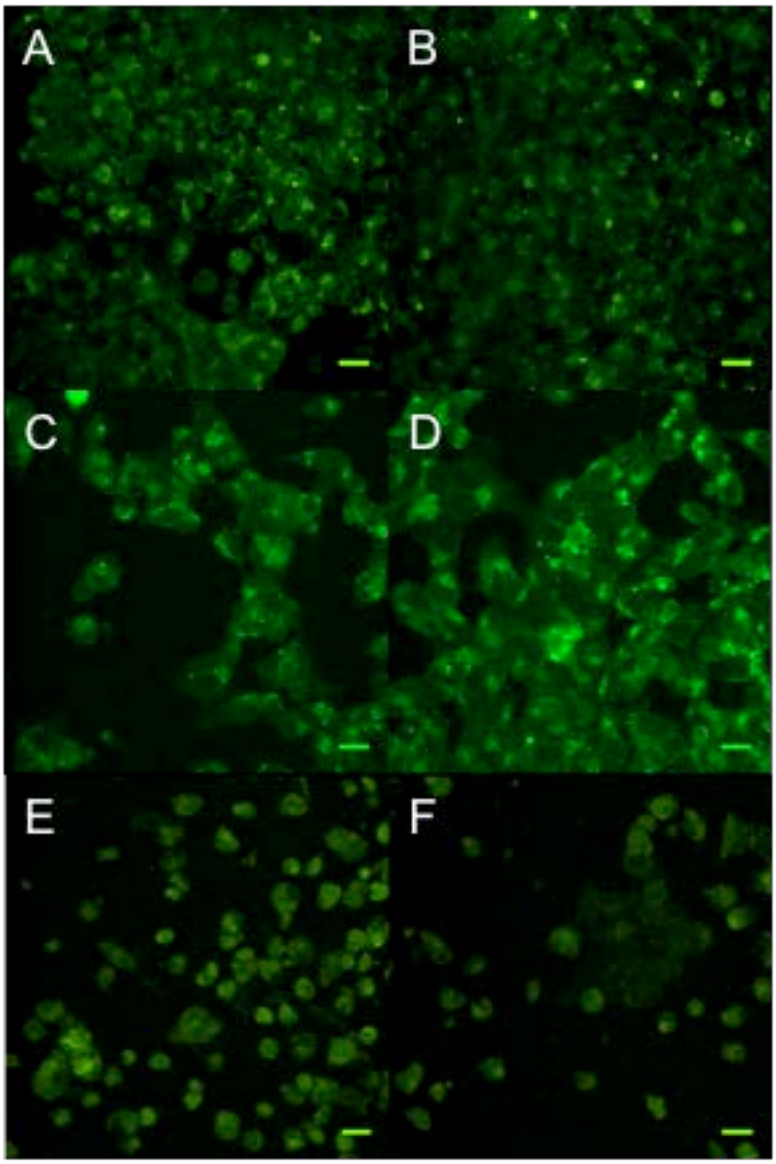

Figure 5.1: Fluorescence images of HEK-293 cells expressing DAT (A, B), NET (C, D), or SERT (E, F) exposed to **3**. Cells in the right column were pretreated with the appropriate reuptake inhibitor while cells on the right were not pretreated.

Probe **3** was exposed to the HEK-293 cells for one min. and images were taken with confocal microscopy. From the images shown in the figure **5.1,** it is clear that the probe 3 was accumulate rapidly in the cells but there is no appreciable difference in images regarding emission intensity and distribution in the cell body with and without inhibitors. However, it doesn't imply that the probe was simply accumulated on the surface of the membrane just by binding interaction and that there is no active transport mechanism by MATs. No appreciable difference is observed between pretreated and untreated cells indicating that the uptake of **3** is not likely to involve these MATs.

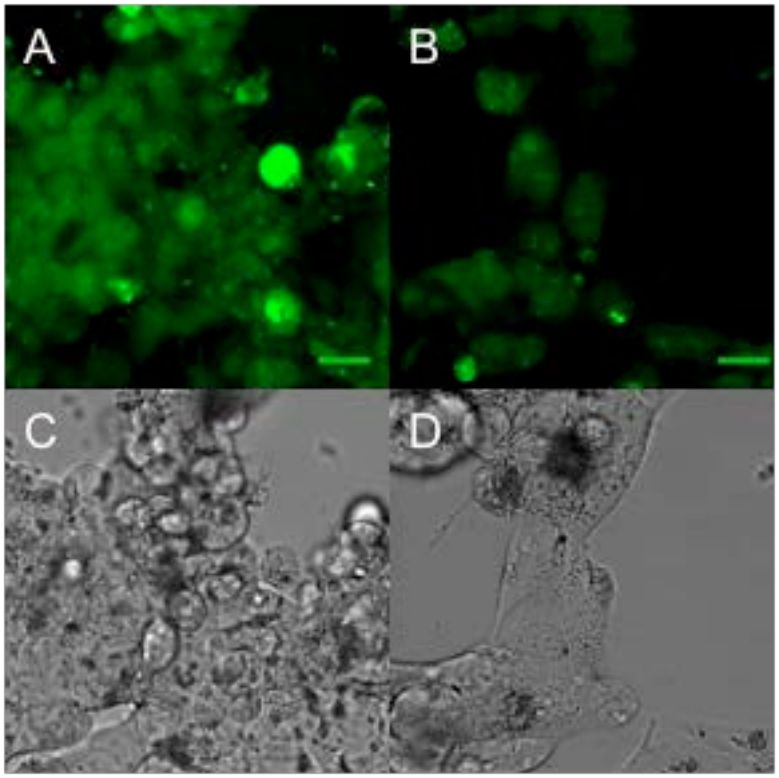

Figure 5.2: HEK-293 cells expressing human dopamine transporter (DAT) treated with **13** (20 uM, 60 s) without (A, C) and with (B, D) 10 uM GBR-12909, a dopamine reuptake inhibitor. Excitation was at 405 nm and emission was collected from 475 to 575 nm. Images were obtained at the same laser intensity with identical detector gain. Z-stacks were obtained at 1 uM increments and summed to give the projections shown in A and B. The corresponding bright field images are shown below (C, D); scale bars are 20 uM.

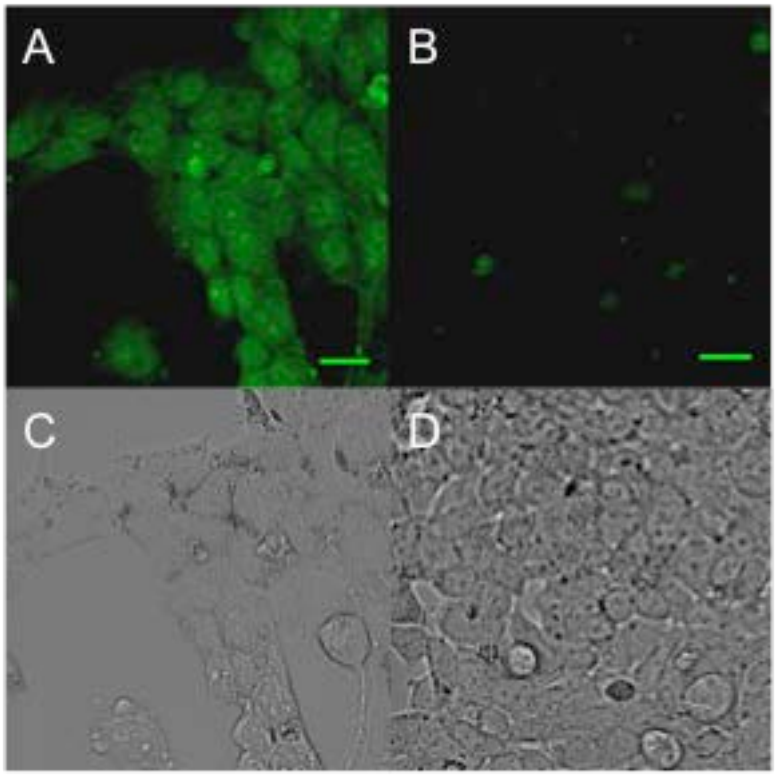

Figure 5.3: HEK-293 cells expressing human norepinephrine transporter (NET) treated with **13** (20 uM, 60 s) without (A, C) and with (B, D) 10 uM desipramine, a norepinephrine reuptake inhibitor. Excitation was at 405 nm and emission was collected from 475 to 575 nm. Images were obtained at the same laser intensity with identical detector gain. Z-stacks were obtained at 1 uM increments and summed to give the projections shown in A and B. The corresponding bright field images are shown below (C, D); scale bars are 20 uM.

The transport of this probe **3** into the cells may not necessarily be by MATs but it could also be because of other several active transports such as the organic cation transporters (OCTs), cationic amino acid transporters (CATs), and the plasma membrane monoamine transporter (PMAT). Then HEK-293 cells were exposed to the fluorescent probe **13**. As shown in **Figure 5.2, 5.3**, **5.4** and **5.5** after 1 minute of exposure of HEK-293 cells expressing DAT, NET or SERT to compound **13** indicated that this probe was accumulated into the cells rapidly.

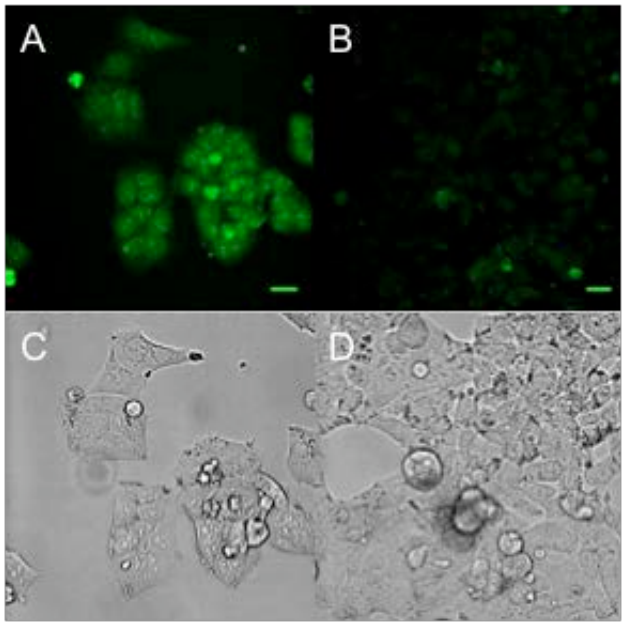

Figure 5.4: HEK-293 cells expressing human serotonin transporter (SERT) treated with **13** (20 uM, 60 s) without (A, C) and with (B, D) 10 uM clomipramine, a serotonin reuptake inhibitor. Excitation was at 405 nm and emission was collected from 475 to 575 nm. Images were obtained at the same laser intensity with identical detector gain. Z-stacks were obtained at 1 uM increments and summed to give the projections shown in A and B. The corresponding bright field images are shown below (C, D); scale bars are 20 uM.

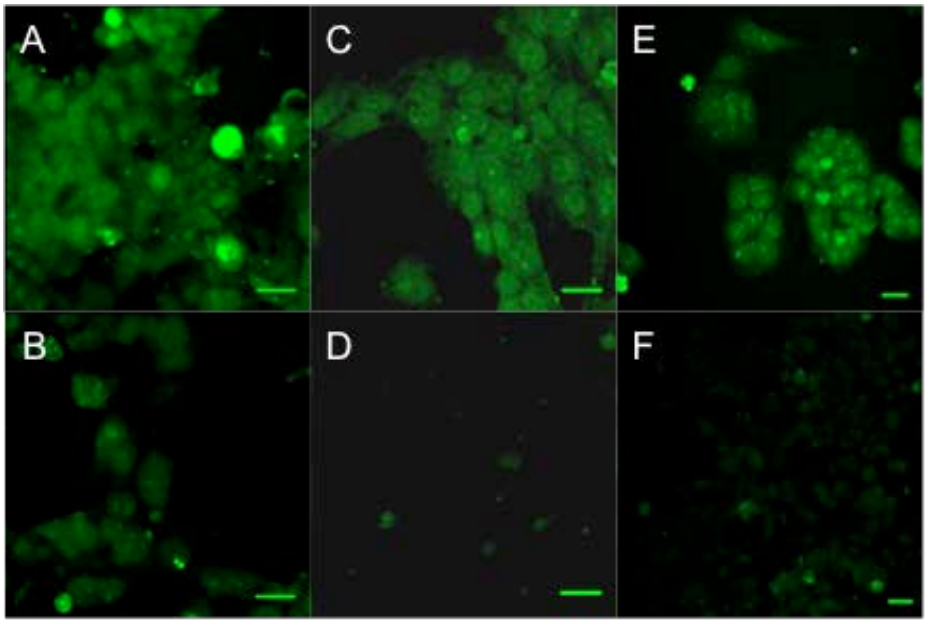

Figure 5.5: Left to right, HEK 293 cells expressing DAT, NET and SERT exposed to **13**. Top row is without inhibitor; bottom row has been treated with GBR-12909, desipramine, and clomipramine, respectively. Accumulation of the probes is limited by these reuptake inhibitors (scale bar for all images is 10 μm).

From these images it is clear that there was significant reduction in the uptake of **13** for the cells expressing DAT, NET, and SERT with inhibitors GBR-12909, desipramine, and clomipramine, respectively. It indicates that the primary mode of interaction between cells and a probe is active transport i. e. probe **13** is transported into the HEK-293 cells through DAT, NET, or SERT.

In order to test whether these probes were accumulated on the surface of the cell membrane just by simple binding interactions or internalized by active transport mechanism by transporters, Hek-293 cells were grown on poly-L-lysine and laminin treated cover slips fixed to a 35 nm cultured dish. These grown cells were exposed to the probe solutions for one minute and images of z-stacks of HEK-293 cells were obtained by confocal microscopy. The new images were obtained by changing cell culture media. Cells exposed with probes excited with 405nm diode laser and emission wavelength were kept in the range 450-600 nm. From the images shown in the **Figures 5.1**, **5.2, 5.3, 5.4** and **5.5** it is clear that both probes are transported into the cells by active transport mechanism via transporters.

5.2. Fluorescent probe for platelets in blood sample

Live Cell and tissue imaging

Biogenic amines are responsible for various important functions in the CNS but they also play a vital role in blood plasma outside the CNS.[55] Serotonin (5-HT), catecholamines (CA), noradrenalin (NA), and adrenaline (Ad) are the biogenic amines present in the plateles of blood and these amines affect

platelets' activities and vessel tone.[56] In biogenic amines, serotonin is an important constituent of platelets. Its change in level significantly affects platelet functions.[57]

Human platelets accumulate serotonin(5-HT) in vesicular and extra-vesicular compartments by active transport process.[58] Platelets accumulate 5-HT from blood plasma mainly via serotonin transporter (SERT).[59] Alternation in the level of 5-HT in blood plasma can cause serious blood related diseases and disorders. The level of 5-HT in blood plasma is depend on its level in platelets and surface SERT.[59] Fluorescent probe **13** was tested for identification of a specific cell type in tissue samples. Platelets expressing SERT in blood sample were exposed to the solution of fluorescent probe **13**. Then images were taken with confocal microscopy. Probe **13** was found to be accumulated selectively in platelets expressing SERT in whole blood samples as shown in the images in **Figure 5.6**.

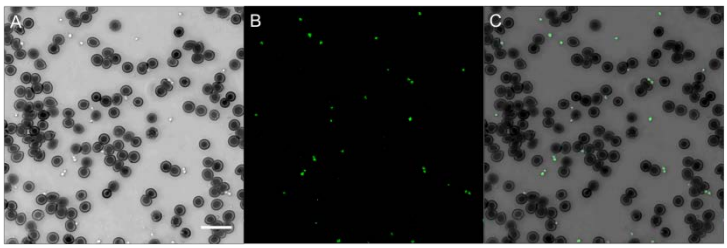

Figure 5.6: 13 was selectively accumulated by platelets expressing SERT in blood sample.

5.3. Fluorescent probe for murine osteocytic cell line, MLO-Y4 Live cell and tissue imaging

Neurotransmitters are responsible for regulating bone metabolism. The osteocytes are capable of synthesizing 5-HT and express both the transporter

and the receptor components of 5-HT. The expression of serotonin transporter (SERT) and receptors (5-HT_{1A} and 5-HT_{2A}) have been shown in the clonal murine osteocytic cell line, MLO-Y4.[60] 5-HT is an important regulatory biogenic amine in the bone cells and these bone cells posses specific pathways that respond to 5-HT.[61] Fluorescent probe **13** was tested to accumulate in bone-derived murine osteocytic cell line MLO-Y4. The samples of murine osteocytic cell line, MLO-Y4 expressing 5-HT, were exposed to the solution of **13**. Then images were taken with confocal microscopy. Additional images were taken after pretreating the sample with clomipramine, a serotonin reuptake inhibitor (SRI). Fluorescent probe **35** was found be accumulated in MLO-Y4 as shown in image A in **Figure 5.7**. The uptake of **13** in MLO-Y4 was significantly blocked by clomipramine as shown in the image B in **Figure 5.7**. Graphs C and D in **Figure 5.7** are for emission intensity and mean intensity of cell bodies with and without clomipramine treatment respectively. From graphs C and D in **figure 5.7** it is clear that clomipramine limits **13** probe uptake significantly in MLO-Y4.

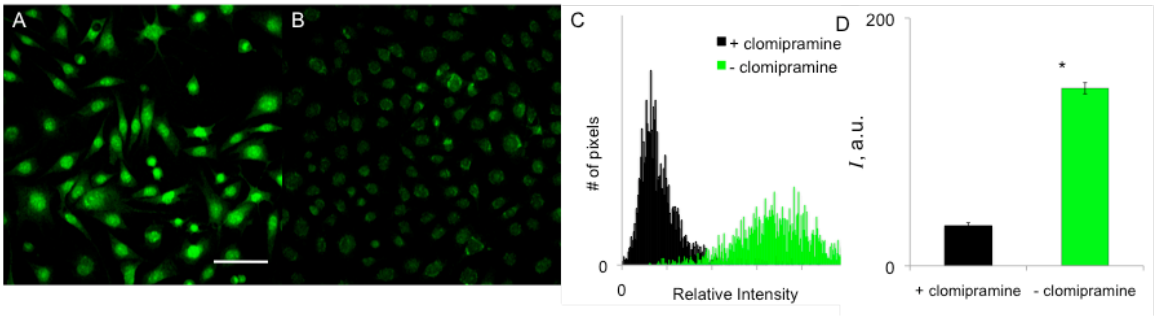

Figure 5.7: 13 (structure in panel D) is accumulated via SERT in MLO-Y4 cells (A). Pretreatment of cells with 10 μm clomipramine, an SRI limits probe uptake (B). Histogram of emission intensity from cell bodies in +/- clomipramine treatment(C). Mean intensity of cell bodies in +/- clomipramine treatment (D).

Chapter IV

CONCLUSION

Fluorescent analog probes are more precise than fluorescent labeled probes in understanding the dynamics of 5-HT regulation in cells. A series of ethyl amine-functionalized fluorophores were synthesized and explored their optical properties. Then their uptake was examined in, the murine osteocytic cell line, MLO-Y4 expressing SERT, platelets expressing SERT of blood samples, and HEK-293 cells expressing DAT, NET and SERT. From confocal microscopy it was found that probe **3** was internalized into HEK-293 cells. Probe **13** was also found to be internalized into HEK-293, platelets of blood samples and Murine osteocytic cell line MLO-Y4 by active transport mechanism via monoamine transporters. Interestingly, the longer wavelength absorption of probes **3** and **13** avoids the high auto fluorescence of the biological sample because of the aromatic amino acid residues and nucleobases which generally excite at short wavelength. These probes, because of their bright images, enabled their imaging process even in the presence of other weaker fluorescent substrates. The excitation and emission wavelengths of probe **3** and **13** are high enough to use commercially available filters. These fluorescent analog probes could be used in understanding the dynamics of neurotransmitters such as, their release, uptake, and transportation, which is a major problem in the case of fluorescently tagged techniques. These results demonstrate that the fluorescent monoamine transporters (FMATS) probe may be potentially useful outside CNS, specifically to determine the impact of reuptake inhibitors on the normal functions of cells.

References

1. G. G. Stokes, *Phil. Trans. R. Soc. Lond.,* **1852**, 142, 463.

2. H. Coons, H. J. Creech and R. N. Jones, *Proc. Soc. Exp. Biol. Med., **1941,*** 47**,** 200.

3. T. C. Südhof, K. Starke and S. Boehm, *Handbook of experimental pharmacology*, **2008**, 184, 23.

4. M. Chalfie, Y. Tu, G. Euskirchen, W. W. Ward and D. C. Prasher, *Science*, **1994**, 263, 802.

5. A. Rück, T. Köllner, A. Dietrich, W. Strauss and H. Schneckenburger, *J. photocem. photobiol. B: Biol.*, **1994**, 24, 63.

6. a) K. Reichert, *Phys. Z*., **1912,** 12, 1010. b) O. Heimstadt, Z. Wiss. Mikrosk, **1912,** 28, 330.

7. a) M. S. T. Goncalves, *Chem. Rev.*, **2009,** 109, 190. b) A. Mayer and S. Neuenhofer, *Angew. Chem. Int. Ed. Engl.*, **1994**, *33,* 1044.

8. W. Wang and H. Li, *Tetrahedron Lett.* **2004**, 45, 8479.

9. A. M. Piloto, S. P. G. Costa and M. S. T. Gonçalves, *Tetrahedron Lett.,* **2005,** 46, 4757.

10. A. M. Piloto, A. S. C. Fonseca, S. P. G. Costa and M. S. T. Gonçalves, *Tetrahedron Lett.,* **2006,** 62**,** 9258.

11. M. L. Capobianco, M. Naldi, M. Zambianchi and G. Barcarolle., *Tetrahedron Lett.,* **2005**, 46, 8181.

12. G. Barbarella, M. Zambianchi, A. Ventola, E. Fabiano, F. Della Sala, G. Gigli, M. Anni, A. Bolognesi, L. Polito, M. Naldi and M. Capobianco, *Bioconjugate Chem.,* **2006**, *17*, 58.

13. M. S. T. Goncalves, *Chem. Rev.*, **2009**, 109, 190.

14. T. Matsuzaki, T. Suzuki, K. Fujikura and K. Takata, *Acta Histochem. Cytochem.,* **1997**, 30**,** 309.

15. T. Suzuki, K. Fujikura, T. Higashiyama and K. Takata, J*. Histochem. Cytochem.,* **1997**, *31*, 49.

16. B. N. G. Giepmans, S. R. Adams, M. H. Ellisman, and R. Y. Tsien, *Science,* **2006**, 312, 217.

17. A. Raj, P. V. D. Bogaard, S. A. Rifkin, A. V. Oudenaarden and S. Tyagi, *Nature Methods,* ***2*****008,** 5, 877.

18. A. M. Femino, F. S. Fay, K. Fogarty, R. H. Singer, *Science*, **1998**, 280, (5363), 585.

19. J. Nath and K. L. Johnson, *Biotech. Histochem,* ***2000****,* 75, 54.

20. D. Bruns, F. Engert, and H. D. Lux, *Neuron*, **1993**, 10, 559.

21. H. W. Meyers, R. Jurss, H. R. Brenner, G. Fels, H. Prinz, H. Watzke, A. Maelicke, *Eur. J. Biochem.*, **1983**, 137(3), 399.

22. P. Cornelius, E. Lee, W. Lin, R. Wang, W. Werner, J. A. Brown, F. Stuhmeier, J. G. Boyd and K. McClure, *J. Biomol. Screen.,* **2009,** 14, 360.

23. D. I. C. Scope, J. R. Barrio and N. J. Leonard, *Science*, **1977**, 195, 296.

24. J. R. Barrio, J. A. Secrist III and N. J. Leonard, *Proc. Nat. Acad. Sci.* U.S.A., **1972**, 69, 2039.

25. J. Ren and D. J. Goss* *Nucleic Acids Res.*, **1999,** *24(18)*, 3629.

26. J. M. Schurr, and B. S. Fujimoto, *Biopolymers,* ***1988***, 27, 1543.

27. J. R. Unruh, G. Gokulrangan, G. S. Wilson, and C. K. Johnson, *Photochem. Photobiol.*, **2005**, 81, 682.

28. G. Vamosi, C. Gohlke and R. M. Clegg, *Biophys. J.* **1996**, 71, 972.

29. O. F. A. Larsen, I. H. M. Van stokkum, B. Gobets, R. V. Grondelle, and H.V. Amerongen, *Biophys. J.,* **2001**, 81, 1115.

30. B. J. Lee, M. Barch, E.W. Castner, J. Völker and K. J. Breslauer, *Biochemistry,* **2007,** 46, 10756.

31. J. R. Unruh, G. Gokulrangan, G. H. Lushington, G. S. Wilson, and C. K. Johnson, *Biophys. J.,* **2005,** 88, 3455.

32. J. J. Hill and C. A. Royer, *Methods Enzymol.,* **1997,** 278, 410.

33. S. P. Davis, M. Matsumura, A. Williams and T. M. Nordlund, *J. Fluoresc.*, **2003**, 13, 249.

34. R. Sapolsky, *Biology and Human Behavior: The Neurological Origins of Individuality, 2nd edition,* **2005**.

35. S.S. Kenneth., *Anatomy and Physiology: The Unity of Form and Function,* 5th edition, **2009.**

36. V K. Yadav, J. H. Ryu, N. Suda, K. F. Tanaka, J. A. Gingrich, G. Schütz, F. H. Glorieux, C. Y. Chiang, J.D. Zajac, K. L. Insogna, J. J. Mann, R. Hen, P. Ducy and G. Karsenty, *Cell,* **2008,** 135(5), 825.

37. T. Klint and P. Weikop, *Therapeutic Strategies*, **2004**, 1, 111.

38. J. Axelrod, L. G. Whitby and G. Hertting, *Science*, **1961,** 133, 383.

39. H. Lavretsky, M. D. Kim, A. Kumar and C. F. Reynolds, *J. Clin. Psychiatry*, **2003,** 64, 1410.

40. R. W. Lam, H. Hossie, K. Solomons and L. N. Yatham, *J. Clin. Psychiatry,* **2004**, 65, 337.

41. J. Zhou, R. He, K. M. Johnson, Y. Ye and A. P. Kozikowski , *J. Med. Chem*., **2004,** 47(24), 5821.

42. J. W. Schwartz, R. D. Blakely and L. J. DeFelice, *J. Biol. Chem.,* **2003,** 278, 9768.

43. J. N. Mason, H. Farmer, I. D. Tomlinson, J. W. Schwartz, V. Savchenko, L. J. DeFelice, S. J. Rosenthal and R.D. Blakely, *J. Neurosci. Methods,* **2005**, 143, 3.

44. R. Wagstaff, M. Hedrick, J. Fan, P. D. Crowe and D. Disepio, *J. Biomol. Screen.,* **2007**, 12, 436.

45. B. J. Venton, H. Zhang, P. A. Garris, P. E. Ehillips, D. Sulzer, and R. M. Wightman, *J. Neurochem.*, **2003**, 87, 1284.

46. N. G. Gubernator , H. Zhang, R. G. W. Staal, E. V. Mosharov, D. B. Bereira, M. Yue, V. Balsanek, P. A. Vadola, B. Mukherjee, R. H. Edwards, D. Sulzer and D. Sames, *Science* , **2009**, 324 (5933), 1441.

47. M. Lee, N. G. Gubernator, D. Sulzer and D. Sames, *J. Am. Chem. Soc.*, **2010**, *132* (26), 8828.

48. A. S. Brown, L. Bernal, T. L. Micotto, E. L. Smith and J. N. Wilson, *Org. Biomol. Chem.*, **2011**, 9, 2142.

49. T. L. Micotto, A. S. Brown and J. N. Wilson, *Chem. Commun.*, **2009**, 7548.

50. A. L. Koner, J. Schatz, W. M. Nau, and U. Pischel, *J. Org. Chem.* **2007**, *72*, 3889.

51. E. B. Veale and T. Gunnlaugsson, *J. Org. Chem.*, **2010**, 75, 5513.

52. S. Ghosh and A. K. Banthia, *Supramol. Chem.*, October, 2004, **16 (7),** 487.

53. Y. Oshiro, S. Sato, N. Kurahashi, T. Tanaka, T. Kikuchi, K. Tottori, Y. Uwahodo, and T. Nishi *, J. Med. Chem.* **1998,** *41,* 658.

54. P. Sandin, P. Lincoln, T. Brown and L. M. Wilhelmsson, *Nature Protocosl*, **2007**, 2(3), 617.

55. A. V. Tuev and V. V. Shchekotov, *Kardiologiia,* **1986**, 26(8), 77.

56. C. C. Smith, *Biochim. Biophys. Acta.,* **1996**, 1291(1), 1.

57. J. Dalsgaard-Nielsen, P. I. F. Honoré, I. Zeeberg, *Acta. Neurol. Scand.*, **1982**, 66(2), 191.

58. J. L. Costa, D. L. Murphy and H. Stark, J. Physiol. **1981**, 316, 153.

59. C. P. Mercado and F. Kilic, *M. I.,* **2010**, 10(4), 231.

60. M. Bliziotes, A. Eshleman, B. Burt-Pichat, X. W. Zhang, J. Hashimoto, K. Wiren and C. Chenu, *Bone*, **2006**, 39(6), 1313.

61. S. J. Warden, A. G. Robling, E. M. Haney, C. H. Turner, and M. M. Bliziotes, *Bone*, **2010**, 46(1), 4.

Appendix A

List of spectra: ^{1}H, ^{13}C and mass Spectra

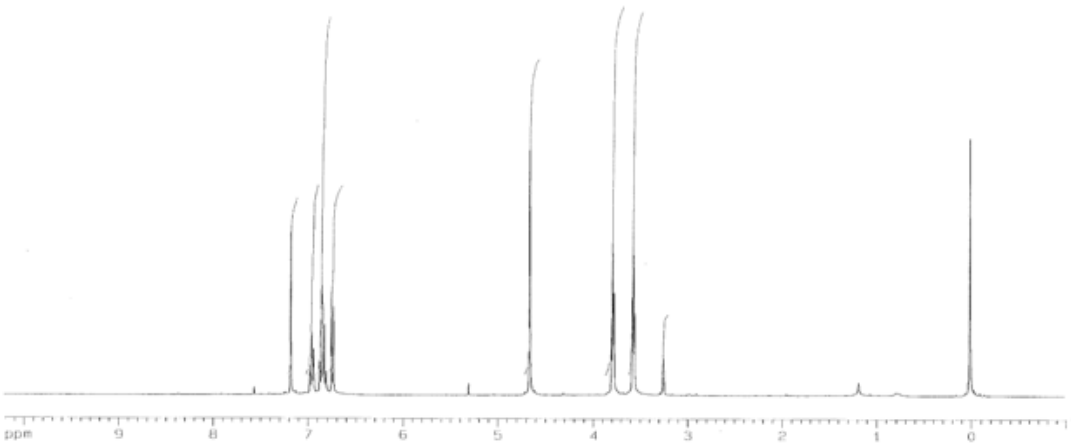

Spectra 1: ^{1}H NMR of **2** in $CDCl_3$+MeOD

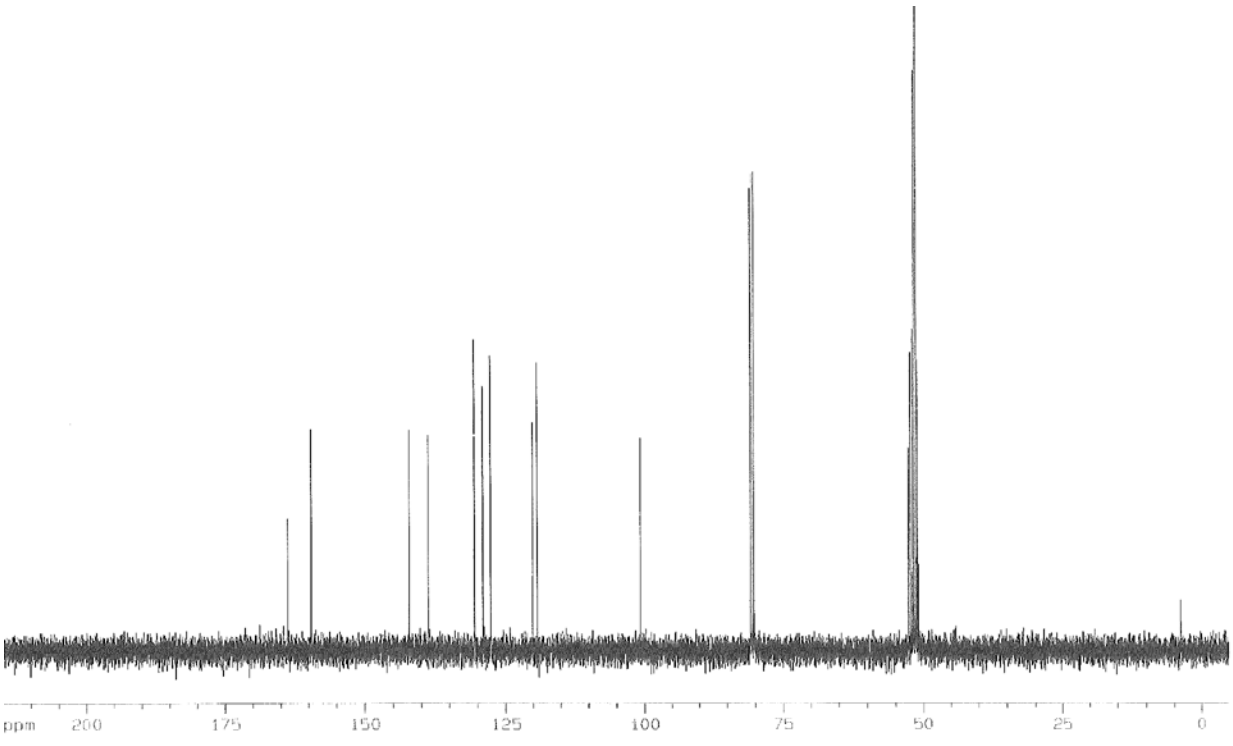

Spectra 2: ^{13}C NMR of **2** in $CDCl_3$+MeOD

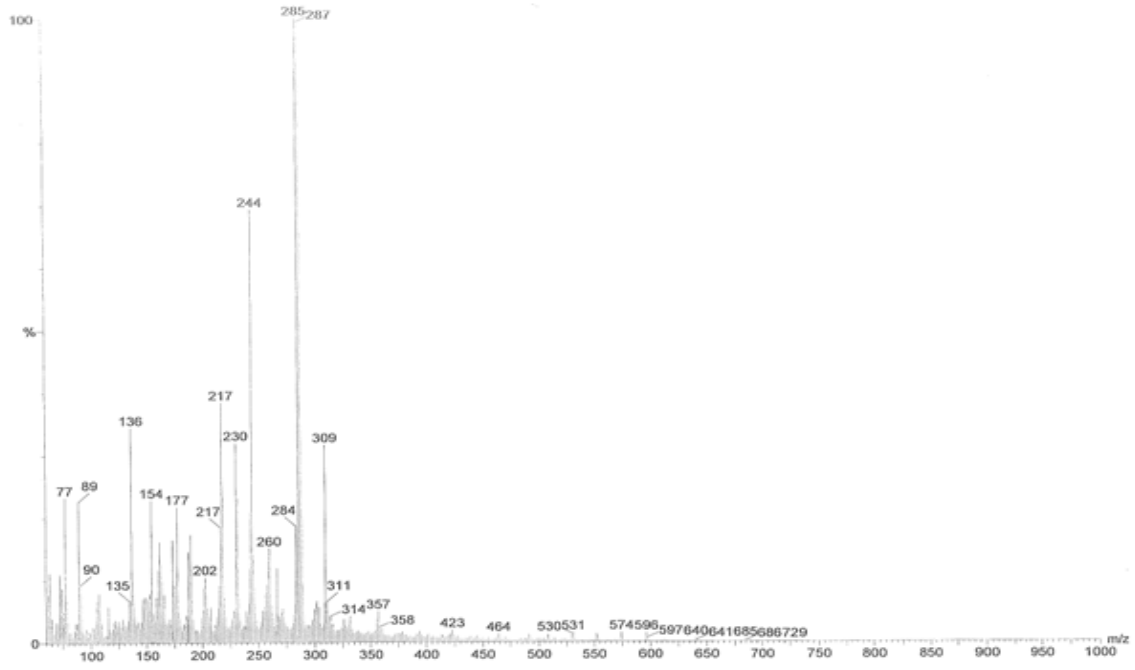

Spectra 3: MS (FAB+) of **2**

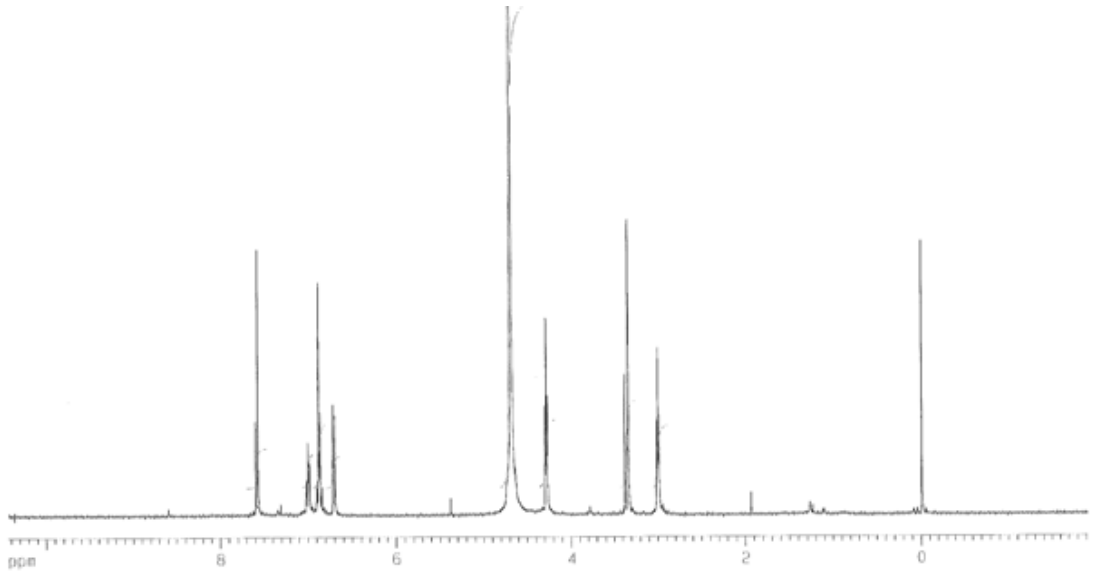

Spectra 4: ^{1}H NMR of **3** in $CDCl_3$+MeOD

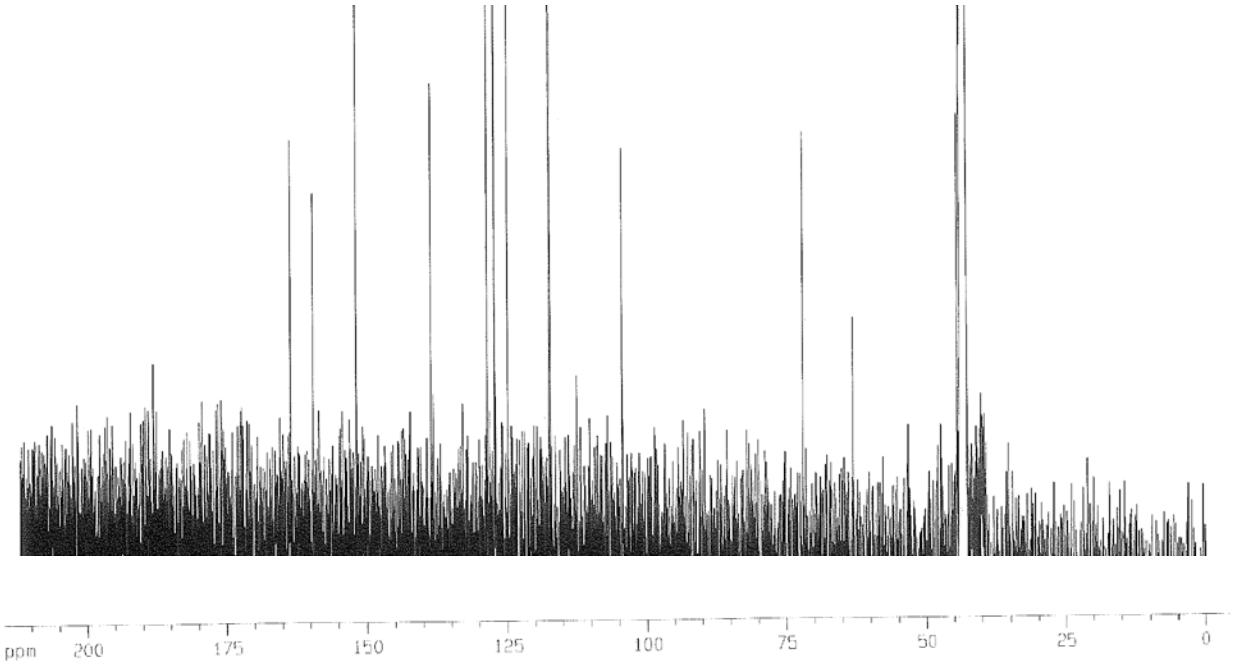

Spectra 5: ^{13}C NMR of **3** in DMSO

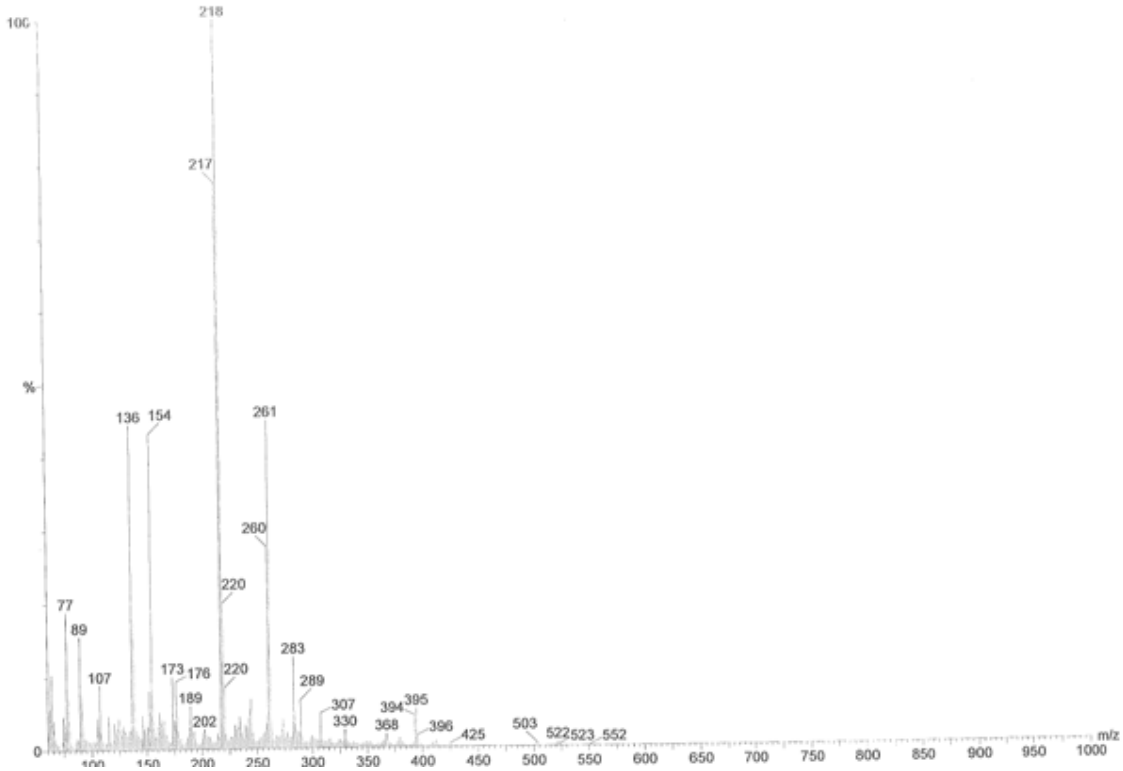

Spectra 6: MS (FAB+) of **3**

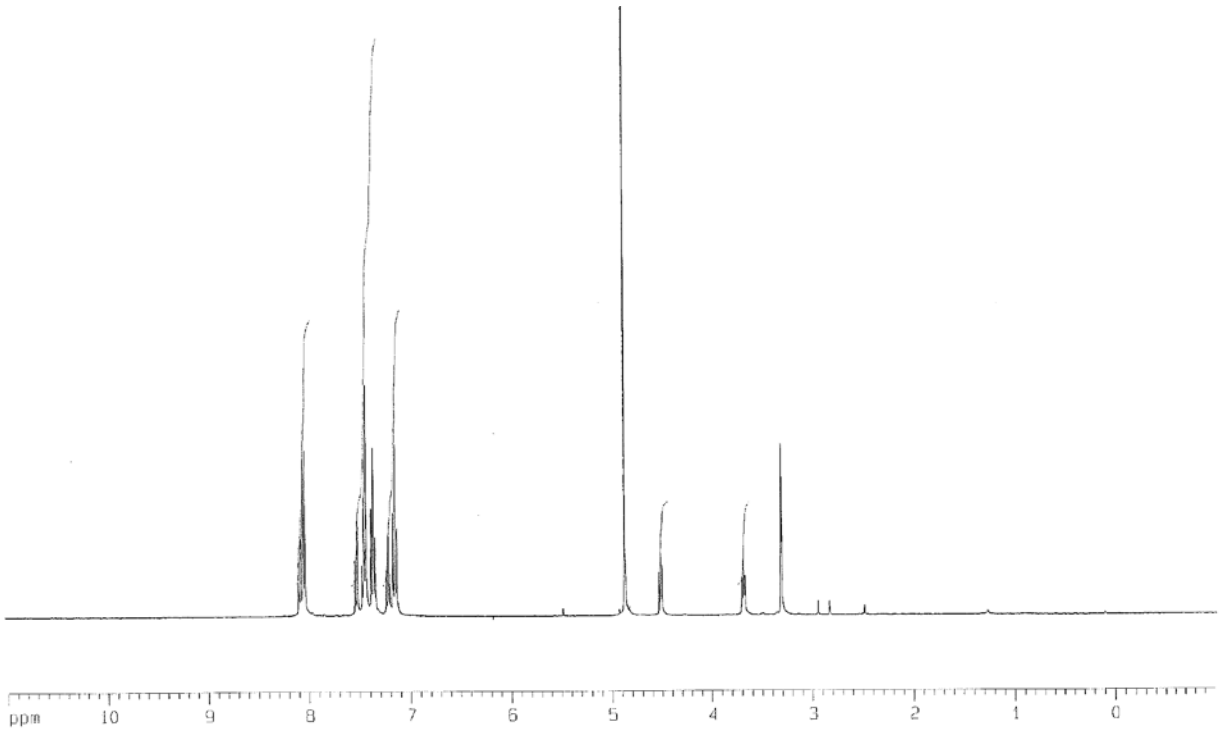

Spectra 7: ^{1}H NMR of **5** in $CDCl_3$

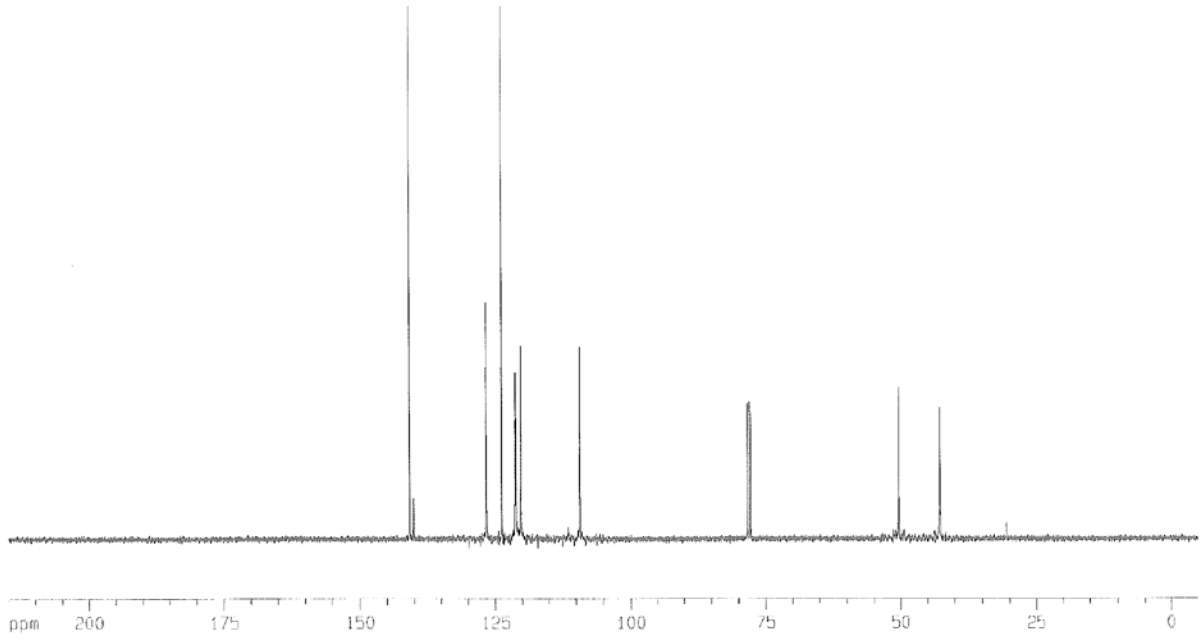

Spectra 8: ^{13}C NMR of **5** in $CDCl_3$

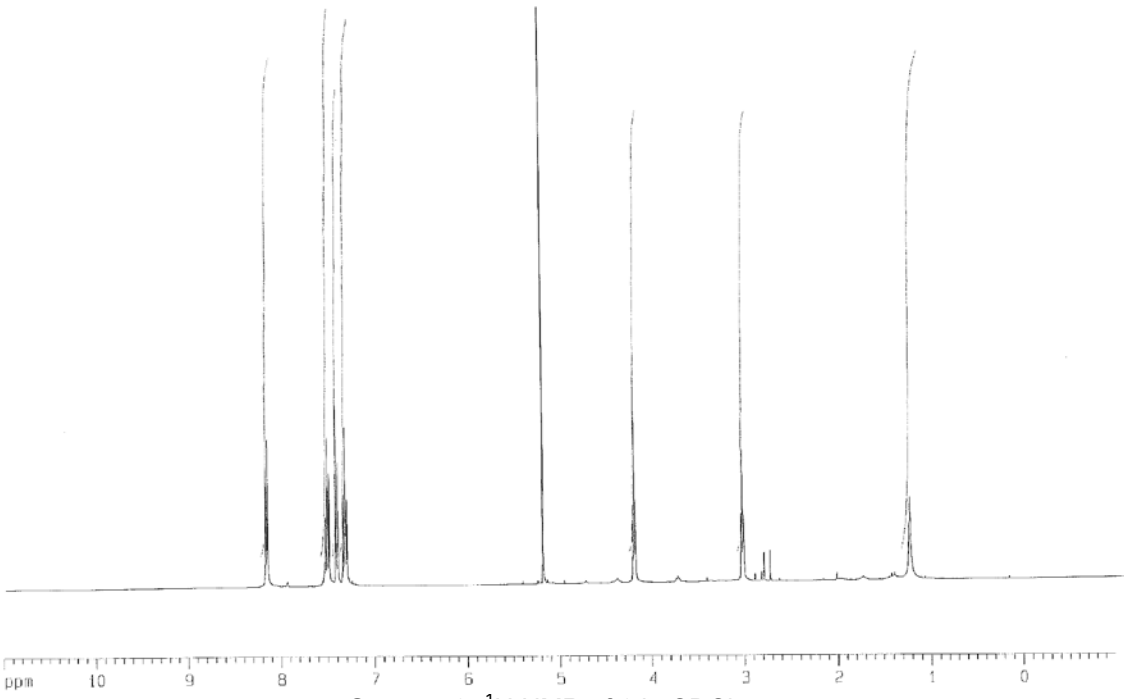

Spectra 9: ^{1}H NMR of **6** in $CDCl_3$

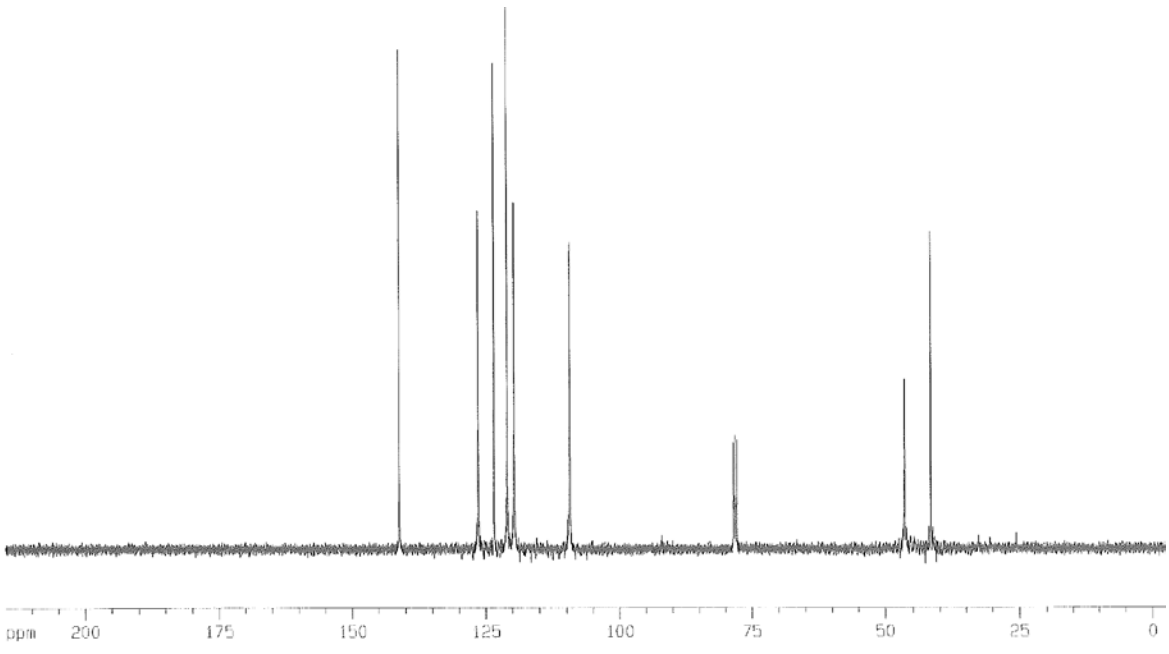

Spectra 10: ^{13}C NMR of **6** in $CDCl_3$

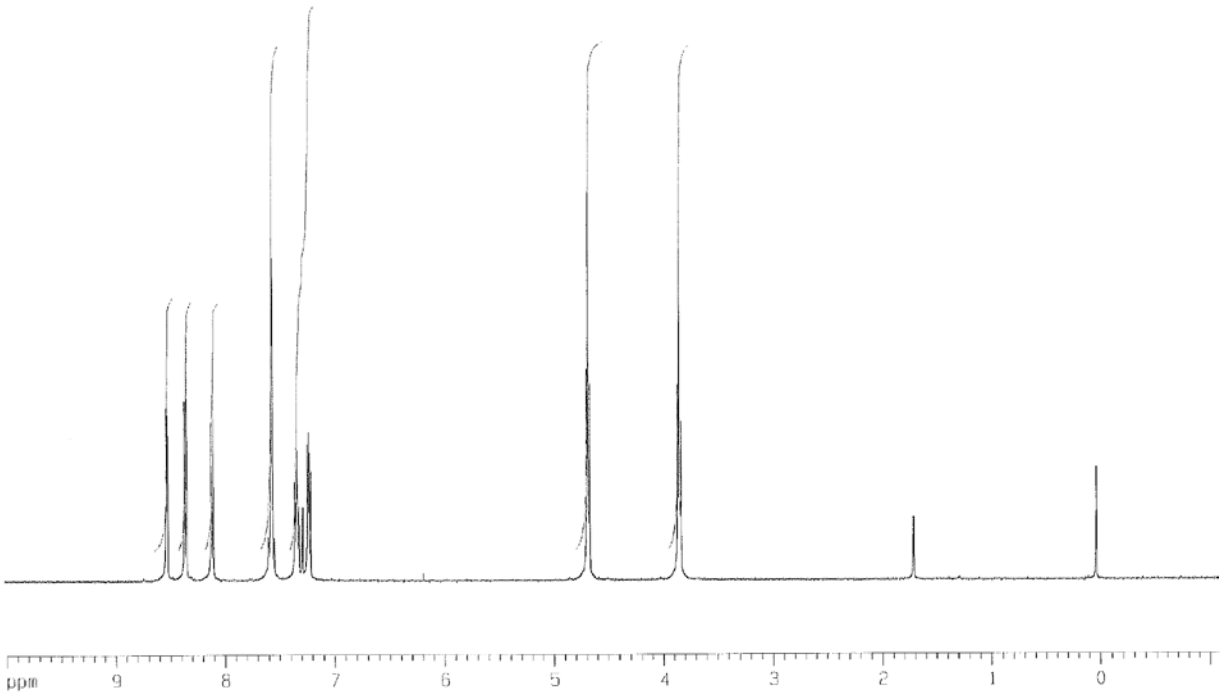

Spectra 11: ^{1}H NMR of **8** in $CDCl_3$

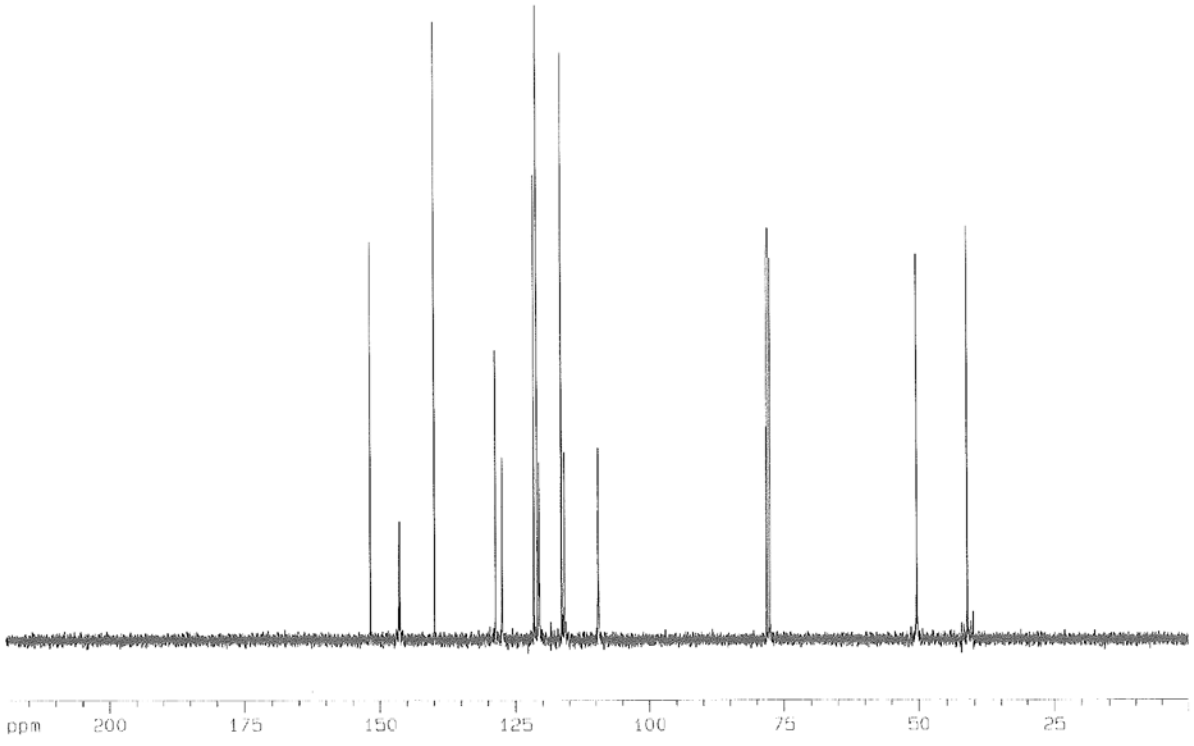

Spectra 12: ^{13}C NMR of **8** in $CDCl_3$

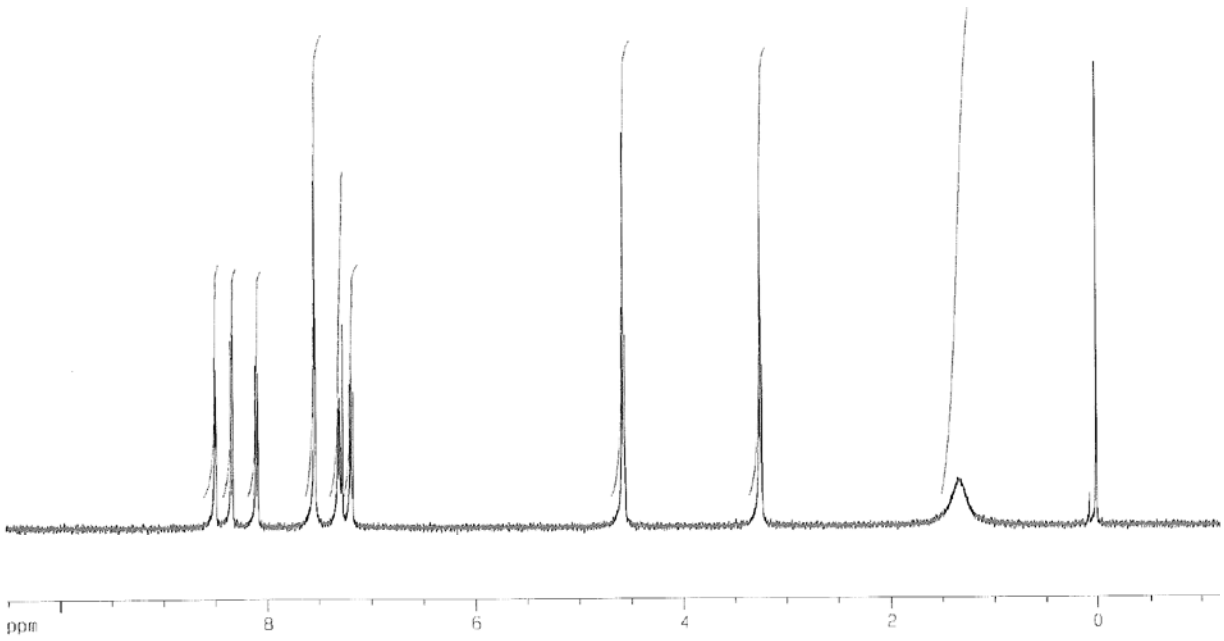

Spectra 13: ^{1}H NMR of **9** in $CDCl_3$

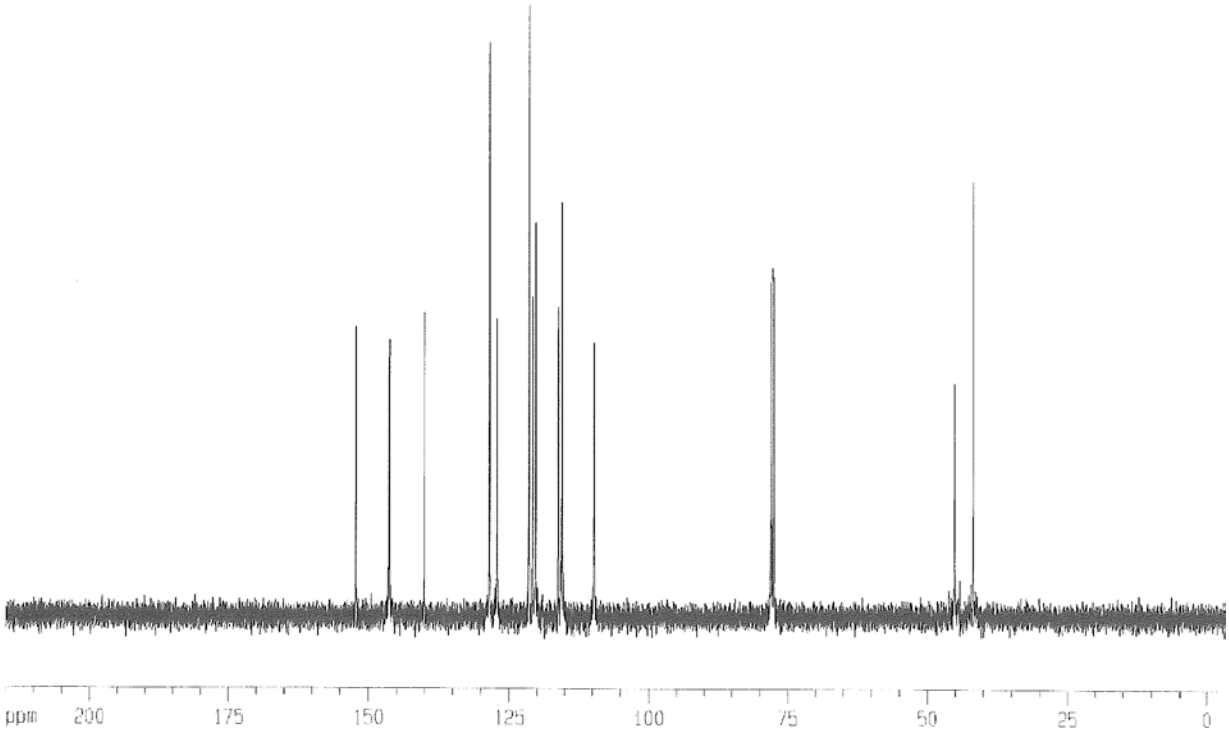

Spectra 14: ^{13}C NMR of **9** in $CDCl_3$

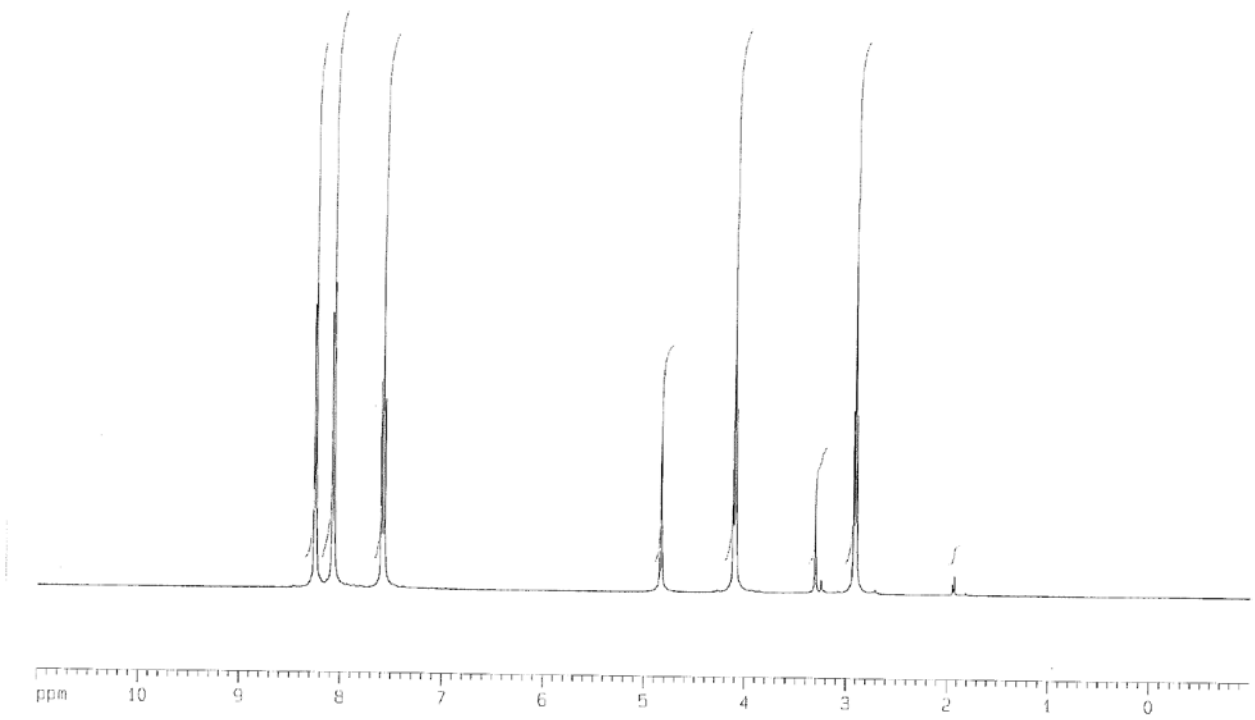

Spectra 15: ^{1}H NMR of **11** in MeOD

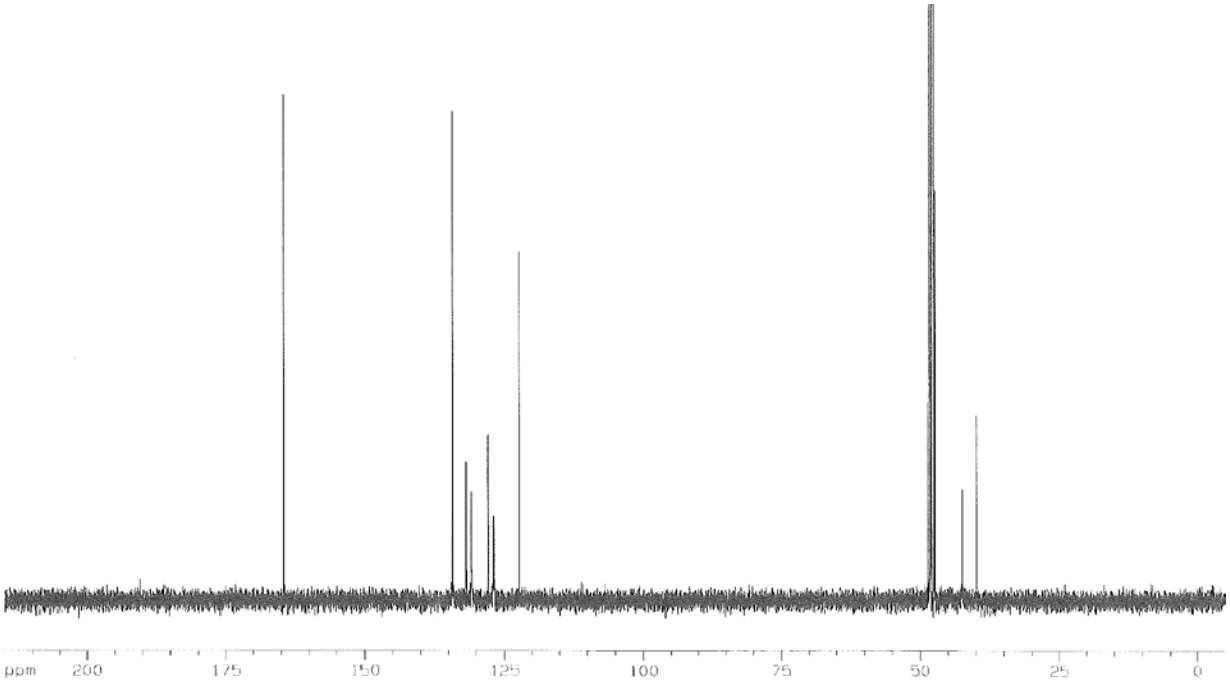

Spectra 16: ^{13}C NMR of **11** in MeOD

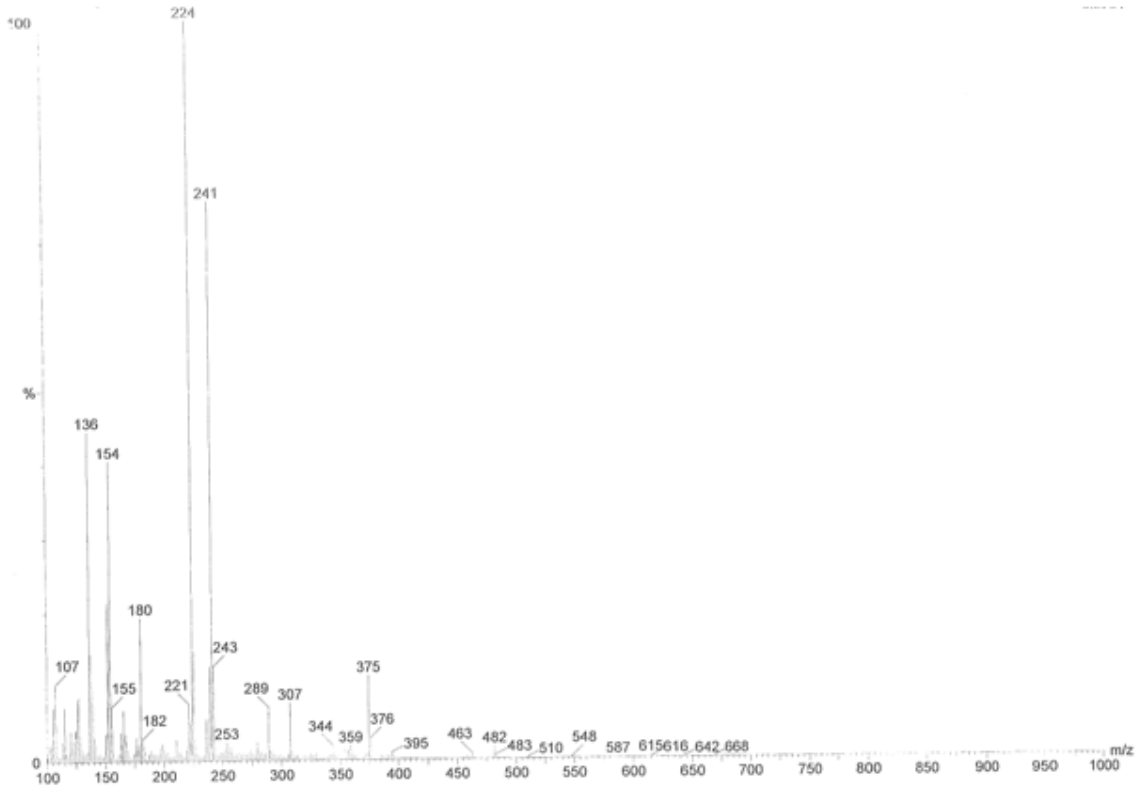

Spectra 17: MS (FAB^+) of **11**

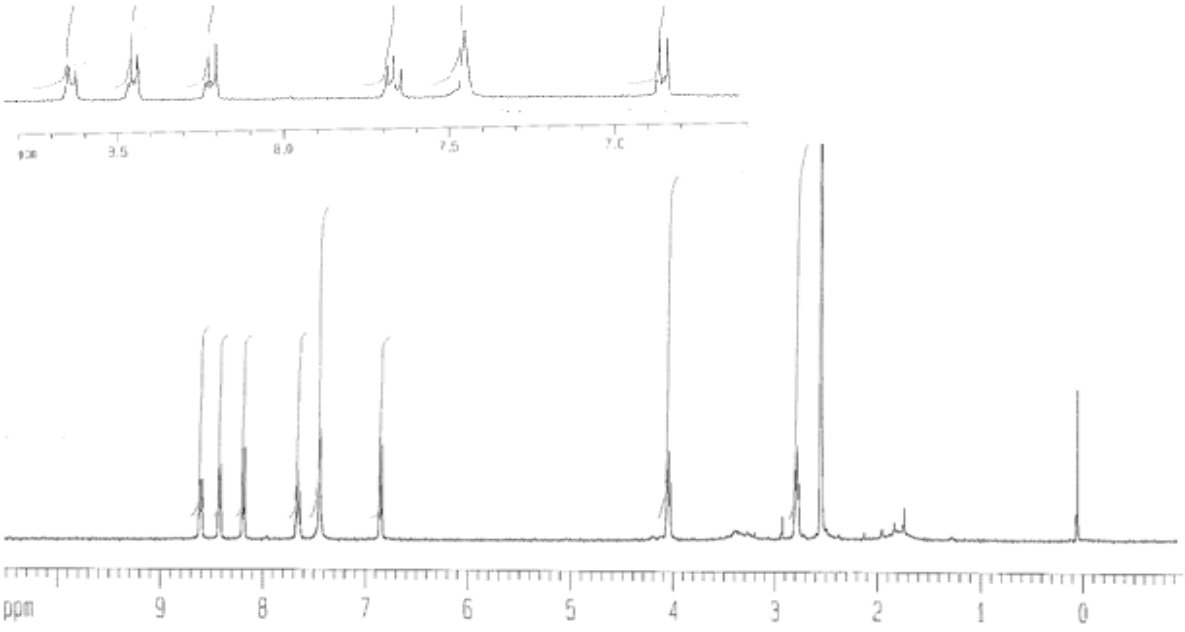

Spectra 18: ^1H NMR of **13** in DMSO

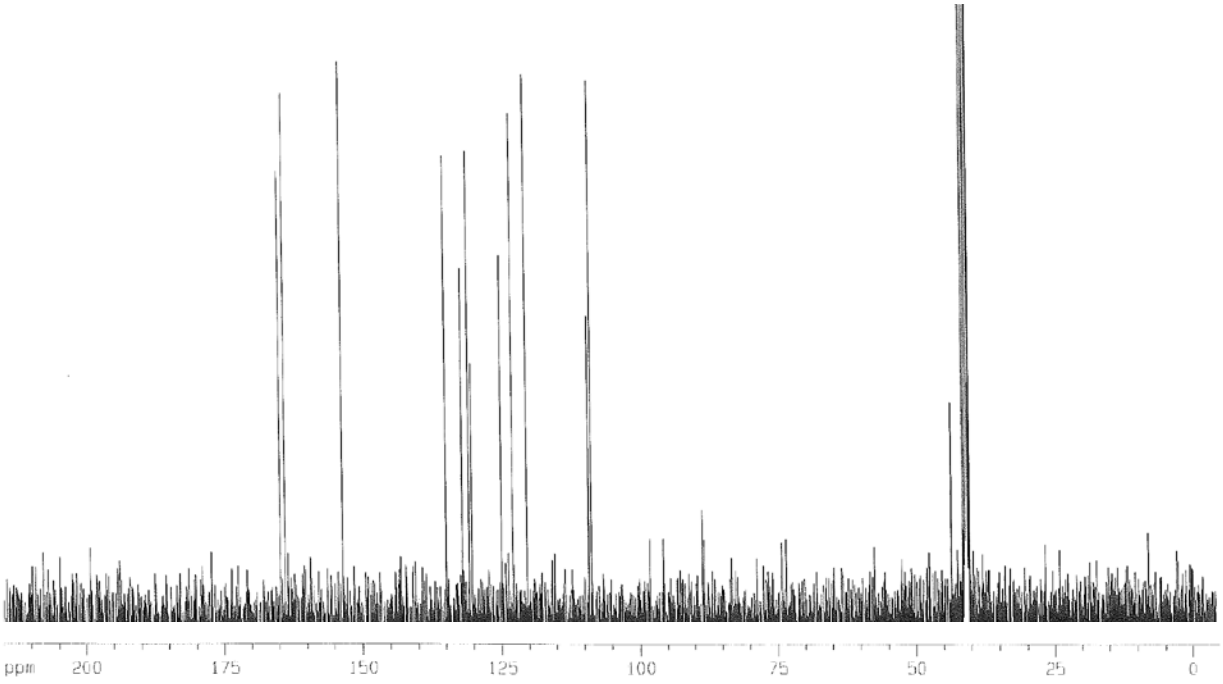

Spectra 19: ^{13}C NMR of **13** in DMSO

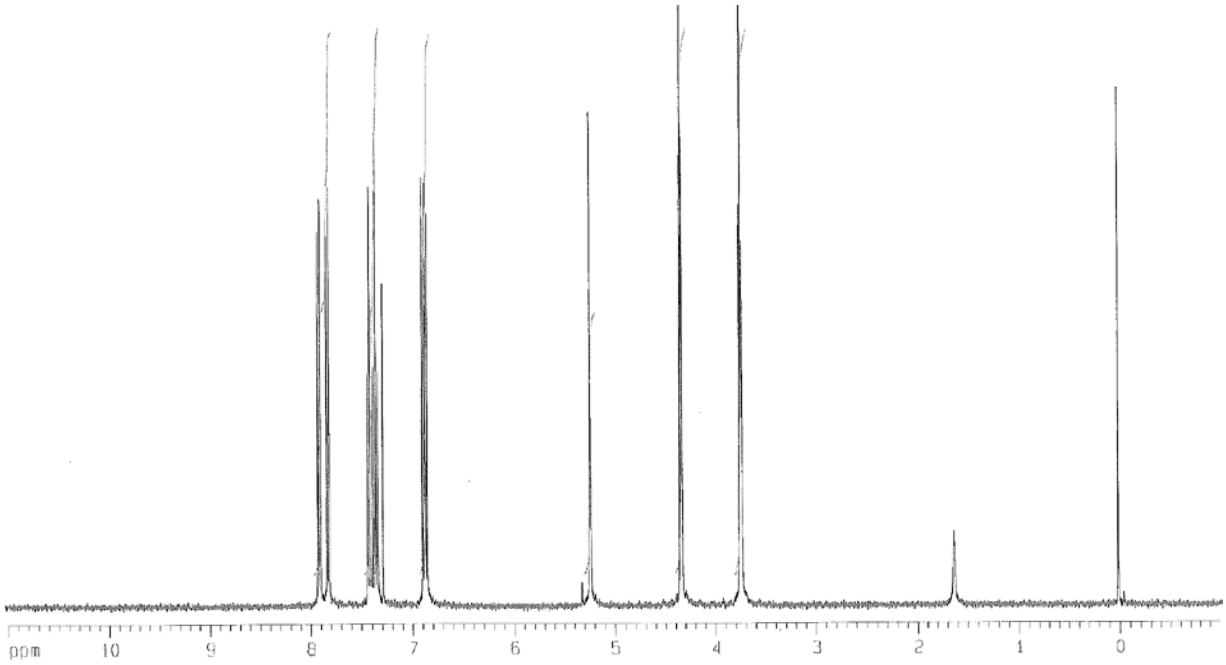

Spectra 20: ^{1}H NMR of **15** in$CDCl_3$

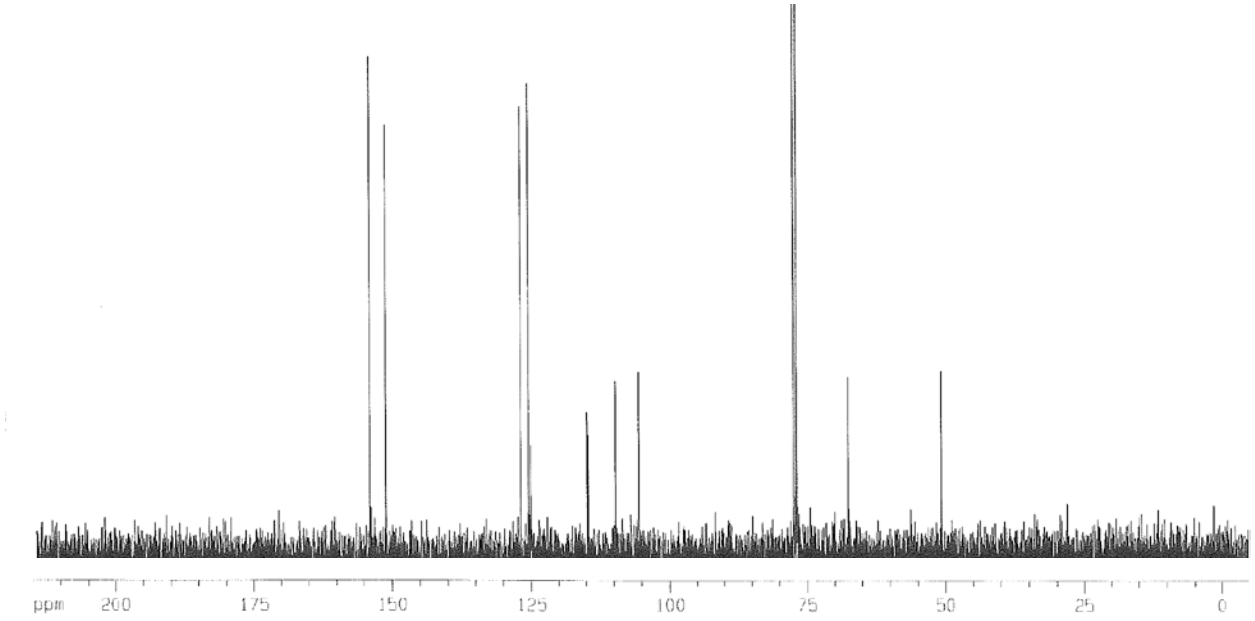

Spectra 21: ^{13}C NMR of **15** in$CDCl_3$

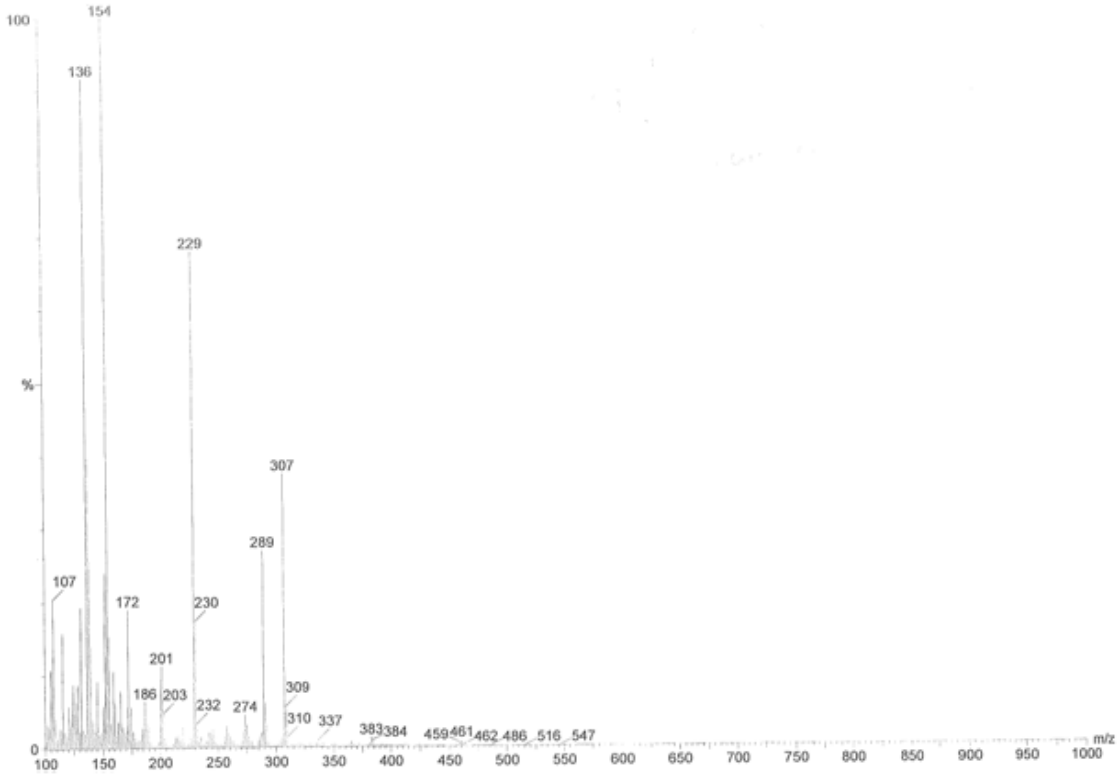

Spectra 22: MS (FAB^+) of **15**

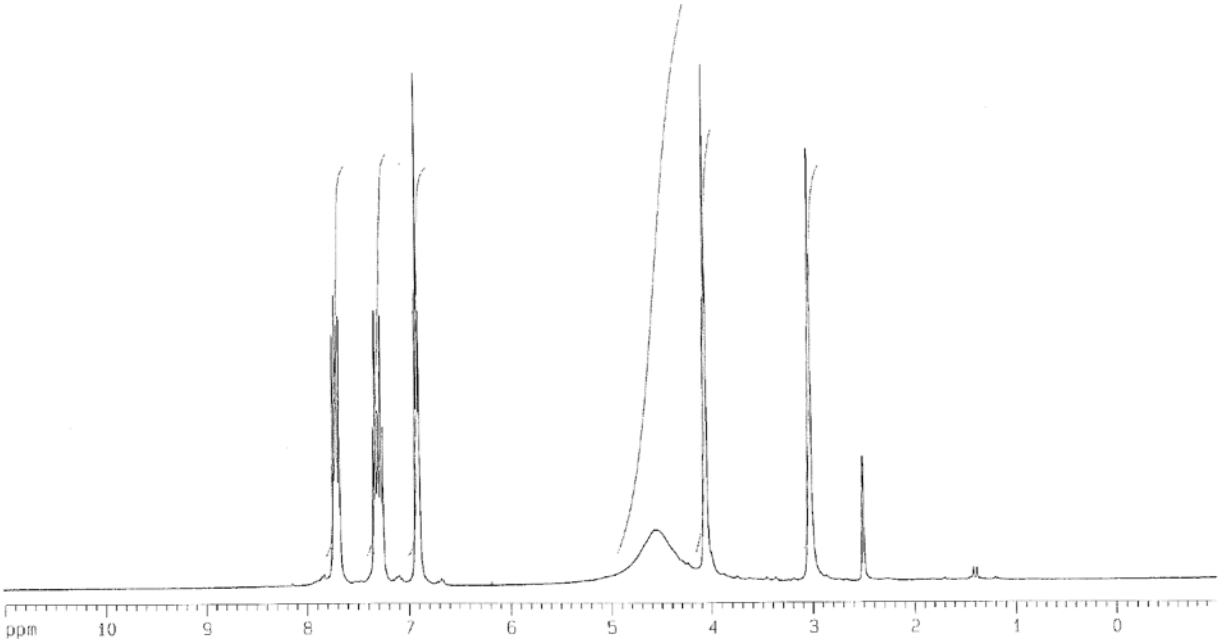

Spectra 23: ^{1}H NMR of **16** in DMSO

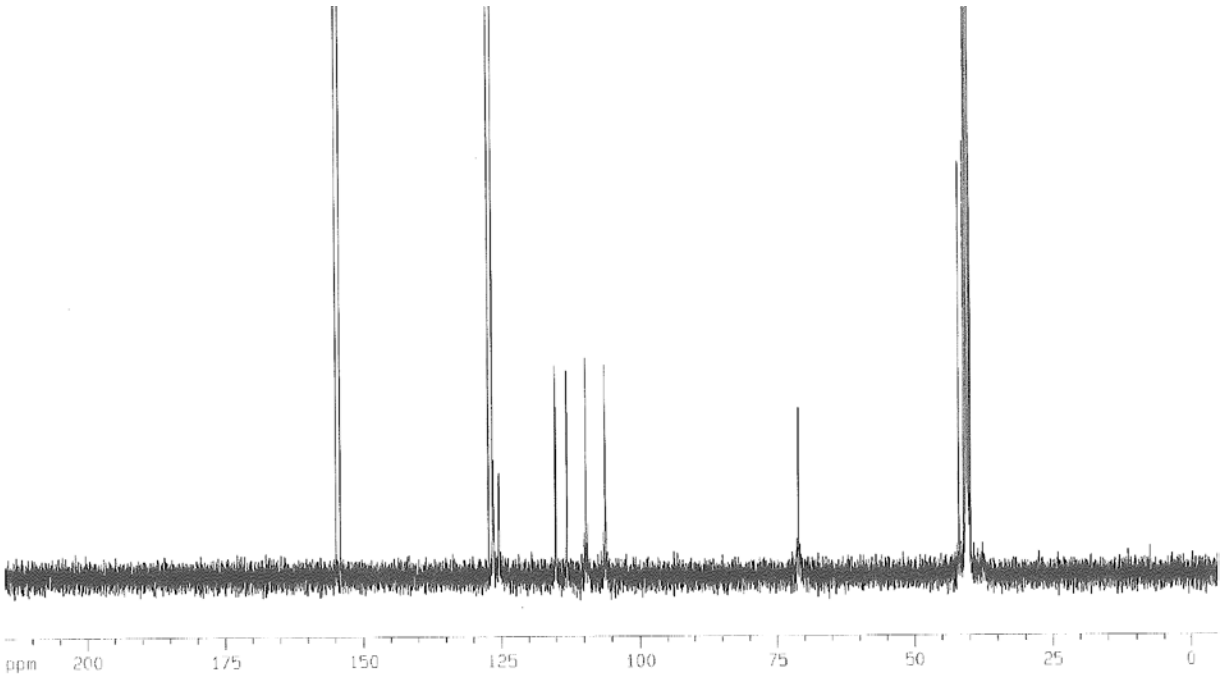

Spectra 24: ^{13}C NMR of **16** in DMSO

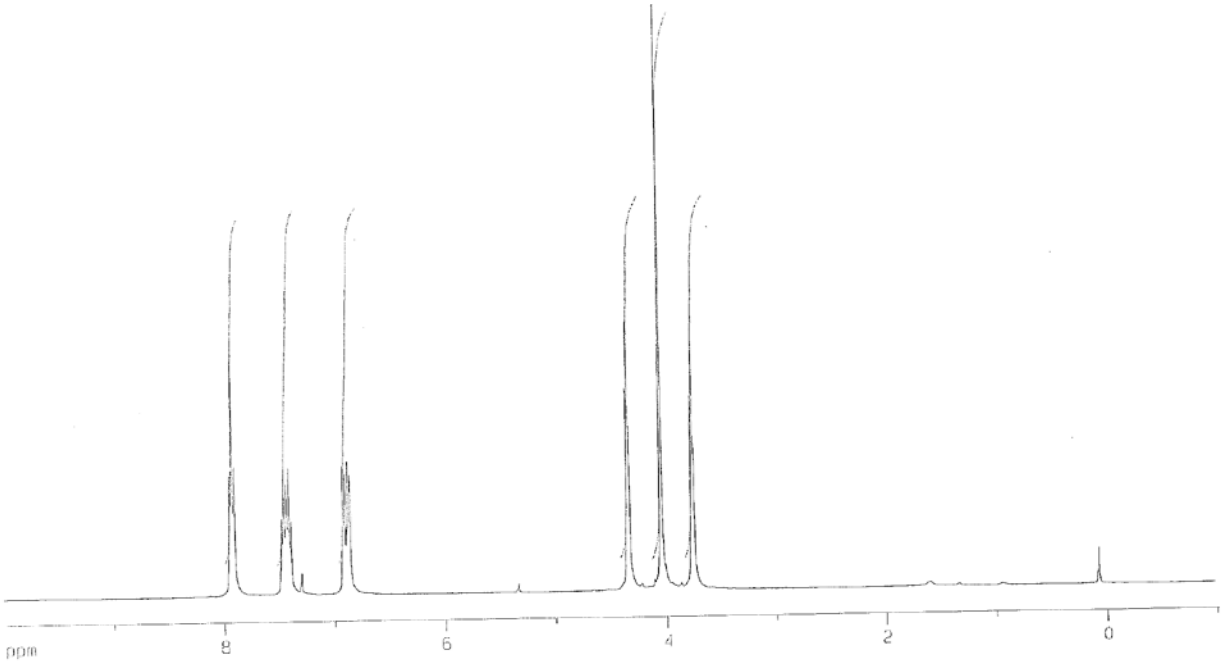

Spectra 25: ^{1}H NMR of **17** in$CDCl_3$

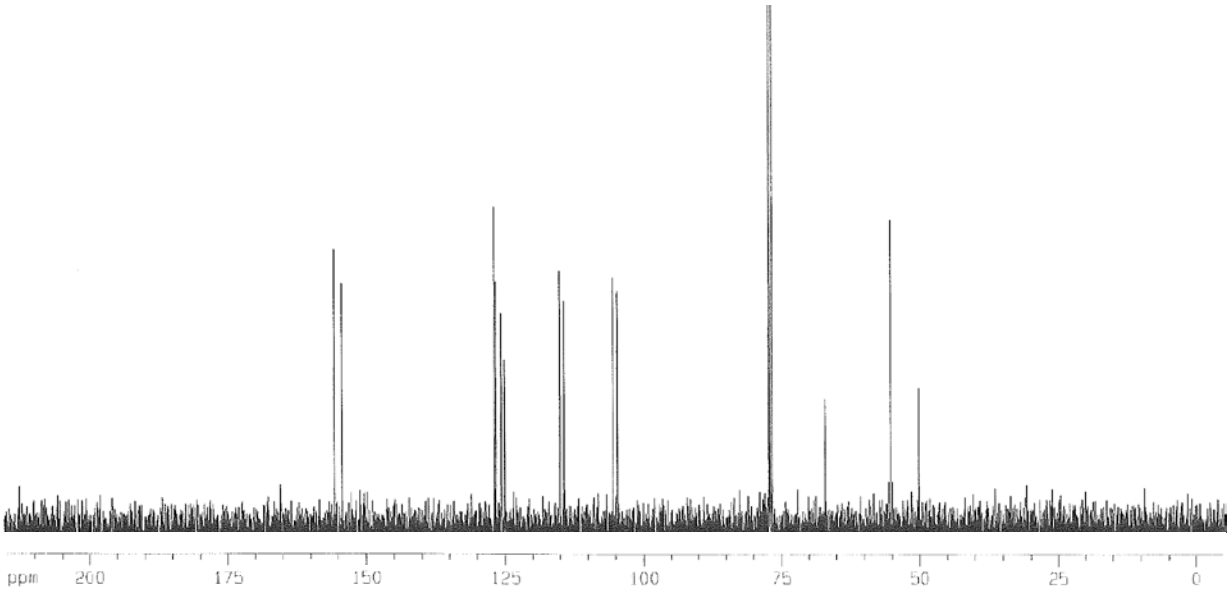

Spectra 26: ^{13}C NMR of **17** in$CDCl_3$

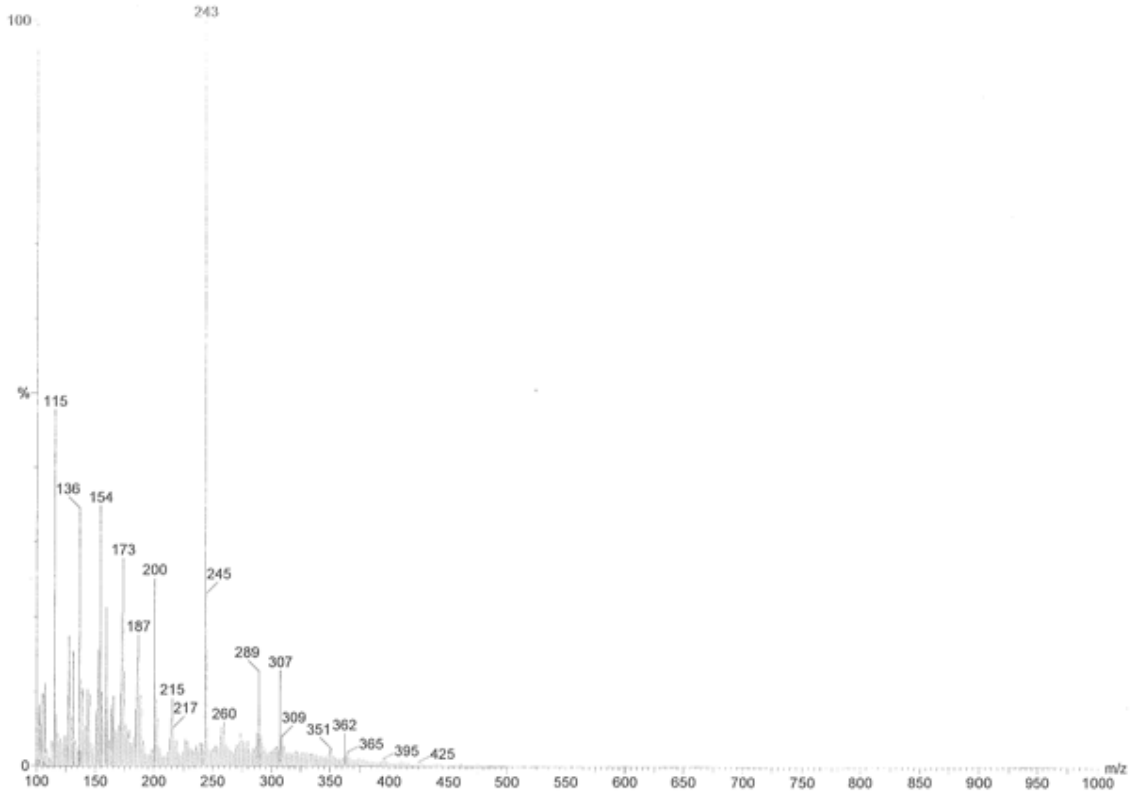

Spectra 27: MS (FAB^+) of **17**

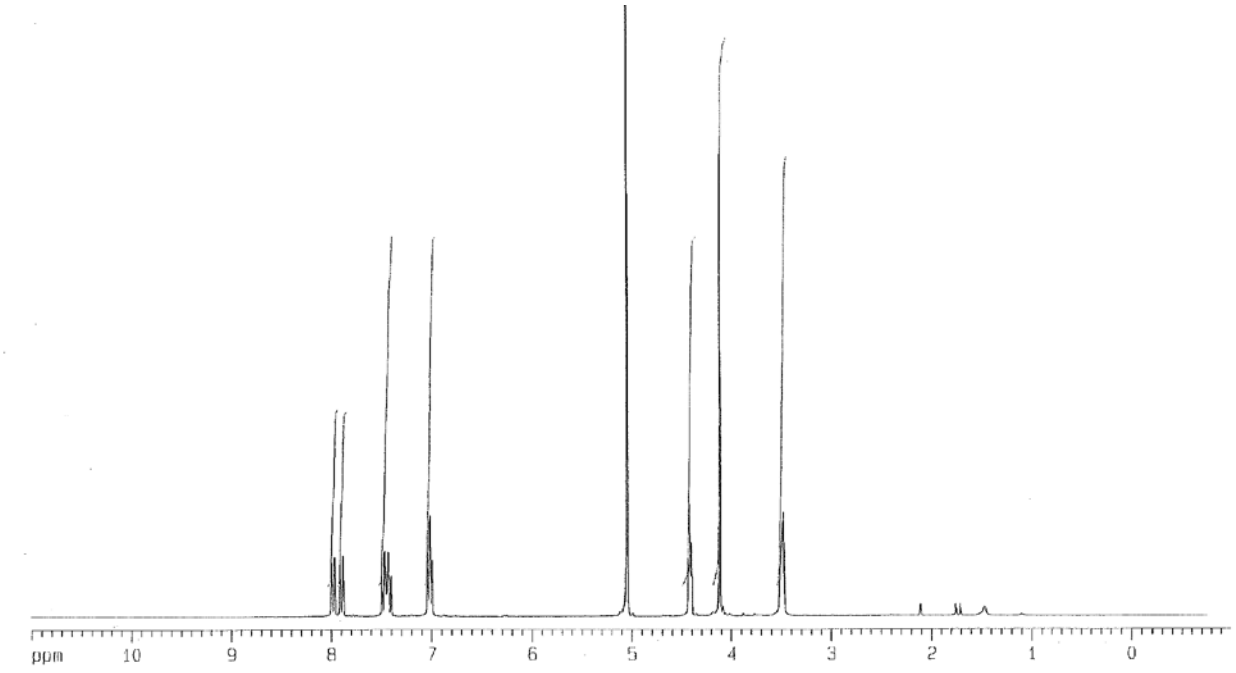

Spectra 28: ^1H NMR of **18** in MeOD

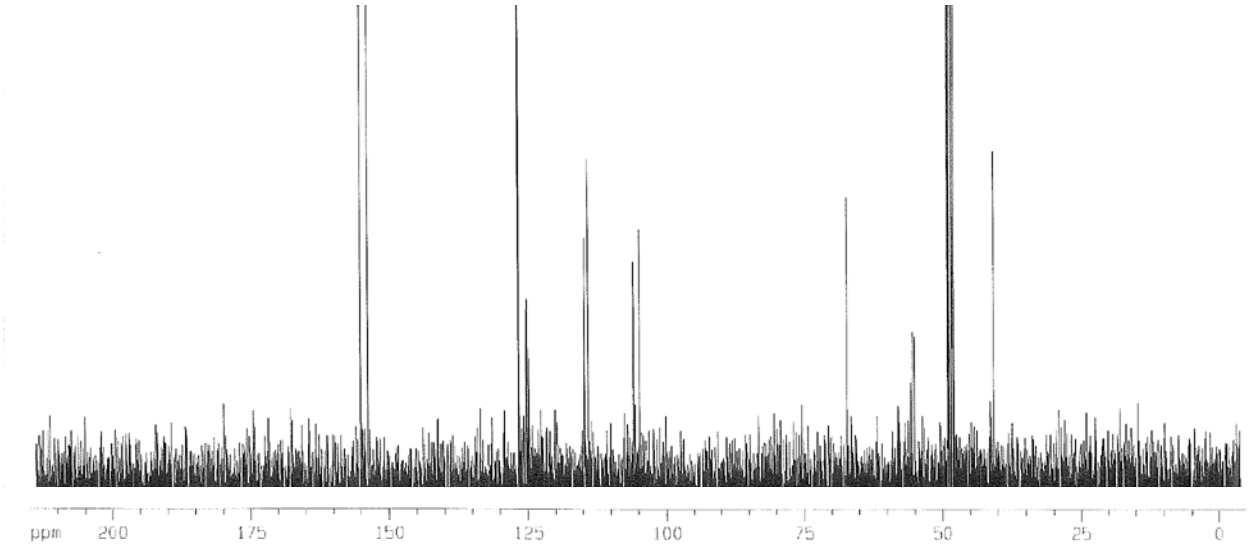

Spectra 29: ^{13}C NMR of **18** in MeOD

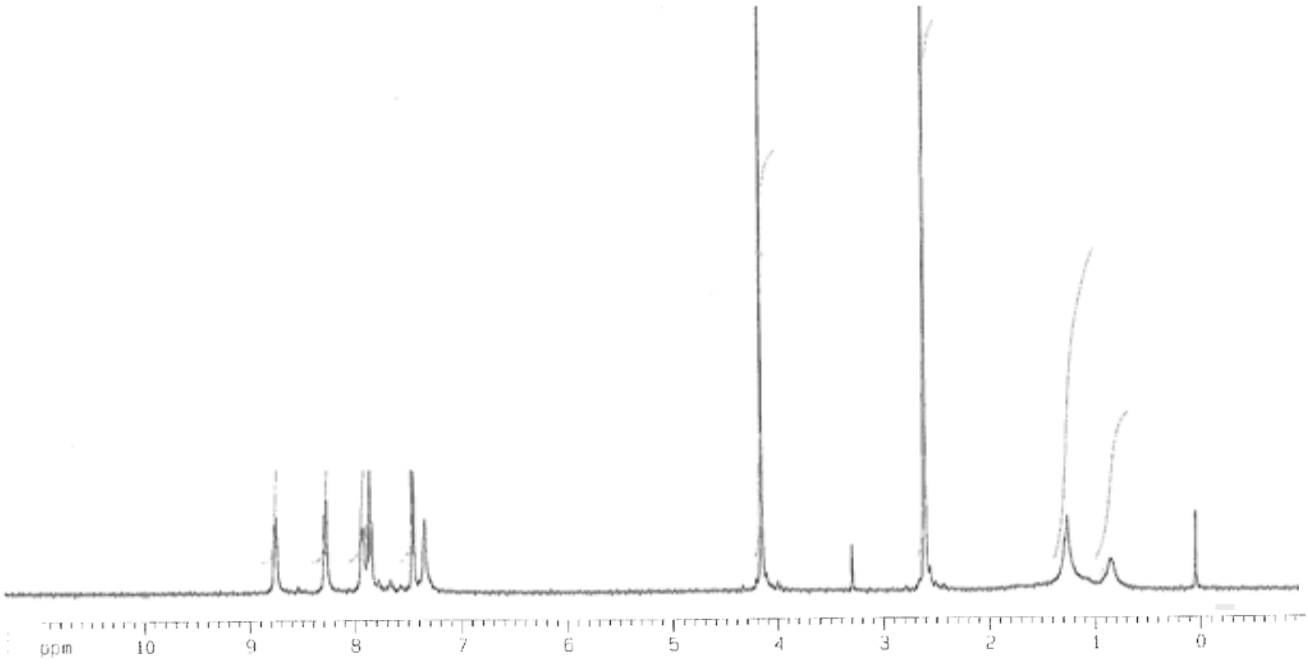

Spectra 30: ^{1}H NMR of **20** in MeOD

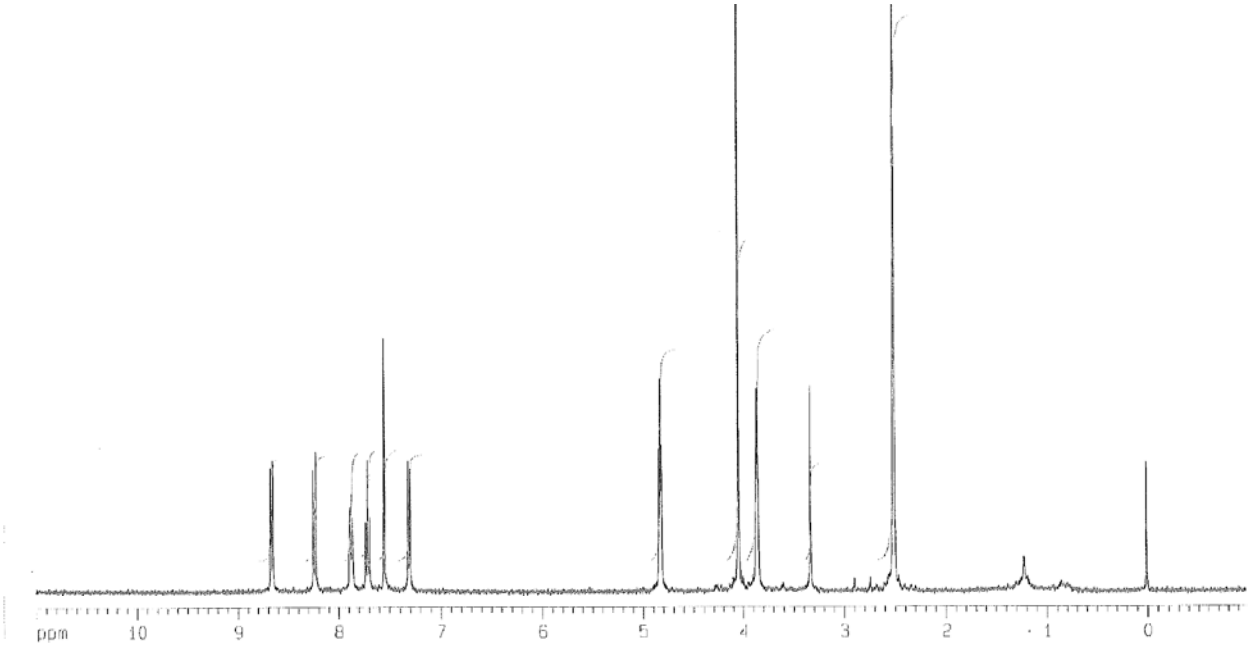

Spectra 31: ^{1}H NMR of **21** in DMSO

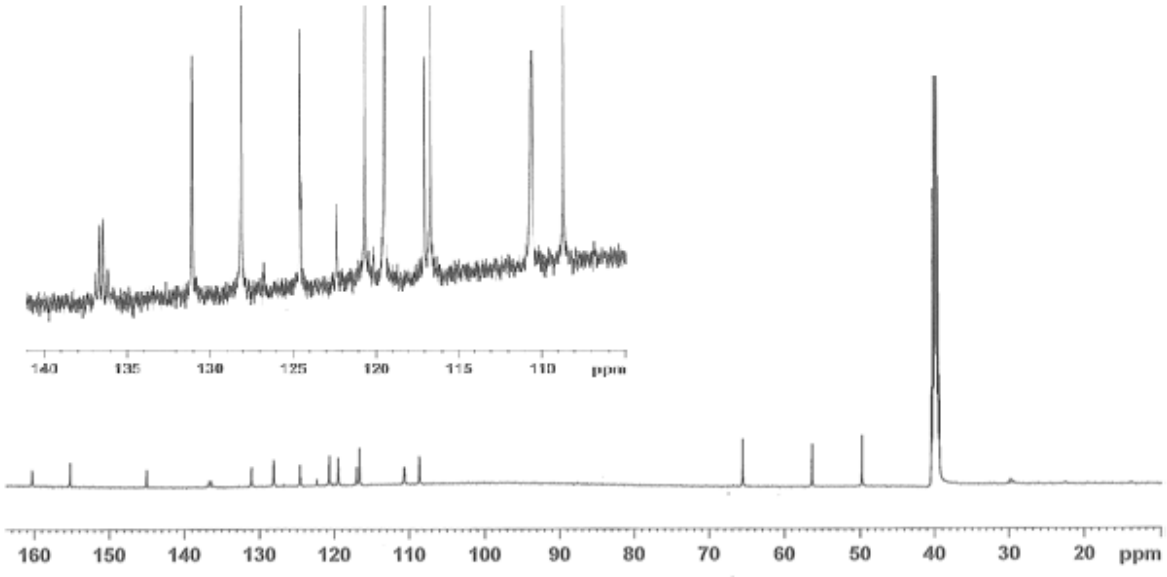

Spectra 32: ^{13}C NMR of **21** in MeOD

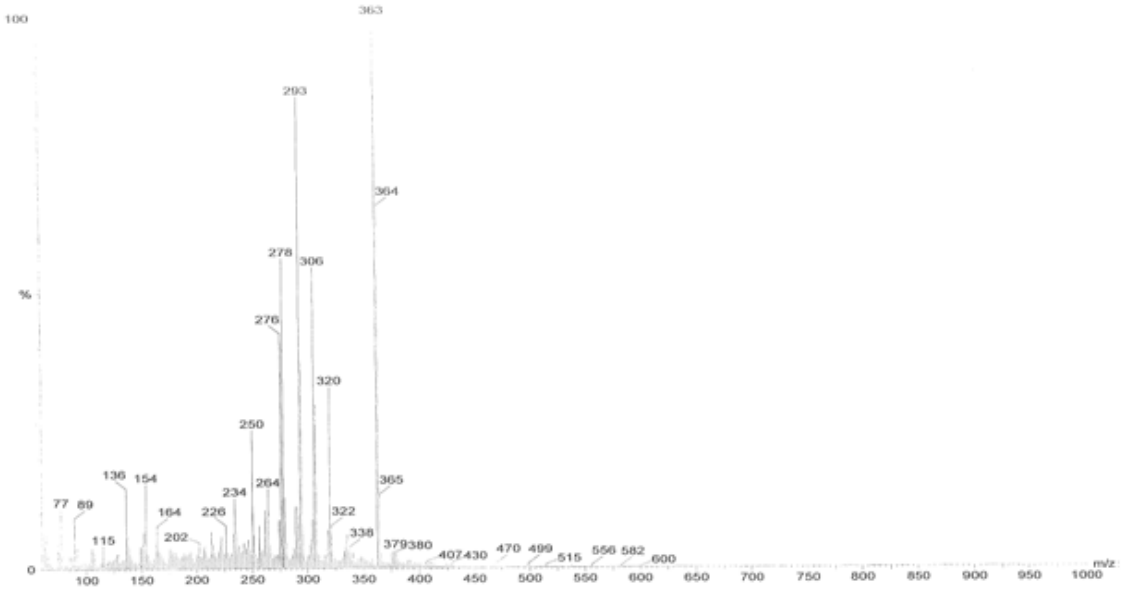

Spectra 33: MS (FAB^+) of **21**

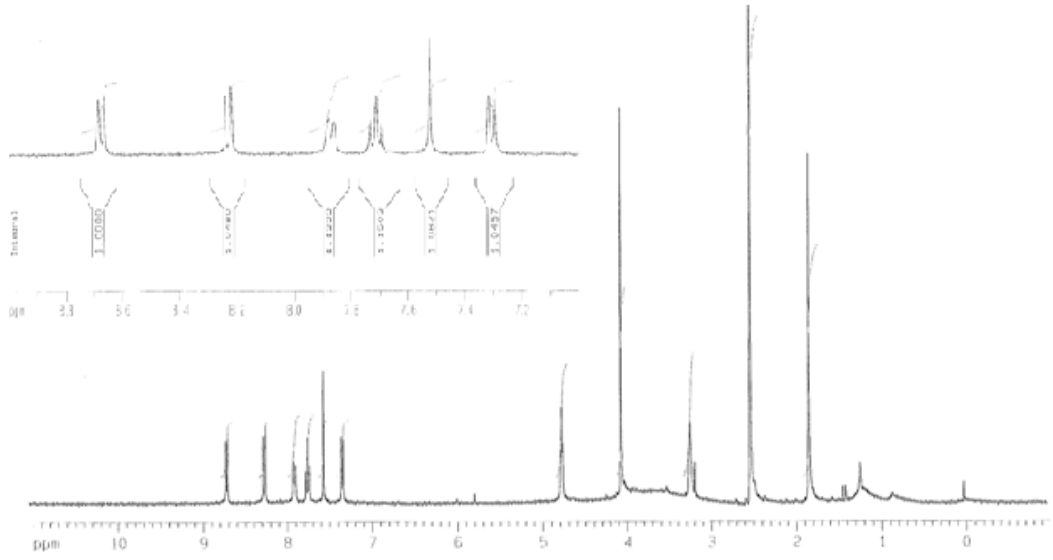

Spectra 34: ^1H NMR of **22** in DMSO

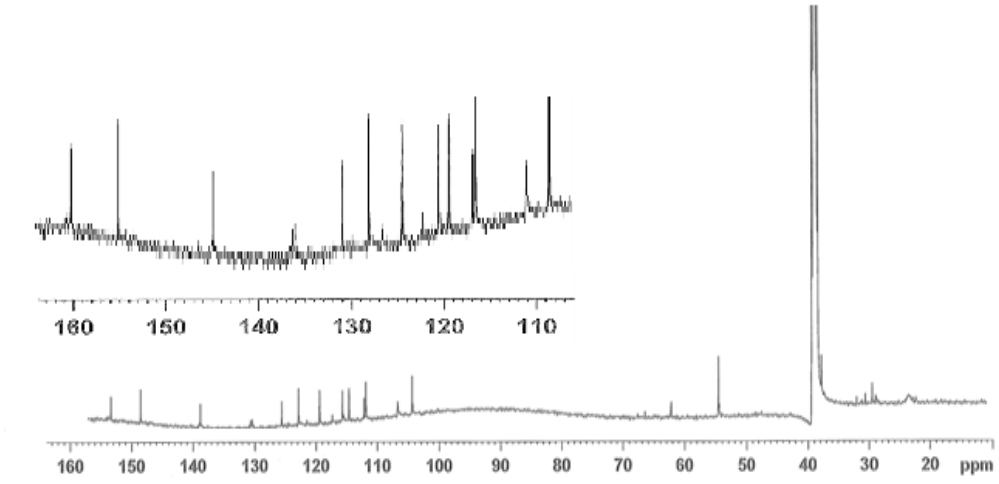

Spectra 35: ^{13}C NMR of **22** in DMSO

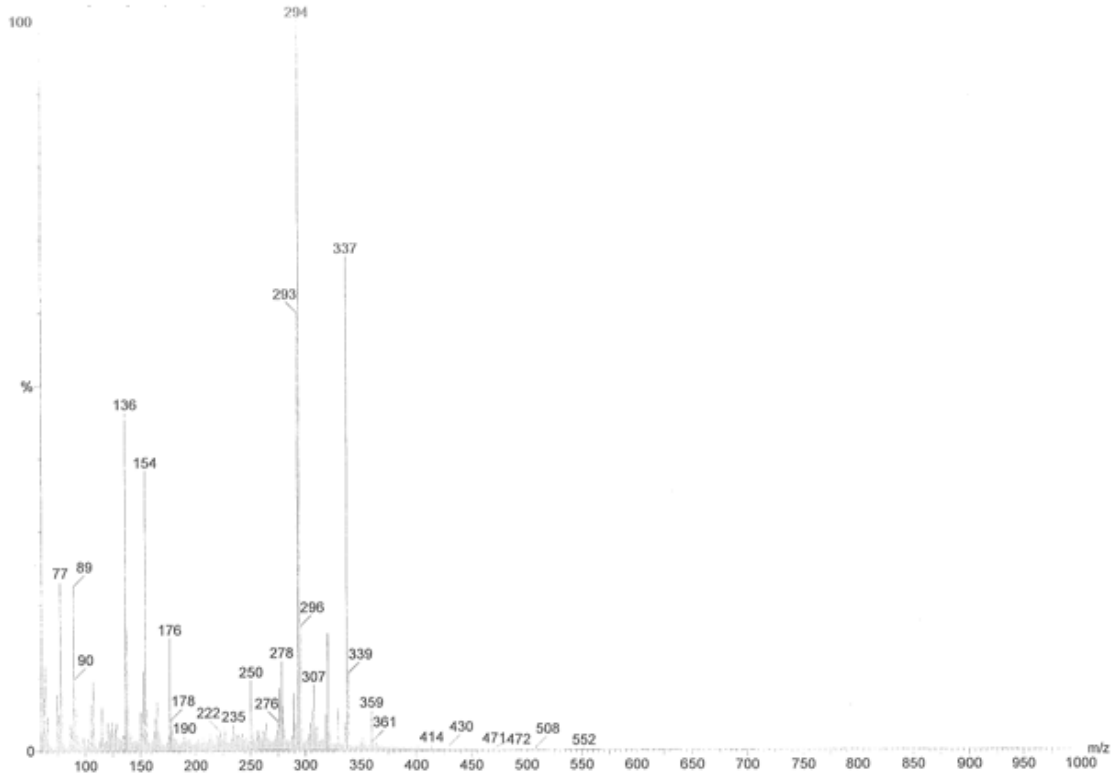

Spectra 36: MS (FAB^+) of **22**

Appendix B

Experimental procedures for probes synthesized but not fully characterized

1. 3-(3-methylbutyl)-3*H*-pyrimido [5, 4-*b*] [1, 4] benzothiazin-2(10*H*)-one (23)

1, 3-diaza-2-oxophenothiazine (1) (500 mg, 2.3 mmol) was placed in a round bottom flask charged with a stir bar, 1-bromo-3-methylbutane (345 mg, 2.3 mmol) and dry NaH (0.68 g, 5.0 mmol). DMF, as sufficient to allow the slurry to stir (~15 mL), was added then the reaction mixture was stirred at room temperature for 5h. After cooling, the reaction was poured into water and extracted three times with ~50 mL of CH_2Cl_2. TLC indicated the presence of both major mono alkylated (4**)** and minor di alkylated products in the organic layer. These were separated on a Biotage Isolera (25 g silica column with CH_2Cl_2 and MeOH). Yield (**23** only): 463 mg, 70%.

2.10-(2-azidoethyl)-3-(3-methylbutyl)-3*H*-pyrimido[5,4-*b*][1,4]benzothiazin-2(10*H*)-one(24)

Product **24** was obtained from the reaction of **23** (400 mg, 1.4 mmol) and 2-azidoethyl tosylate (0.7 mg, 2.7mmol) according to the method described for the preparation of **2**. Yield: 362 mg, 73%.

3.10-(2-aminoethyl)-3-(3-methylbutyl)-3*H*-pyrimido[5,4-*b*][1,4]benzothiazin-2(10*H*)-one(25)

Product **25** was obtained from the reaction of **24** (250 mg, 0.7 mmol) and 1.0 M solution of PMe_3 according to the method described for the preparation of **3**. Yield: 148 mg, 64%.

4. 3-[2-(dimethylamino) ethyl]-3*H*-pyrimido [5, 4-*b*] [1, 4] benzothiazin-2(10*H*)-one (26)

Product **26** was obtained from the reaction of 1(500 mg, 2.3 mmol) , 2-chloro-*N*,*N*-dimethylethanamine hydrochloride(332 mg, 0.43mmol) and NaH(0.2 g, 8.3mmol) according to the method described for the preparation of **23**. Yield: 416 mg, 62.7%.

5. 3-benzyl-3*H*-pyrimido [5, 4-*b*] [1, 4] benzothiazin-2(10*H*)-one (27)

Product **27** was obtained from the reaction of **1**(500 mg, 2.3 mmol), Benzyl bromide (300 mg, 1.76 mmol) and Noah (0.2 g, 8.3mmol) according to the method described for the preparation of **23**. Yield: 481 mg, 68%.